Politecnico di Torino

Collegio di Ingegneria Chimica e dei Materiali

Corso di Laurea in Ingegneria dei Materiali

Tesi di Laurea Magistrale

Key Factors in Controlling Stille Coupling Reactions Catalyzed by Palladium Complexes: Density Functional Theory (DFT) Calculation Analyses

---

Supervisor:
Prof. Takashi Yumura

Co-supervisor:
Prof. Marco Sangermano

Author:
Ruben Tavano

Abstract

Stille coupling reactions are one of the most common coupling reactions used nowadays. For many years only phosphorous ligands have been considered in the catalysts for this type of reaction but recent studies have shown that also arsenic ligands are very promising. In this study, DFT calculations were applied to the Stille coupling reaction of different systems (with various substrates and catalysts) in order to obtain the energy values associated to the various steps of the reaction.

In trial 1, oxidative addition was found to be a rate-determining step (but the considered halogen atom could effectively modulate the energy levels of this step), while transmetalation was found to be a rate-determining step only with phosphorous ligands.

In trial 2, different substituent groups were attached to the substrate (with a fixed halogen atom). In this trial, the energy levels of the transition states associated to the oxidative addition and the transmetalation were clearly lowered in the first considered system where an electron-withdrawing group was used as the substituent group of the substrate.

The use of arsenic ligands in Stille coupling reactions is interesting because it can significantly lower the energies associated to almost every transition state of the reaction, and the use of specific substituent groups in the ligand can enhance this behavior. The study of different substrates has also found that the use of specific halogen atoms and substituent groups in the substrate can strongly influence the reaction and highly enhance the reaction yield.

Summary

Riassunto

Introduzione

I polimeri funzionali sono stati utilizzati in molti settori diversi negli ultimi anni e questo aumento della loro popolarità si deve alle nuove tecniche di sintesi che hanno consentito un enorme aumento dell'efficienza produttiva. Tra i processi che sono stati utilizzati per la sintesi di polimeri funzionali, la reazione di Stille ha avuto sicuramente un ruolo importante in quanto ha consentito di ottenere molti polimeri semiconduttori per numerose applicazioni come i dispositivi OLED e OFET, e le PSCs. Tuttavia, grazie alla grande versatilità di questo tipo di reazione, si stanno studiando ulteriori applicazioni nell'ambito della sensoristica e delle telecomunicazioni: lo sviluppo di questi particolari polimeri coniugati, facilmente sintetizzabili attraverso le reazioni di Stille si trova ancora in uno stato iniziale ma avrà certamente un profondo sviluppo negli anni a venire.

La reazione di Stille solitamente prevede l'accoppiamento di una specie organica elettrofila e di un composto organostannico (anche detto organostannano) attraverso l'utilizzo di un catalizzatore basato sul palladio. In seguito alla reazione si ha la formazione di un prodotto accoppiato con la creazione di un legame singolo carbonio-carbonio (la reazione tipo è rappresentata in Figura 1).

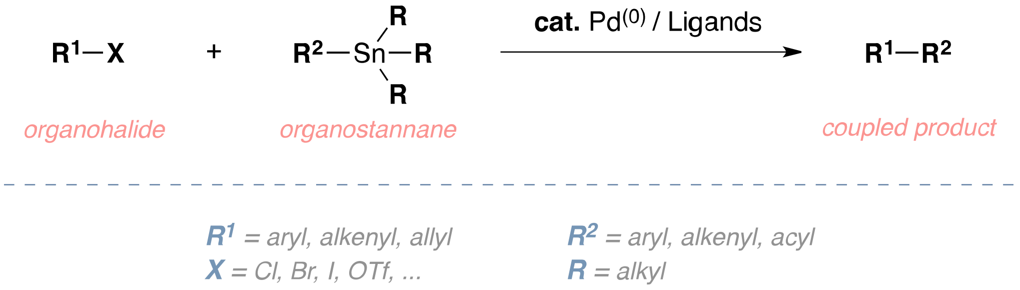

Figura 1 Schema basilare di una reazione di Stille

Questo tipo di reazione venne scoperto nel 1976 da Colin Eaborn il quale sintetizzò il primo prodotto accoppiato attraverso l'uso di un catalizzatore al palladio, ma il più grande sviluppo si ebbe a partire dal 1978 con il lavoro di John Stille (il quale darà anche il nome alla reazione). Stille studiò con grande attenzione questo tipo di reazione ed in seguito alla stesura da parte sua di un'importante review, a partire dal 1986, la reazione di Stille attirò un grande interesse nella comunità scientifica e accademica, che avrebbero portato questa reazione ad un grande utilizzo in ambito industriale. Purtroppo, Stille morì in un incidente aereo poco dopo aver spiegato in modo piuttosto completo il meccanismo di reazione, ma il suo contributo fu comunque molto importante per comprendere più in dettaglio le caratteristiche della reazione.

La reazione che venne per prima considerata da Stille procedeva attraverso quattro step principali, illustrati in Figura 2:

- Nel primo step il catalizzatore PdL_2 subisce una addizione ossidativa con la specie elettrofila in modo da formare $RPdL_2X$.
- Successivamente questa specie subisce una transmetallazione con l'organostannano $R^{I}SnR^{II}_3$ così da formare $RPdL_2R^{I}$.
- La specie ottenuta evolve attraverso un'isomerizzazione trans-cis in modo da prepararsi per l'ultimo step.
- In seguito all'isomerizzazione la specie ottenuta subisce un'eliminazione riduttiva che porta alla specie accoppiata finale $R\text{-}R^{I}$ e alla rigenerazione del catalizzatore PdL_2.

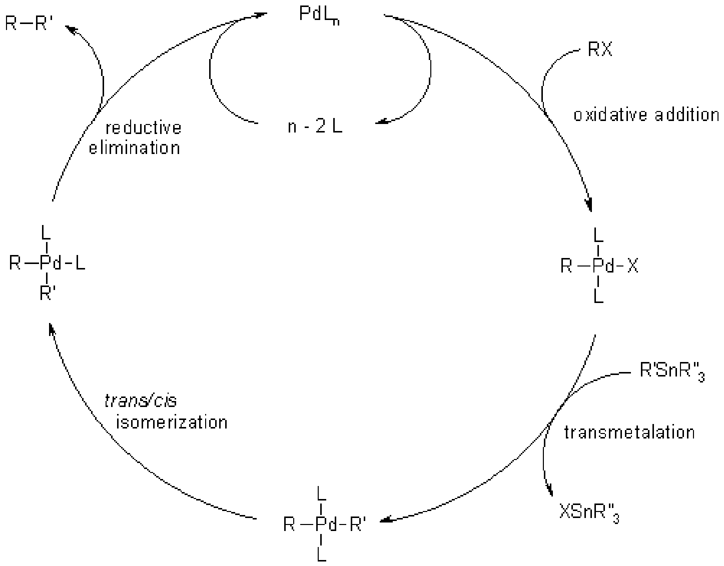

Figura 2 Meccanismo semplificato ipotizzato da Stille

Studi successivi hanno poi dimostrato che le reazioni di Stille presentavano un meccanismo molto più complesso, dipendente dal tipo di catalizzatore, di solvente, dagli additivi e da numerosi altri fattori. Ad esempio, se si usano catalizzatori con dei ligandi bidentati si può agire sull'isomerizzazione che può avere luogo dopo il primo step inibendola e portando ad una diversa evoluzione della reazione. Un'altra possibile modificazione del percorso della reazione si ha nel meccanismo della transmetallazione. Questo step può essere visto come S_E2 (per la rottura elettrofila del legame Sn-C ad opera del complesso contenente palladio) ma può anche essere visto come S_N2 (per la sostituzione del ligando sul complesso contenente palladio). Il complesso di palladio ha solitamente una struttura tetracoordinata a 16 elettroni con geometria quadrata planare che può evolvere attraverso due percorsi principali:

- Nel primo caso si ha un percorso associativo che coinvolge un complesso a 18 elettroni con struttura intermedia bipiramidale trigonale, e con la sostituzione che è regolata dal ligando con il maggior effetto trans;
- Nel secondo caso si ha un percorso dissociativo che coinvolge un complesso a 14 elettroni con struttura intermedia a T, e con la sostituzione che è regolata dal ligando con la maggior capacità di indebolire il legame trans rispetto ad esso.

Lo stato intermedio nella rottura elettrofila può avere una struttura aperta o ciclica, a seconda del percorso che si considera, come mostrato in Figura 3.

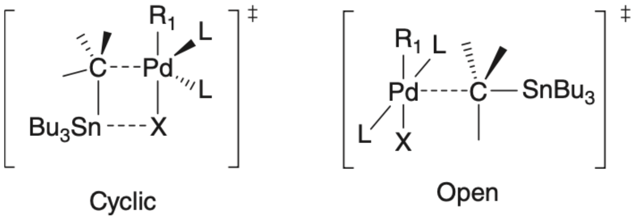

Figura 3 Stati di transizione con geometria ciclica o aperta

Stille osservò nei suoi esperimenti unicamente specie che portavano ad ottenere una geometria aperta per lo step intermedio, ma negli anni successivi si è scoperto che se si utilizzano degli organoalogenati la reazione procede invece attraverso uno stato di transizione ciclico.

Queste sono solo alcune delle complessità che sono state osservate durante lo studio delle reazioni di Stille, con numerosi fattori da considerare ogni qual volta si voglia procedere con questo tipo di reazione. Un meccanismo più completo (mostrato in Figura 4), che tiene conto di moltissimi dei fattori che influenzano la reazione, è stato ipotizzato all'inizio del XI secolo.

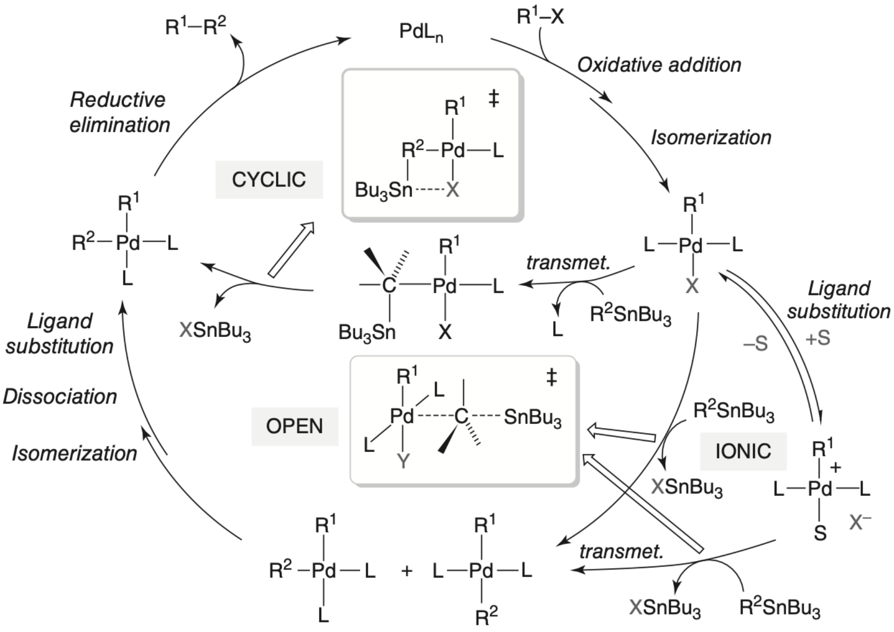

Figura 4 Meccanismo completo per la reazione di Stille

Tra i fattori che influenzano la reazione di Stille il più importante è sicuramente il catalizzatore. Solitamente si usano specie contenenti Pd(II) le quali devono poi essere ridotte a Pd(0) con appositi agenti riducenti in modo da poter procedere con la reazione. La componente principale del catalizzatore al palladio sono i gruppi ligandi, che sono in grado di influenzare l'evoluzione della reazione. Molto comuni sono i ligandi voluminosi (perlopiù contenenti fosforo) che portano ad una stabilizzazione delle strutture intermedie nell'addizione ossidativa, nella transmetallazione e nell'eliminazione riduttiva. Anche il comportamento elettronico dei catalizzatori è molto importante poiché la presenza di un atomo centrale differente nel ligando (ad esempio arsenico al posto del fosforo) o di gruppi aventi un effetto elettronico specifico legati all'atomo centrale (gruppi elettro-donatori o elettro-accettori), può influenzare profondamente la reazione. Negli ultimi anni, a causa di problemi legati alla stabilità e alla reattività dei ligandi basati sul fosforo, un crescente interesse si è sviluppato nei confronti dei ligandi basati sull'arsenico. In un recente studio (da cui parte questo lavoro di tesi), il Prof. Imoto, ha studiato la reazione considerando numerose specie diverse, con catalizzatori contenenti arsenico e gruppi legati agli atomi di arsenico dotati di differenti effetti elettronici, andando a vedere con quale tipologia di catalizzatori si ottenevano le minori barriere energetiche per i vari step, e di conseguenza i migliori rendimenti della reazione.

Nello stesso studio vengono considerati differenti substrati (specie organiche elettrofile) di partenza, poiché anche il substrato che si considera gioca un ruolo chiave nella reazione. L'uso di alogeni e gruppi sostituenti diversi, influenza notevolmente la forza dei legami che si devono rompere per far procedere la reazione e modifica, inoltre, i livelli energetici degli orbitali, rendendo gli step della reazione più semplici a seconda delle specie considerate.

Anche gli additivi possono essere utilizzati in modo da facilitare la reazione: sali di litio come LiCl sono in grado di accelerare la reazione trasformando il catalizzatore in un'altra specie se questo non è sufficientemente nucleofilo, sali di rame come CuI agiscono da trappole per i ligandi liberi in modo da impedire che la transmetallazione venga inibita (specialmente nel caso di ligandi forti come PPh_3), sali di potassio o cesio contenenti fluoro riescono ad aumentare la reattività dell'organostannano grazie alla formazione di speciali complessi che facilitano la transmetallazione.

Il solvente utilizzato è molto importante poiché, specialmente se si considerano delle policondensazioni, oltre che a solubilizzare i reagenti, serve a mantenere la catena polimerica in crescita in modo da ottenere elevati pesi molecolari e ridotta polidispersione. Inoltre, il solvente può direttamente partecipare alla reazione reagendo con il complesso al palladio legandosi ad esso come se si trattasse di un ligando vero e proprio.

Infine, anche la temperatura gioca un ruolo chiave. Aumentando la temperatura si può aumentare la resa della reazione ma bisognerà anche prestare attenzione alla degradazione dei reagenti. Per questo motivo solitamente le temperature utilizzate sono tra i 60 °C e i 100 °C.

In questo lavoro diverse reazioni di Stille sono state studiate attraverso analisi di chimica computazionale (con simulazioni basate su density functional theory o DFT) per individuare in dettaglio quali sono i fattori che influenzano la reazione tra l'organostannano e l'organoalogenato. L'utilità di questo studio va cercata nella grande quantità di combinazioni che sono state studiate e che hanno consentito di capire in modo più approfondito l'effetto che i diversi ligandi e substrati hanno sulla reazione di Stille.

Nel primo trial diversi ligandi terziari basati su arsenico o fosforo sono stati considerati: ogni atomo di fosforo o arsenico è legato a tre gruppi identici (Ph o fenile, $PhCF_3$ o para-trifluorometil benzene, PhOMe o para-anisil benzene) in modo da ottenere un totale di sei ligandi diversi. Inoltre, diversi substrati sono stati considerati con differenti atomi di alogeno: il substrato è X-Ph-OMe in cui X indica l'atomo di alogeno che può essere bromo, cloro o iodio. L'organostannano viene invece mantenuto invariato (si tratta di una molecola di (tributilstannil)vinile). In questo modo, per il trial 1, un totale di 18 sistemi reattivi è stato considerato.

Nel secondo trial, partendo dalla migliore combinazione di specie ottenuta nel trial 1, il substrato è stato modificato in modo da considerare differenti gruppi sostituenti in posizione para rispetto all'alogeno. I valori precedentemente ottenuti per il gruppo OMe sono stati confrontati con quelli ottenuti per un singolo atomo di idrogeno ed un gruppo NO_2, in modo da ottimizzare ulteriormente la reazione studiata. In questo modo, per il trial 2, un totale di 6 sistemi reattivi è stato considerato.

Metodi

Lo studio attraverso chimica computazionale con l'utilizzo di simulazioni DFT prevede inizialmente di creare dei file in formato .gjf attraverso il programma GaussView 6.0, file in cui sono contenute le geometrie iniziali. Ogni step della reazione è rappresentato da una o più geometrie che andranno successivamente ottimizzate in modo da ottenere delle strutture rappresentate da un punto stazionario sulla curva di potenziale: queste geometrie potranno essere degli intermedi di reazione nel caso in cui il punto stazionario sia un minimo, mentre potranno essere degli stati di transizione nel caso in cui il punto stazionario sia un punto di sella. Il processo di ottimizzazione è eseguito attraverso il programma Gaussian 16.0 con il quale, oltre all'ottimizzazione della geometria (che consente anche di ottenere i valori dell'energia totale per i vari step della reazione), si possono preformare delle analisi vibrazionali in modo da capire se le geometrie sono state correttamente ottimizzate (nel caso in cui le geometria siano correttamente ottimizzate si hanno modi di vibrazione tutti positivi per gli intermedi di reazione, mentre si ha un modo di vibrazione immaginario per gli stati di transizione) e così da ottenere le energie libere di Gibbs, che saranno fondamentali per capire quali sono le diverse rese della reazione per i vari sistemi. Queste informazioni sono tutte contenute in file .out che forniscono anche informazioni legate alle energie degli orbitali dei diversi atomi e alle cariche presenti sui diversi atomi. Una volta ottenute tutte le informazioni, i valori relativi di energia totale ed energia libera di Gibbs sono stati calcolati rispetto alle energie dello stato iniziale, così da avere importanti indicazioni sulle energie di attivazione. Le energie libere di Gibbs relative infine, sono state utilizzate per ottenere delle rappresentazioni energetiche che consentono un facile confronto tra i vari sistemi considerati.

Risultati

La reazione che è stata considerata in questo studio è riportata in Figura 5. Nel caso del secondo trial il gruppo OMe del substrato è stato sostituito con un atomo di idrogeno o con un gruppo NO_2.

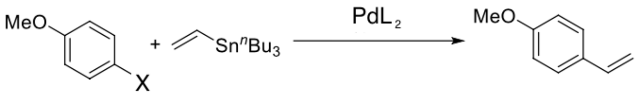

Figura 5 Reazione di Stille considerata nel primo trial

Secondo quanto riportato in letteratura, ed in particolare dal Prof. Imoto che ha contribuito a questo progetto, il ciclo catalitico della reazione inizia tra il catalizzatore PdL_2 e l'organoalogenato X-Ph-OMe, mentre l'organostannano Bu_3SnEt viene aggiunto in un secondo momento. Inizialmente si ha la dissociazione del catalizzatore bi-ligato PdL_2 in modo da impedire che ci siano ingombri sterici che possono inibire la reazione, andando a formare un catalizzatore mono-ligato PdL. In seguito si ha l'addizione ossidativa del substrato al nuovo complesso PdL, con inizialmente la formazione di un primo complesso (derivante dai due reagenti) che evolve successivamente a formare il complesso MeOPh−PdX−L dove OMePh, L, e Pd(II) sono allineati. Il prodotto dell'addizione ossidativa deve poi isomerizzare in modo da ottenere una geometria più stabile, scambiando la posizione del ligando L e dell'alogeno X. In seguito all'isomerizzazione, si ha l'aggiunta dell'organostannano che segna l'inizio della transmetallazione: attraverso interazioni catione Pd(II)-π tra le due specie si ha la formazione di un complesso con struttura quadrata planare in cui l'estremità $SnBu_3$ dell'organostannano migra verso l'alogeno e al contempo l'estremità vinilica migra verso l'atomo di palladio. Al termine della transmetallazione si è ottenuto un nuovo organostannano Bu_3SnX e il nuovo complesso Et−PdPhOMe−L con L, Et e Pd allineati. L'ultimo step è l'eliminazione riduttiva, in cui si ha l'accoppiamento tra le due estremità organiche del complesso al palladio per ottenere OMePhEt e la rigenerazione del catalizzatore mono-ligato PdL (necessario per procedere con ulteriori cicli catalitici). Il ciclo catalitico considerato è riportato in Figura 6.

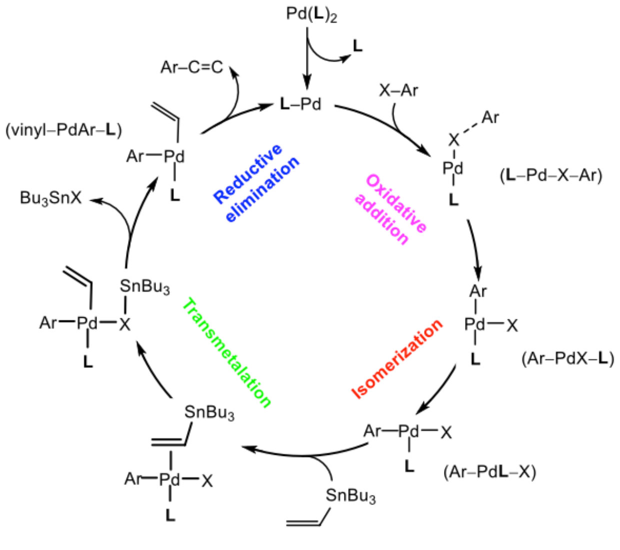

Figura 6 Ciclo catalitico considerato per la reazione di Stille

La specie più importante per la reazione è il catalizzatore. Come già detto, trattandosi in questo caso di un catalizzatore PdL_2 con dei ligandi voluminosi, sarà necessaria una dissociazione del catalizzatore in PdL così da facilitare il primo step della reazione. In seguito alle analisi effettuate, le lunghezze di legame tra l'atomo di palladio e gli atomi di arsenico o fosforo sono state ottenute: nel primo caso si ha una lunghezza di 2,3 Å, nel secondo caso si ha una lunghezza di 2,2 Å. Anche le cariche presenti sull'atomo di palladio in PdL sono molto importanti per ottenere informazioni sulla stabilità delle specie: valori simili sono stati ottenuti nel caso di ligandi contenenti arsenico e fosforo, mentre un trend crescente con $PhCF_3$ < Ph < PhOMe è stato osservato per i diversi gruppi sostituenti (con valori pari a -0,13/-0,12 per As o P, -0,16 e -0,19). Di fondamentale importanza è anche lo studio dei livelli energetici degli orbitali HOMO del catalizzatore che sono in grado di influenzare notevolmente le energie dell'addizione ossidativa. Se si considerano i gruppi PhOMe, Ph and $PhCF_3$ in catalizzatori con arsenico si hanno HOMO a -4,55 eV, -4,76 eV e -5,34 eV. Nel caso di ligandi con fosforo, I livelli associati agli HOMO per PhOMe, Ph, and $PhCF_3$ sono -4,74 eV, -4,80 eV, e -5,27 eV.

Lo studio delle geometrie ottimizzate per il substrato ha consentito di ottenere informazioni importanti legate alla reazione.

Per il primo trial (con il solo gruppo OMe come sostituente in posizione para rispetto all'alogeno), se si considera un atomo di cloro come alogeno si ottiene la minore lunghezza di legame tra l'atomo di carbonio in Ph e l'alogeno pari a 1,8 Å, un valore intermedio si ottiene se si considera un atomo di bromo con una lunghezza di legame pari a 2,0 Å, e una lunghezza di 2,2 Å si ottiene se si considera un atomo di iodio come alogeno (questi valori sono strettamente legati all'elettronegatività di Pauling per i vari alogeni, che cresce nell'ordine I < Br < Cl). Sono state inoltre ottenuti i valori di carica presenti sull'alogeno nel substrato a seconda di quale atomo si considera: nel caso di Cl si è osservata una carica pari a -0,04, nel caso di Br si è osservata una carica pari a 0,03, e nel caso di I si è osservata una carica pari a 0,13. Per i diversi substrati sono inoltre stati studiati i livelli energetici degli orbitali con valori diversi a seconda di quale alogeno si considera. Nel caso dei substrati è di fondamentale importanza il valore associato all'energia dell'orbitale σ^* tra l'alogeno e il carbonio in Ph poiché questo orbitale è quello direttamente coinvolto nell'addizione ossidativa. L'energia associata a σ^* per il cloro è pari a 0,75 eV, per il bromo è pari a -0,42 eV, e per lo iodio è pari a -1,09 eV.

Per il secondo trial, in cui il gruppo OMe è stato sostituito con H o NO_2 e l'atomo di alogeno è mantenuto invariato (in questo caso si tratta di I), differenti caratteristiche sono state ottenute. Nel caso della lunghezza di legame si hanno valori pari a 2,2 Å per H e pari a 2,1 Å per NO_2. Nel caso della carica presente sull'atomo di iodio si hanno valori pari a 0,11 per H e pari a 0,17 per NO_2. Nel caso dell'energia associata all'orbitale σ^*, valori pari a -1,08 eV e -1,61 eV sono stati ottenuti rispettivamente per H e NO_2.

I valori di energia libera di Gibbs relativa per i vari step della reazione, ottenuti nel primo trial, se si considerano ligandi contenenti arsenico sono riportati in Tabella 1, quelli relativi a ligandi contenenti fosforo sono riportati in Tabella 2 (i valori tra parentesi indicano la differenza di energia rispetto all'energia associata al primo complesso, lo stato precedente all'addizione ossidativa).

Tabella 1 Riassunto dei valori di energia libera di Gibbs relativa per i vari step della reazione al variare del ligando (contenente arsenico) e dell'atomo di alogeno (valori in kcal/mol)

L	PdL+L	1st complex	TS_{OA}	TS_{ISO}	TS_{TM}	TS_{RE}
Cl_As($PhCF_3$)$_3$	21,31	20,66	24,13 (3,47)	14,80 (−5,86)	13,60 (−7,06)	5,49 (−15,17)
Cl_AsPh_3	21,62	19,95	24,59 (4,64)	13,65 (−6,30)	12,88 (−7,07)	4,94 (−15,01)
Cl_As(PhOMe)$_3$	21,79	20,15	25,05 (4,90)	13,06 (−7,09)	14,13 (−6,02)	4,48 (-15,67)

Br_As(PhCF$_3$)$_3$	21,31	17,60	23,36 (5,76)	12,30 (−5,30)	16,18 (−1,42)	5,49 (−12.10)
Br_AsPh$_3$	21,62	18,35	24,32 (5,97)	10,59 (−7,76)	15,98 (−2,37)	4,94 (−12,11)
Br_As(PhOMe)$_3$	21,79	18,88	24,76 (5,88)	9,64 (−9,24)	16,92 (−1,96)	4,48 (-14,40)
I_As(PhCF$_3$)$_3$	21,17	14,07	21,22 (7,15)	7,45 (−6,62)	19,05 (4,98)	6,92 (−7,15)
I_AsPh$_3$	21,62	15,07	22,26 (7,19)	5,96 (−9,11)	18,67 (3,60)	6,23 (−8,84)
I_As(PhOMe)$_3$	21,79	15,15	21,50 (6,35)	5,43 (−9,72)	19,34 (4,19)	6,19 (-8,96)

Tabella 2 Riassunto dei valori di energia libera di Gibbs relativa per i vari step della reazione al variare del ligando (contenente fosforo) e dell'atomo di alogeno (valori in kcal/mol)

L	*PdL+L*	1st complex	*TS$_{OA}$*	*TS$_{ISO}$*	*TS$_{TM}$*	*TS$_{RE}$*
Cl_P(PhCF$_3$)$_3$	21,43	18,28	23,70 (5,42)	17,85 (−0,43)	17,34 (-0,94)	7,25 (−11,03)
Cl_PPh$_3$	21,82	20,17	25,00 (4,83)	15,92 (-4,25)	16,98 (-3,19)	7,17 (−13,00)
Cl_P(PhOMe)$_3$	22,17	20,65	25,56 (4,91)	15,25 (−5,40)	17,57 (-3,08)	6,55 (-14,10)
Br_P(PhCF$_3$)$_3$	21,43	17,79	23,76 (5,97)	14,47 (−3,32)	19,74 (1,95)	7,25 (−10,54)
Br_PPh$_3$	21,82	18,87	24,86 (5,99)	13,13 (-5,74)	19,98 (1,11)	7,17 (−11,71)
Br_P(PhOMe)$_3$	22,17	20,02	25,41 (5,39)	12,00 (−8,02)	20,79 (0,77)	6,55 (-13,47)
I_P(PhCF$_3$)$_3$	21,43	14,92	21,92 (7,00)	10,50 (−4,42)	23,77 (8,85)	8,81 (−6,11)
I_PPh$_3$	21,82	16,04	22,88 (6,84)	8,48 (-7,56)	22,40 (6,36)	8,56 (−7,48)
I_P(PhOMe)$_3$	22,17	16,49	22,51 (6,02)	7,93 (−8,56)	23,48 (6,99)	8,81 (-7,68)

I valori di energia libera di Gibbs relativa per il secondo trial sono riportati in Tabella 3.

Tabella 3 Riassunto dei valori di energia libera di Gibbs relativa per i vari step della reazione al variare del gruppo sostituente nel substrato e dell'atomo principale nel ligando (valori in kcal/mol)

L	*PdL+L*	1st complex	*TS$_{OA}$*	*TS$_{ISO}$*	*TS$_{TM}$*	*TS$_{RE}$*
NO$_2$_As(PhOMe)$_3$	21,79	16,11	19,93 (3,82)	2,75 (−13,36)	13,31 (−2,80)	0,93 (-15,18)
NO$_2$_P(PhOMe)$_3$	22,17	17,28	23,00 (5,72)	4,97 (−12,31)	17,15 (−0,13)	2,94 (-14,34)
H_As(PhOMe)$_3$	21,79	15,40	21,31 (5,91)	5,43 (−9,97)	18,67 (3,27)	6,25 (-9,15)
H_P(PhOMe)$_3$	22,17	16,66	22,48 (5,82)	7,90 (-8,76)	22,95 (6,29)	8,21 (-8,45)

Osservando i valori riportati nelle tabelle si possono fare numerose considerazioni.

Per quanto riguarda il primo trial sia nel caso dei ligandi contenenti arsenico che nel caso dei ligandi contenenti fosforo si sono notati dei trend analoghi: i valori di energia associati al primo complesso, allo stato di transizione dell'addizione ossidativa e allo stato di transizione dell'isomerizzazione decrescono al variare dell'alogeno nel substrato nell'ordine Cl < Br < I, il trend opposto è invece stato osservato per gli stati di transizione della transmetallazione e dell'eliminazione riduttiva (quest'ultima presenta valori quasi identici per Cl e Br). È evidente però, che i valori associati ai sistemi contenenti arsenico sono praticamente sempre minori rispetto ai valori associati ai sistemi contenenti fosforo. L'effetto dei diversi gruppi sostituenti legati all'atomo centrale nei ligandi appare trascurabile, con valori molto vicini in tutti i casi (un effetto leggermente maggiore si osserva solo sull'isomerizzazione).

Per quanto riguarda il secondo trial, la scelta di utilizzare ligandi contenenti arsenico rispetto a ligandi contenenti fosforo si mostra nuovamente vantaggiosa poiché consente di abbassare le energie associate ai vari step. L'utilizzo di NO$_2$ nel substrato consente di ottenere valori energetici più bassi rispetto ai sistemi del primo trial e anche rispetto ai sistemi in cui si è utilizzato H (questi sistemi presentano valori del tutto paragonabili a quelli ottenuti per il trial 1).

In entrambi i trial si è notato che gli step caratterizzati dalle maggiori barriere energetiche sono la dissociazione del catalizzatore, l'addizione ossidativa e la transmetallazione. Per questo motivo ci si dovrà concentrare sull'ottimizzazione di questi "energy demanding steps" in modo da massimizzare la resa della reazione.

Discussione

La dissociazione del catalizzatore è uno step che non dipende dal substrato considerato in quanto l'unica specie coinvolta in questo processo è PdL_2. Questo step è necessario poiché l'ingombro sterico causato dai ligandi voluminosi renderebbe la reazione pressoché impossibile. In tutti i sistemi considerati si sono ottenuti valori energetici per la dissociazione paragonabili con piccole differenze che dipendono unicamente da leggere variazioni nella forza di legame tra l'atomo principale del ligando e l'atomo di palladio. In particolare, si sono ottenuti valori minori nel caso dei ligandi contenenti arsenico (come si può notare dalla maggior lunghezza del legame Pd-As rispetto al legame Pd-P) e si è osservato una tendenza crescente nei valori energetici associati alla dissociazione del catalizzatore con $PhCF_3$ < Ph < PhOMe come gruppi sostituenti nel ligando.

L'addizione ossidativa è uno degli step più importanti della reazione poiché è solitamente accompagnata da valori di energia di attivazione molto elevati. Per studiare nel dettaglio questo processo è necessario prima considerare la stabilità del primo complesso, che è il punto di partenza per l'addizione ossidativa. La stabilità del primo complesso è strettamente legata alle cariche presenti sugli atomi principali dei due reagenti coinvolti (in questo caso il palladio del catalizzatore mono-ligato e l'alogeno del substrato). Non vi sono differenze significative nella stabilità al variare dell'atomo principale del ligando ma importanti differenze sono invece presenti al variare del gruppo sostituente nel ligando e del substrato. Nel primo trial, la carica presente sull'alogeno nel substrato dipende unicamente dal tipo di alogeno considerato, mentre i valori presenti sull'atomo di palladio sono in tutti e tre i casi negativi e simili: la stabilità sarà quindi maggiore nel caso di cariche positive sull'atomo di alogeno che siano in grado di bilanciare la carica negativa presente sull'atomo di palladio (in questo caso lo iodio è l'atomo di alogeno che riesce maggiormente a stabilizzare il primo complesso, come visibile nei valori di energia riportati in Tabella 1 e Tabella 2). Se si considera un substrato contenente iodio e un catalizzatore con un ligando contenente arsenico legato a $PhCF_3$ si ottiene una carica netta pari a zero, motivo per cui questa combinazione di specie porta al primo complesso più stabile. Nel secondo trial, la carica presente sull'alogeno nel substrato dipende invece dal gruppo sostituente che si considera in posizione para rispetto allo iodio: valori energetici simili sono stati ottenuti poiché la differenza di carica rispetto al primo trial non è significativa.

Per quanto riguarda l'addizione ossidativa vera e propria bisognerà considerare i livelli energetici degli orbitali nelle due specie coinvolte. Si avrà infatti l'attivazione del legame C-X del substrato in seguito al trasferimento di elettroni dall'orbitale HOMO del catalizzatore all'orbitale σ* presente tra l'atomo di carbonio e l'alogeno nel substrato. La facilità con cui questo trasferimento di elettroni si realizza, si traduce direttamente in valori di energia di attivazione minori per l'addizione ossidativa. Nel primo trial i gap minori sono ottenuti se si considera un substrato contenente iodio (poiché in questo caso l'energia del LUMO è la più bassa tra tutti i substrati), insieme ad un ligando contenente arsenico e gruppi elettro-donatori: in questo caso si ottiene un gap pari a 3,46 eV che porta all'unica energia di attivazione avente un valore minore rispetto all'energia richiesta per la dissociazione del catalizzatore, mostrando quindi una maggiore stabilità nell'addizione ossidativa rispetto alle altre combinazioni di specie. Nel secondo trial, non si ha praticamente alcun effetto se si considera H al posto di OMe nel substrato, mentre la scelta di utilizzare NO_2 porta ad un divario ancora minore (pari a 2,94 eV) che si traduce in una energia di attivazione per l'addizione ossidativa ancora inferiore. Queste considerazioni sull'energia di attivazione sono ulteriormente comprese se si considerano i valori delle costanti di Hammett per i diversi gruppi sostituenti in posizione para rispetto allo iodio nel substrato: è stato possibile ottenere una relazione lineare tra la differenza di energia per l'addizione ossidativa rispetto al primo complesso e il valore della suddetta costante (pari a -0,16 per OMe, 0 per H, e 0,74 per NO_2). Questa scoperta consente, a parità di reazione, di stabilire a priori quali energie di attivazione aspettarsi per l'addizione ossidativa conoscendo unicamente il valore della costante di Hammett per il sostituente (che è tabulato). Inoltre, considerando che la transmetallazione non è un rate determining step nel caso di ligandi contenenti arsenico, si possono ipotizzare a grandi linee i rendimenti della reazione unicamente conoscendo il substrato considerato.

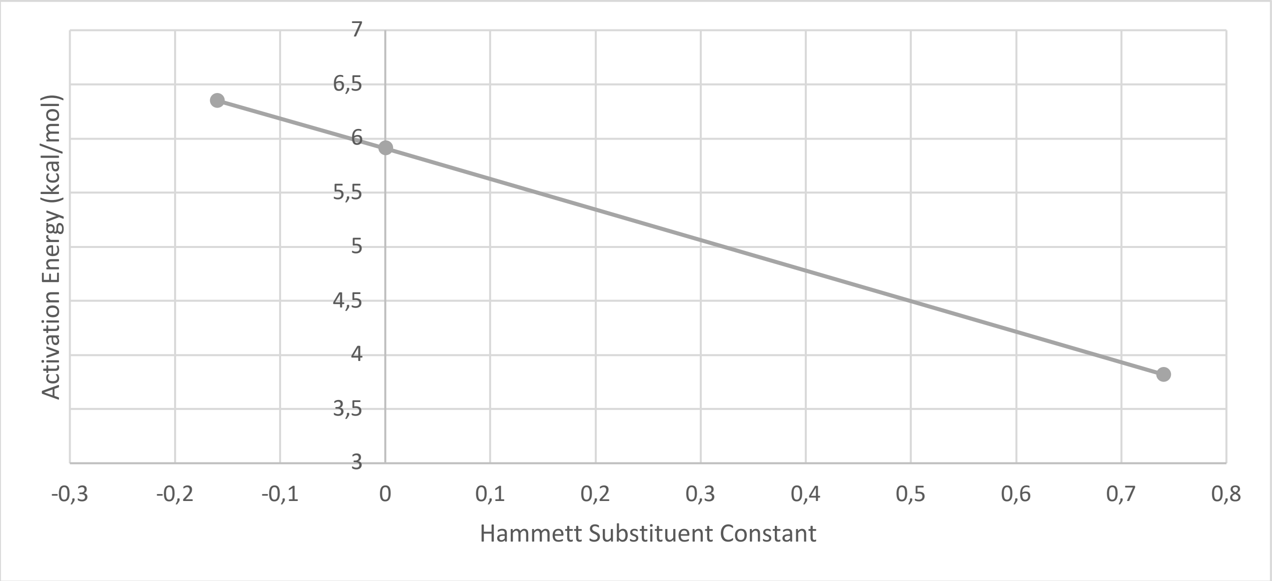

Figura 7 Grafico in cui sono mostrati i diversi valori di energia di attivazione (misurati dal primo complesso) in relazione alle costanti di Hammett dei sostituenti

Nell'isomerizzazione va considerato l'ingombro sterico delle specie coinvolte. Per questo motivo se si considerano ligandi contenenti arsenico, che portano a lunghezze di legame con l'atomo di palladio maggiori, si ottengono valori energetici inferiori rispetto a ligandi contenenti fosforo. Anche le forze dei legami andranno considerate poiché al crescere della forza di legame tra le specie coinvolte si avranno valori energetici superiori. Per questo motivo nel primo trial si hanno valori associati all'isomerizzazione che crescono nell'ordine I < Br < Cl per gli atomi di alogeno e nell'ordine $PhCF_3$ > Ph > PhOMe per i gruppi sostituenti nel ligando. Nel secondo trial, la presenza di un gruppo elettro-accettore come NO_2 al posto di un gruppo elettro-donatore come OMe, porta a legami più deboli come visibile dai valori di energia minori per lo stato di transizione dell'isomerizzazione (l'uso di H invece non porta ad alcuna variazione).

La transmetallazione è tra gli step più importanti per la reazione di Stille, insieme alla dissociazione del catalizzatore e all'addizione ossidativa. L'uso di ligandi contenenti arsenico è un metodo molto efficace per ridurre l'energia di attivazione di questo step in quanto si tratta di un processo influenzato principalmente da fattori sterici. Per questo motivo nel primo trial si hanno valori notevolmente minori nel caso di ligandi contenenti arsenico poiché si ottengono in questo delle lunghezze di legame Pd-As maggiori rispetto a quelle Pd-P: in questo modo si ha un efficace diminuzione delle repulsioni dovute ad effetti sterici. La tipologia di gruppo sostituente nel ligando che si considera non ha invece alcun effetto in quanto si sono ottenuti valori paragonabili per tutti e tre i gruppi sostituenti. Ha un importante rilevanza il tipo di alogeno che si considera nel substrato poiché la dimensione dell'atomo cresce nell'ordine Cl < Br < I e questo si traduce in un maggior ingombro sterico anche ad opera dell'atomo di alogeno, come visibile dal trend di valori al variare dell'alogeno. Anche la forza di legame tra lo stagno e l'alogeno e tra il palladio e l'alogeno va considerata: in questo caso si hanno delle forze del legame che crescono nello stesso ordine delle dimensioni degli alogeni con la forza dei legami Sn-X che cresce più velocemente rispetto alla forza dei legami Pd-X, confermando quanto osservato sulla sola base delle considerazioni geometriche. Nel secondo trial, queste forze di legame sono notevolmente influenzate dalla presenza di un gruppo elettro-accettore come NO_2 nel substrato che è in grado di abbassare ulteriormente l'energia di attivazione associata alla transmetallazione.

Infine, l'eliminazione riduttiva è sempre caratterizzata da valori energetici ridotti. Vi è tuttavia una grande dipendenza dal ligando e dal substrato considerati poiché si dovrà tener conto della diversa forza di legame tra le estremità vinilica (proveniente dall'organostannano) e organica (proveniente dal substrato) e l'atomo di palladio. Questo legame è influenzato dall'atomo principale e dai vari gruppi sostituenti nel ligando: legami più deboli sono presenti se si considerano ligandi contenenti arsenico e se si considera PhOMe come gruppo sostituente. Anche l'alogeno è in grado di influenzare l'energia relativa ottenuta per l'eliminazione riduttiva. Nel calcolo dell'energia relativa, infatti, si deve tenere in considerazione anche l'organostannanoalogenato ottenuto in seguito alla transmetallazione in cui la forza di legame X-Sn e quindi l'energia associata a questa specie, varia a seconda dell'alogeno considerato (nel caso dello iodio si ottengono infatti valori energetici superiori rispetto al cloro e al bromo). Nel secondo trial, l'utilizzo di NO_2 riesce ad abbassare enormemente l'energia associata all'eliminazione riduttiva poiché la presenza di un gruppo elettro-accettore (al posto di H o di un gruppo elettro-donatore), consente di indebolire significativamente la forza di legame tra il carbonio dell'estremità derivante dal substrato e l'atomo di palladio, portando ad avere un valore di energia di attivazione prossimo a zero e rendendo di conseguenza l'accoppiamento finale molto più facile.

Conclusioni

In questo progetto si sono considerati molti sistemi differenti (con diversi gruppi sostituenti e atomi principali nel ligando e con diversi gruppi sostituenti e atomi di alogeno nel substrato), così da capire in dettaglio l'influenza che i diversi catalizzatori e substrati hanno sulla reazione di Stille. Attraverso lo studio con chimica computazionale, i livelli energetici associati ai vari step per ogni sistema considerato sono stati ottenuti così da poter confrontare i diversi valori.

Il primo trial ha mostrato che i valori energetici ottenuti per i ligandi contenenti arsenico sono più bassi di quelli ottenuti per i ligandi contenenti fosforo. Sebbene l'addizione ossidativa sia un rate-determining step in entrambi i casi (dato che i valori sono soltanto marginalmente minori se si usa l'arsenico), l'uso di ligandi basati sull'arsenico abbassa notevolmente l'energia associata allo stato di transizione della transmetallazione, rendendola un rate-determining step unicamente nel caso di ligandi basati sul fosforo. L'uso di diversi atomi di alogeno legati al substrato ha portato a valori energetici per l'addizione ossidativa e l'isomerizzazione che crescono nell'ordine I < Br < Cl e valori energetici per la transmetallazione e l'eliminazione riduttiva che crescono nell'ordine opposto. Dai valori ottenuti per il primo trial è chiaro come l'energia di attivazione associata alla transmetallazione sia efficacemente abbassata dall'uso di ligandi contenenti arsenico, mentre l'energia di attivazione associata all'addizione ossidativa sia efficacemente abbassata dall'uso di substrati contenenti iodio e di gruppi elettro-donatori nel ligando.

Il secondo trial ha confermato quanto già ottenuto riguardo alla tipologia di atomo centrale nel ligando, con valori minori di energia se si considera l'arsenico. Inoltre, sostituendo il gruppo OMe del substrato con un gruppo elettro-accettore come NO_2, valori significativamente minori per le energie di attivazione sono stati ottenuti, con un effetto particolarmente importante sull’addizione ossidativa.

In conclusione, dopo aver studiato in dettaglio numerose tipologie di sistemi, si può stabilire che, dal punto di vista unicamente energetico, le migliori specie reattive da considerare per il catalizzatore sono i ligandi contenenti arsenico e gruppi elettro-donatori in posizione para rispetto ad esso, mentre per il substrato sono atomi di iodio come alogeni e gruppi elettro-accettori come sostituenti in posizione para rispetto all’alogeno.

Ulteriori studi saranno necessari per capire ancor più nel dettaglio i meccanismi coinvolti, così da ottimizzare ulteriormente le rese della reazione. Inoltre, attraverso lo studio di nuovi catalizzatori (che siano dotati di minori energie di dissociazione), nuovi substrati (che portino a minori energie associate all’addizione ossidativa) e nuovi organostannani (che portino a minori energie associate alla transmetallazione), i rendimenti della reazione di Stille potranno essere notevolmente incrementati aumentando così la diffusione di questa reazione già oggi molto utilizzata, ampliandone le applicazioni. Infine, uno studio accurato dei costi legati alle varie specie reattive e dell’impatto ambientale che l’uso di queste specie può avere, sarà richiesto per poter applicare su larga scala quanto ottenuto in questo studio simulativo.

1 Introduction

Functional polymers have gained a lot of interest in recent times due to the great variety of applications they are involved in. Many fields like biotechnology, consumer electronics and energy storage appliances rely on the use of functional polymers and a big impact on human society has already been experienced. The key aspects of this importance are the new efficient and scalable synthesis techniques and the great versatility that is typical of this kind of materials, making it quite easy for scientists to obtain new functional materials for specific use scenarios.

In the second half of last century new peculiar techniques have been discovered such as ROMP (ring-opening metathesis polymerization), a type of metathesis polymerization in which cyclic olefins react with an appropriate catalyst opening the ring structure to relief the strain (Figure 1); controlled Ziegler-Natta polymerization, a type of reaction in which alpha olefines react to obtain tactically controlled polymers through specific catalysts; ATRP (atom transfer radical polymerization), a type of living radical polymerization in which a transition metal catalyst creates an equilibrium with the starting species leading to low radical concentrations and a narrow molecular weight distribution [1].

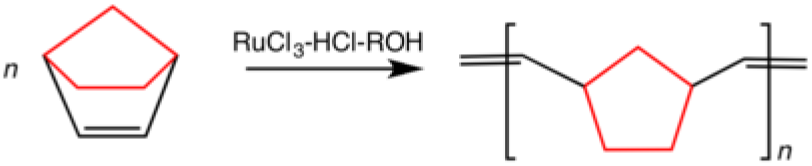

Figure 1 Typical ROMP reaction used to obtain polynorbornene

In the same years ATRP reactions were studied, new polycondensations based on transition-metal complexes that could catalyze the formation of carbon-carbon bonds were discovered. The most important reactions of this kind are Suzuki, Negishi, Heck and Stille coupling reactions. Stille reaction in particular, owes its importance to the high reaction yields and the compatibility with various functional groups and for this reason it is very used for the synthesis of organic functional materials. Nowadays the main application of Stille coupling reaction is the synthesis of conjugated semiconducting polymers that made it possible to obtain new technologies like organic photovoltaic solar cells, organic light-emitting diodes and field effect transistors. Because of its great versatility, Stille coupling reaction has also recently been studied in completely new fields like medical diagnosis and agrochemicals.

Stille coupling reaction refers to the reaction between an organic electrophile and an organostannane (sometimes called organotin) with a palladium catalyst in order to generate a new carbon-carbon single bond. A simple scheme for this reaction can be seen in Figure 2.

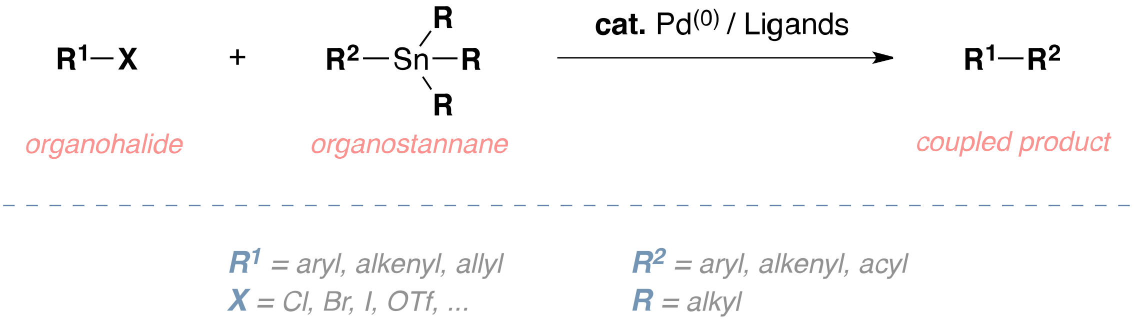

Figure 2 Simple Stille coupling reaction scheme [2]

The first evidence of this type of reaction was made by Eaborn in 1976. He prepared aryltin compounds by using a palladium complex to catalyze the reaction between bromobenzene and bis(tributyltin), as shown in Figure 3 [3].

$$\mathrm{ArBr} + \mathrm{Bu_3SnSnBu_3} \xrightarrow{\mathrm{Pd(PPh_3)_4}} \mathrm{ArSnBu_3} + \mathrm{ArAr} + \mathrm{BrSnBu_3}$$

Figure 3 Aryltin compounds synthesis as reported by Eaborn in 1976

A year later, in 1977, Kosugi and Migita, used a similar method to obtain the first carbon-carbon bonds from cross-coupling between arylhalides and organostannanes. An example is shown in Figure 4 [4].

$$\mathrm{ArX} + \mathrm{Bu_3SnR'} \xrightarrow{\mathrm{Pd(PPh_3)_4}} \mathrm{ArR'} + \mathrm{XSnBu_3}$$

Figure 4 Cross-coupling reaction of arylhalides and organostannanes as reported by Kosugi in 1977

After these successful experiments, Stille decided to conduct extensive studies on this type of reaction, that would later be named after him. His first studies considered the synthesis of ketones from acyl chlorides and organostannanes and after many experiments he was able to reveal many characteristics of this reaction. In a famous review written in 1986 he summarized all the results he had obtained and, after his detailed work, Stille coupling reaction quickly became one of the preferred methods for obtaining functional polymeric materials [5]. A few years later, in the early 1990s, Yu was able to obtain high molecular weight polymers from organo-ditin monomers and dihalide monomers through a Stille polycondensation process. Heteroaromatic diblock copolymers like PPT were synthetized as shown in Figure 5 [6].

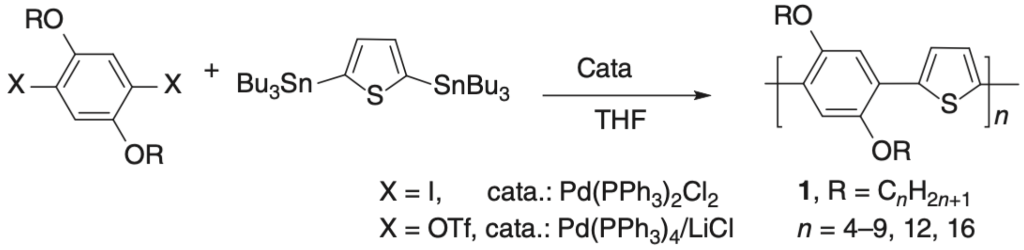

Figure 5 Synthesis process of PPT by Stille polycondensation

1.1 Reaction Mechanism

The first reaction that was studied by Stille was the coupling of benzoyl chloride and (tributylphenyl)stannane with $Pd(Bn)Cl(PPh_3)_2$ (where PPh_3 is triphenylphospine) as the catalyst. The catalysts are active Pd(0) species that are usually generated by the reduction of Pd(II) complexes by the organostannane at the beginning of the reaction. After studying this reaction, Stille proposed a particularly simple mechanism that consisted in various subsequent steps:

- In the first step the PdL_2 complex undergoes an oxidative addition with the organic electrophile substrate R-X to form $RPdL_2X$.
- This specie then undergoes a transmetalation with the $R^ISnR^{II}_3$ organostannane to form $RPdL_2R^I$.
- Usually, a trans-cis isomerization is then needed in order to make the final step possible.
- The final step is a reductive elimination that leads to the $R\text{-}R^I$ product and regenerates the PdL_2 active species.

This simplified cyclic mechanism that was first proposed by Stille can be seen in Figure 6. Even if this mechanism was widely accepted, it was immediately clear that there were a lot of variables that needed to be considered. In fact, the reaction is highly dependent on the conditions with catalysts, ligands, solvents, additives and temperature all playing a key role in the evolution of the reaction.

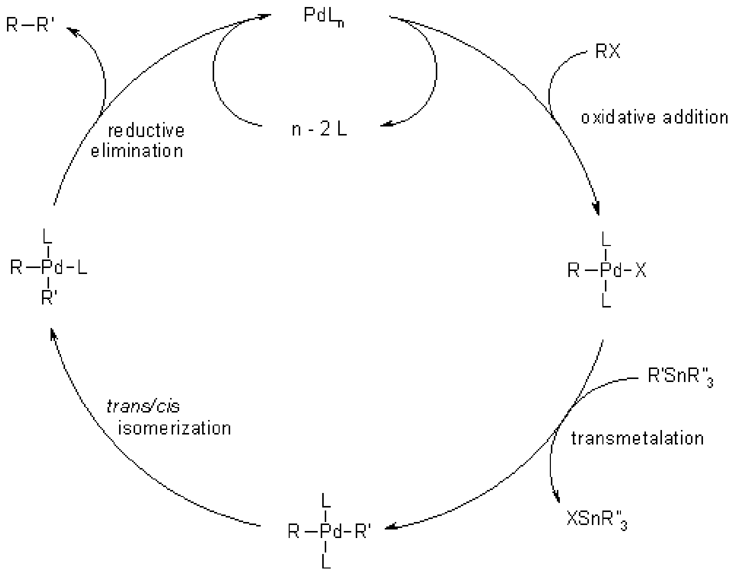

Figure 6 Simplified Stille coupling mechanism [7]

A lot of studies were conducted in order to understand in detail the main steps of the reaction. For example, it was found that the first step for C-X (with sp^2 carbon) has a three-center transition state that forms a cis-product which is rapidly isomerized to form the most stable trans product. But this is not always the result: if bidentate ligands are used instead of normal ligands the final product of this step can also be the cis-complex (a comparison of the two cases can be seen in Figure 7) [8].

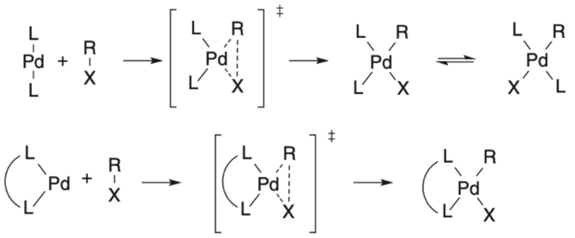

Figure 7 Oxidative addition step with normal ligands (upper) and bidentate ligands (lower) [9]

In some particular cases the cis-complex is the favored product. By studying the oxidative addition of chlorobenzene to $Pd(dippp)_2$ (dippp is 1,3-bis(diisopropylphosphanyl)propane) in dioxane, Milstein *et al.* have observed that the cis-product and the trans-product are formed in parallel pathways but in this case the cis-complex was the most stable one, both kinetically and thermodynamically [10].

The least known step of the reaction is the transmetalation step because it greatly differs from other similar palladium-catalyzed reactions. In this step the organostannane reacts with the Pd center leading to Sn-C bond cleavage and Pd-C bond formation. The main difference is that Sn-C bond is not as strong or polar as other metal-carbon bonds. In a very complete review published in 2004, Espinet and Echavarren pointed out that this step involves the electrophilic cleavage of Sn-C bond (S_E2 reaction) by the Pd(II) complex (derived from the oxidative addition) but this could also be seen as a ligand substitution (S_N2 reaction) on the Pd(II) complex [11]. These types of complexes are usually 16-electron, square planar and tetracoordinated complexes which can experience ligand substitution via two possible pathways. One pathway is associative, which would involve an 18-electron, trigonal bipyramidal intermediate with the substitution being defined by the ligand with the highest trans effect (that leads the lowest energy transition state). The other pathway is dissociative, which would involve a 14-electron, T-shaped intermediate with substitution being defined by the ligand with the highest trans influence capable of weakening the bond trans to it. [12]. The intermediate in the electrophilic cleavage considered in order to explain the S_E2 is a transition state that could be open or cyclic as can be seen in Figure 8. In his studies, Stille considers this intermediate to be open which explains why the transmetalation step is often very fast. The same open transition state is also observed in the coupling of organotriflates with $AsPh_3$ as ligand [13]. However, if the ligand is kept but the substrate is changed to an organohalide, the trans complex reacts with the organostannane through a cyclic transition state releasing the ligand, thus explaining the inverse dependence on the concentration of ligand on the reaction rate [14]. All these findings show the complexity of the transmetalation step, which may go through different pathways according to different reaction conditions.

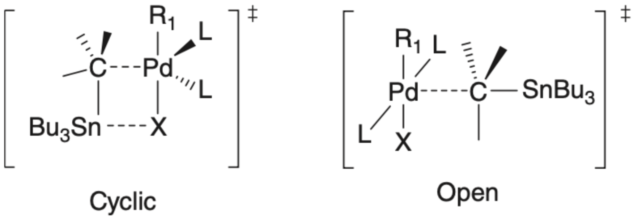

Figure 8 Cyclic and open transition states in transmetalation step

The reductive elimination step is needed in order to obtain the final product and also to regenerate the Pd(0) species that start the cycle. The obtained product from the transmetalation step needs to undergo a trans to cis isomerization in order to place the two species that will be coupled in cis position to each other. For this step apart from the simple isomerization of the four substituted groups bonded to palladium, a particular intermediate step was observed with a dissociation of the ligand before the transmetalation step to obtain a 14-electron T-shaped complex as shown in Figure 9. In this case ArPdXL (with L that is a PPh_3 group) was observed after the dissociation and by reacting with the organostannane, ArPdXL complex is obtained. This complex will later undergo a fast reductive elimination in order to produce the final Ar-R product [15]. The rate of this last step is dependent on many factors, such as the ligands considered, and sometimes it can be a slow step (for example with chelating ligands that make the isomerization more difficult).

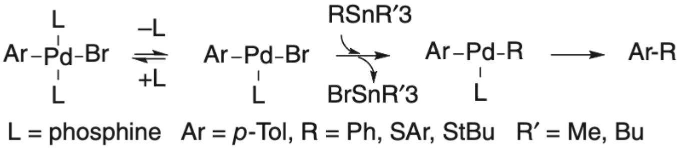

Figure 9 Reaction path after the ligand dissociation through a T-shaped complex

To better understand the complex mechanism of Stille coupling reactions a more complete representation has been proposed by Espinet *et al.* in 2015. This representation can be seen in Figure 10 [9].

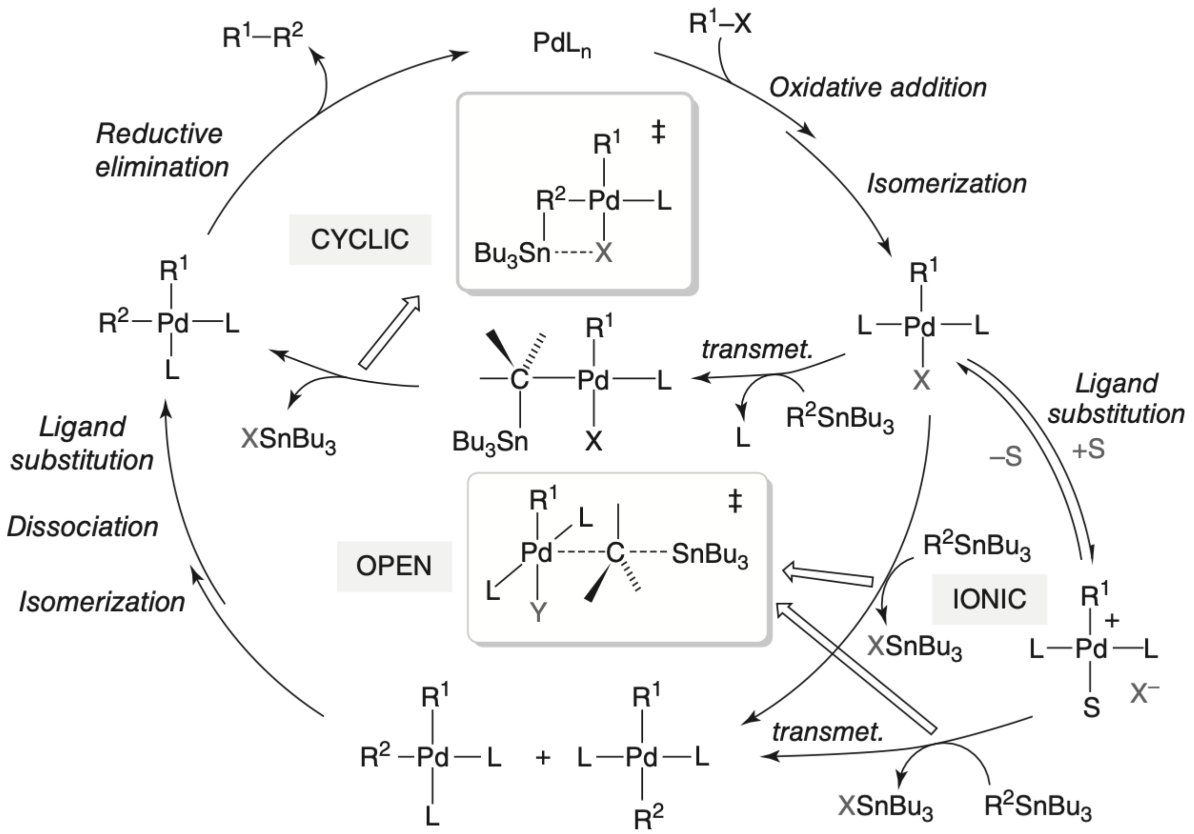

Figure 10 More complex mechanism for Stille coupling reaction

1.2 Influencing Factors

It is clear that the reaction mechanism for Stille coupling reactions is quite complex to comprehend and predict, especially considering the enormous amount of different chemical species that can be used for this type of reaction. Some examples of the diverse pathways have already been discussed in the previous paragraph, but a more detailed approach will be applied in this paragraph in order to show the experimental findings related to the different species involved.

1.2.1 Catalyst

One of the most important species is the catalyst which is considered. Many palladium compounds are used, both Pd(II) and Pd(0), but Pd(II) species need to be reduced with an appropriate reducing agent. $Pd(PPh_3)_4$ and $Pd_2(dba)_3$ are the most common palladium catalysts industrially used for the Stille coupling but $Pd_2(dba)_3$ is the most used one because of its superior stability against air and moisture [16]. The ligand is the most important element in the catalyst and accurate studies are necessary in order to obtain a proper catalytic system. The key aspects in this case are its size, bulkiness and electron-donating ability.

In their studies Yu *et al.* observed that if a Pd(II) catalyst is used, a stoichiometric excess of organostannane is needed so that a Pd(0) complex can be generated. They have also observed how different ligands influence the obtained polymer with a reactivity trend as $AsPh_3$ > P(2-furyl)$_3$ > PPh_3 [17]. Bulky phosphorous ligands are very common even if they are not that stable. The most common bulky phosphorous ligands are shown in Figure 11 and their use led to highly effective and highly selective reactions even at room temperature [18].

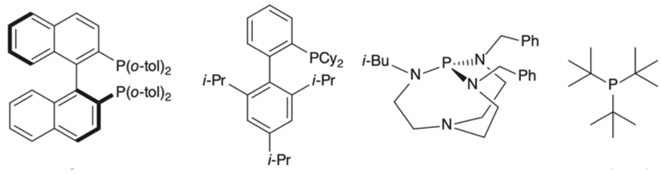

Figure 11 Structure of some common bulky phosphorous ligands

The great effectiveness of this kind of ligands is thought to be related to the stabilization of monoligated palladium intermediates due to the bulk of the phosphorous ligand. In the oxidative addition step, the monoligated Pd(0) species facilitate a nucleophilic attack to the Ar–X bond while the electron richness of the phosphorous provides efficient electron donation to the σ^* orbital of Ar–X, even if this bond has very low nucleophilicity. In the transmetalation step, a three-centered, 14-electron Pd(II) complex is stabilized by the ligand, making it easier for the organostannane, which has a low polarity Sn-C bond, to carry out a nucleophilic attack. In this case trans to cis isomerization is not needed in order to induce the reductive elimination as in the case of a tetracoordinated Pd(II) complex, further inducing reductive elimination. This mechanism has been proposed by Espinet in 2015 and it can be seen in Figure 12.

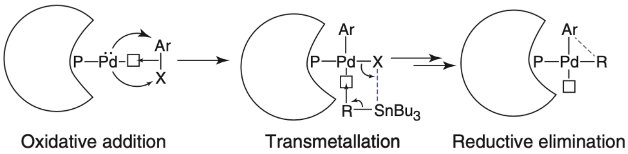

Figure 12 Mechanism of Stille coupling reaction assisted by bulky ligands [9]

The electronic effect of the ligands is almost as important as their size. It has been observed that the reduction of $Pd(OAc)_2(PPh_3)_2$ to Pd(0) complex is enhanced by electron-withdrawing groups at the para position of the aryl groups on the phosphorous [19]. It has also been observed that arsenic complexes, such as $Pd(dba)(AsPh_3)_2$, can be more stable than similar phosphorous complexes like $Pd(dba)L_2$ (where L is PPh3 or tri(2-furyl)phosphine (TFP)) due to their better electron-donating ability [20]. A kinetic study on a system consisting in iodobenzene (as substrate) and vinyltributyltin (as organostannane) with $Pd_2(dba)_3$ (as catalyst and palladium source) with different ligands has shiwb that the coupling rate when using TFP and $AsPh_3$ is three and four orders of magnitude higher, respectively, than that of PPh_3. It was deducted that there is an inhibitory effect on the cross-coupling by strong ligands, such as PPh_3 and TAP. Strong electron-donating ligands are also more easily oxidized deactivating the catalyst [21].

Even if the most common catalysts are usually phosphorous-based, a growing interest is associated to arsenic-based ligands. In a recent work, Prof. Imoto, confirmed that the use of arsenic ligands can be energetically preferable when compared to phosphorous ligands. Prof. Imoto's group performed experiments on Stille coupling reactions between iodine or bromine substituted substrates (but not chlorine substituted substrates because difficulties in the reaction have been encountered during the studies) and various palladium catalysts (various arsenic ligands have been studied but because of steric repulsion, only para substituted groups have been considered), and they obtained different yields of products depending on substrates and catalysts. They performed experimental works mainly on OMe-Ph-I substrates, but they also considered other substituted groups where OMe is replaced. According to the obtained results, higher yields are observed when NO_2 is used instead of OMe. By using DFT calculations it was found that arsenic ligands lead to significantly lower energy values for the transmetalation step when compared to phosphorous ligands. They also found that electron-donating groups lead to smaller activation energies for the oxidative addition (while electron-withdrawing groups have no effect) and for the transmetalation (while electron-withdrawing groups lead to higher values for this step) [22].

1.2.2 Substrate

Even if the role of the substrate seems not as important as that of the catalyst, the final product of the Stille coupling reaction is highly dependent on the chosen substrate. The most common substrates are organic halides with the organic part (usually an aromatic group) that will be coupled with the group from the organostannane after the reductive elimination and the halogen atom that can greatly influence the pathway of the reaction by modifying the energy levels of the transition states. In a very interesting study, Lam *et al.* have studied the way different halogen atoms can influence the oxidative addition step of the Stille coupling reaction. They found that weaker C-X bonds in an aryl halide substrate lead to lower energy gaps for this step. They also considered different types of aryl halides (with electron-donating or electron-withdrawing groups in para position) and found out that electron-withdrawing groups lead to lower oxidative addition barriers due to the lower σ^* and π^* orbitals energy in C-X, stabilizing the oxidative addition transition state [23].

The influence of the substrate is not only present on the oxidative addition step but also on the transmetalation step. In particular, the effect of the leaving halogen from the transmetalation transition state has been confirmed: more electronegative halogen atoms tend to lower the activation barrier for the transmetalation step, while less electronegative halogen atoms tend to make the transmetalation more difficult. The observed behavior is consistent with the measurements of the bond strengths for Sn-X and Pd-X, with Sn-X bond strength that increases faster than the Pd-X bond strength going down in the halogen column of the periodic table [24].

1.2.3 Additive

Usually, inorganic salts are used as additives in Stille coupling reactions. The most common ones are LiCl, CuI, KF and CsF with an action that is greatly dependent on the reaction conditions.

LiCl is a very common additive used since the reaction was first studied. By using LiCl and other bromide and iodide salts the coupling is accelerated with a transformation of species like triflato complexes into chloro complexes (this is the typical reaction that was studied by Stille) that can then enter the catalytic cycle [25]. But this accelerating effect is not always present: for example, in the coupling of vinyl triflate and aryl tributylstannane with $Pd_2(dba)_3$ as catalyst, LiCl was found to retard the reaction when TFP or PPh_3 is used as ligand, but accelerate the reaction when $AsPh_3$ is used. This behavior is thought to depend on the oxidative addition step that can be promoted by the additive if the catalyst is not very nucleophilic while it can be retarded if the catalyst is nucleophilic meaning that the step has already taken place [21].

CuI is another salt that enhances coupling in Stille reaction through a mechanism known as "copper effect". By using CuI as additive in the palladium catalyzed coupling of iodobenzene and vinyltributyltin in dioxane, an influence on the kinetics was observed: a more than 100-fold rate increase was observed with a strong ligand, such as PPh_3, and almost no difference was observed with a soft ligand, such as $AsPh_3$. The proposed mechanism considers CuI as a scavenger for the free ligand, especially for strong ligands, which are able to inhibit the transmetalation step. In addition, it was observed that in very polar solvents such as NMP and in the absence of strong ligand, a Sn/Cu transmetalation takes place to produce an organocopper species, which more easily can undergo transmetalation to the Pd(II) complex. It was also observed that a stoichiometric ratio of Pd:L:Cu=1:4:2 (where L are the ligands) leads to the best results with enhanced reaction rate and yield. Further CuI additions decrease the yield, because too much CuI removes ligand from the active catalytic species, thus reducing the catalyst stability [26].

Additives like KF and CsF are Lewis bases that can activate the tin compounds due to their fluorophilicity. It is suggested that a pentavalent tin complex with a higher reactivity in the transmetalation step is formed thanks to the coordination of F^- to tin compounds [16]. Other bases such as NaOH or amines have been studied because of their role in stabilizing tin compounds with coordination but the observed efficacy is way lower than fluorine salts [27] [28].

1.2.4 Solvent

The most used solvents in Stille reactions are benzene, toluene, xylene, THF (or tetrahydrofuran), dioxane, chloroform, DMF (or dimethylfluoride) and NMP (or *N*-methylpyrrolidone). The choice of the solvent is really important because it can strongly influence the reaction due to the wide range of solubility towards organic molecules and polarity. The solvent does not only solubilize the reagents, but it can also take part in the reaction by dissociating the ligand or by acting as a ligand to the palladium catalyst. For example, it was observed that, in the coupling of PhI with tributyl(vinyl)tin and $Pd(dba)(AsPh_3)_2]$ as catalyst in DMF, the transmetalation step takes place in the solvent-coordinated trans-$PdPhI(AsPh_3)(DMF)$ complex [29]. Moreover, the solvent can affect the configuration of the final product based on its polarity and coordinating ability.

In polymerization by Stille coupling the solvent is even more important because it must also keep the growing polymer chain in solution as long as possible in order to obtain polymers with high molecular weight and narrow polydispersity. For example, DMF is highly polar and can coordinate to the catalyst center as ligand, but many of the commonly used polymers show low solubility in DMF. On the other hand, the most used polymers in this reaction show good solubility in toluene, which is less polar and coordinating. A mix of the two solvents with a toluene/DMF 4:1 ratio can provide benefits of each individual solvent while avoiding the disadvantages, enabling a good yield of high molecular weight polymers [17].

1.2.5 Temperature

Even though Stille coupling reactions usually take place at temperatures higher than room temperature, heating plays a less important role than the other parameters already discussed. Temperature generally does not change the reaction pathway, but it can affect the Stille coupling in many aspects. For example, increasing the temperature may improve the reaction rate and perhaps the solubility of the species. But it can also lead to side reactions and decomposition if the reagents are not stable against heat, enormously decreasing the reaction yield. However, high temperature above 100 °C is usually employed for polymerization because it increases solubility and reaction rate without affecting stability.

In order to optimize the reaction, lower reaction temperatures, and shorter reaction times are desirable to save resources. Apart from more complex systems that can react at room temperature [27], new ways of heating have been studied in order to increase heating efficiency. Microwave irradiation has been used in the Stille reaction in order to reduce the reaction time to just a few minutes, with only a limited reduction in yield. In this case, energy is directly transferred to the reactants and the temperature of the whole volume rises at the same time [30].

1.3 Applications of Stille Coupling Reactions

Stille polycondensation is an ideal reaction for the synthesis of functional polymeric materials due to its great versatility. One of the first industrial applications has the polycondensation of PPT (or poly(phenylene-tiophene)) which showed nonlinear optical behavior and liquid crystal properties [31]. The possibility of obtaining fine-tuned properties like fusibility, solubility and characteristic temperatures with Stille polycondensation led to a large diffusion of such processes in many different applications.

1.3.1 Organic Photovoltaic Polymers

Stille polycondensation is broadly used to produce the donor-acceptor semiconducting polymers that are needed in organic photovoltaic solar cells. Polymer-based solar cells (or PSCs) can convert the solar energy into electricity and due to the potential low cost, the extreme lightness, the potential in flexible devices and the high volumes of production that are obtainable, the interest in this application is high. The most common device is the bulk heterojunction in which donor and acceptor materials are mixed in order to obtain a biphasic interpenetrating network between two electrodes. Usually, the acceptor material derives from fullerene, and the donor material is a conjugated polymer, but many studies are conducted in order to substitute fullerene with another polymer.

Acceptor polymeric materials are developing rapidly because of lower costs compared to fullerenes and easier tuning of physical properties. The required properties for this type of material are:

- Strong and broad adsorption within the visible range;
- Well matched energy levels with the used donor polymers;
- Good solubility and miscibility with the used donor polymers so that a bulk heterojunction structure is obtained;
- High electron mobility for efficient charge transport.

Perylene-diimides (or PDI) are studied as promising acceptor materials due to their high electron mobility and strong intermolecular π-interaction. A first study on PSCs with PDI as acceptor material showed that low molecular weight and low dispersity are obtained and that a relatively high electron mobility is reached ($1,3x10^{-2}$ $cm^2V^{-1}s^{-1}$) [32]. By mixing PDI with some other polymers, such as DTT and DIO, the power conversion efficiency (or PCE) could be raised from around 1% to almost 3,5%. DTT was found to improve the mixing of acceptor and donor polymers while DIO was found to promote the crystallization of the donor polymer [33]. Another possible acceptor polymer derives from naphthalene-diimide (or NDI) monomer, and the first studies showed a high electron mobility of around 0,45-0,85 $cm^2V^{-1}s^{-1}$ [34].

Donor polymers play an important role in bulk heterojunction solar cells because they are the component that adsorbs light generating an electrical current. The required properties for this type of material are:

- Low band gap in order to adsorb as much solar energy as possible;
- Well matched energy levels with the used acceptor polymers;
- Good solubility and miscibility with the used donor polymers so that a bulk heterojunction structure is obtained.

The first studies focused on PPV based polymers, but large band gaps and low photocurrents were obtained, so this type of polymer was abandoned. The interest moved to polythiophenes like P3HT or BDT. By using this class of polymers excellent solar performances were obtained with high molecular weights due to their good solubility. In 2010 a PCE of 7,4% was obtained and by further tuning of the structure a record PCE of 9,2% was obtained a few years later [35]. Benzothiadiazole (or BT) is also very interesting for PSCs applications. In some recent studies, the use of BT derived DFBT combined with PDTP and mixed with a polythiophene like P3HT, led to a PCE of 10,6% because the complementary nature of the different polymers made it possible to adsorb throughout the visible and n-IR region [36].

A particular class of polymers for PSCs has a special structure made of donor-acceptor alternating copolymers. This type of polymers has electron-rich and electron-deficient moieties that alternate along the polymer chain. In this case the HOMO and LUMO energy levels are mostly influenced by the HOMO energy level of the donor and the LUMO energy level of the acceptor, so that the energy levels of the final polymers can be modified by changing the single building blocks separately. These building blocks need to have proper electron-donating or electron-accepting capabilities, available sites for side chain functionalization and a conjugated polymer propagation ability.

1.3.2 Organic Light Emitting Diode Polymers

The electroluminescence of organic materials was firstly observed in anthracene crystals. This characteristic was more recently used in order to manufacture OLED (organic light emitting diode)-based displays, a technology that is very common nowadays. The structure of an OLED device is usually characterized by an emitting layer between two electrodes: after an external electric field is applied, electrons and holes are injected from the electrodes into the middle layer, where excitons are formed. The excitons then undergo recombination to excited states which generate radiative emission after decaying. In order to obtain high efficiency and good light output, the injection and the transport of electrons and holes needs to be accurately planned. For this reason, a multilayer structure is usually used with the most common ones made of a transparent and conductive indium tin oxide anode, a hole transporting layer, an emissive layer, an electron transporting layer and a metal cathode [37].

The development of new materials can tune the emission color, the electron affinity and the charge mobility of the OLED but the performances usually depend on energy level matching between the layers. The efficiency of OLEDs is usually measured through EQE which indicates the ratio of emitted photons over the charges injected into the material. In order to obtain high effective OLEDs it is very important to control the reaction conditions and the impurities concentration so the Stille coupling is a very effective production method for this devices.

PPV has been widely used for OLEDs and, even if the main production method is thermal decomposition or photoirradiation on metal electrodes, very precise functionalization can be carried out by Stille coupling reactions, making the material more soluble or modifying the characteristic emission wavelength. Other materials consist in pyridine derivatives (that can be coupled with PPV to increase EQE [38]) and thiophene-based conjugated polymers. For example, CPDTs that derive from thiophene have been considered in the realization of OLEDs: by using dithiophenesilole and oligothiophene monomers to produce conjugated polymers (with $CuCl_2$ additive in THF solvent in order to obtain the best results), multilayer devices with yellow emission and high luminance of 500 cd m^{-2} at 13 V were obtained [39].

1.3.3 Organic Field Effect Transistor Polymers

Organic field effect transistors (or OFETs) are another very important application of organic semiconducting materials. These devices are flexible, processable in solution, cheap to produce and lightweight. A typical FET device is made of a substrate, a gate electrode, a dielectric insulating layer, a source, a semiconducting material and a drain electrode. When a bias is applied to the gate electrode an electric field is generated at the polymer-insulator interface, which shifts the HOMO and LUMO energy levels of the polymer. A conducting channel is formed between source and drain electrode and charge carriers can flow through the polymer to the electrodes in order to generate current. For this type of application semiconducting polymers with high carrier mobility are required (correlated to high crystallinity). Its energy levels should match the work function of the electrodes and a good chemical and thermal stability is required.

Thiophene-based polymers have been one of the first considered polymers for FET applications. By using P3HT and fused thiophene via Stille polycondensation, discrete mobilities around 0,2-0,7 $cm^2V^{-1}s^{-1}$ and good stability were obtained if compared to just P3HT-based polymers [40].

IID has also been used for FET applications with side modifications required in order to improve the solubility of the polymer. By studying IID-based polymers high hole mobilities of up to 3,62 $cm^2V^{-1}s^{-1}$ were obtained by considering a side branching with the shortest π- π distance [41]. An evolution of this application made it possible to obtain piezoelectric transistors with high pressure sensitivity, fast response time, high stability and low power consumption for electronic skin [42].

Diketopyrrolopyrrole (or DPP) monomer has been recently studied because by incorporating siloxane side chains, ambipolar charge transport properties have been observed. Hole mobilities of up to 3,97 $cm^2V^{-1}s^{-1}$ and electron mobilities of up to 2,20 $cm^2V^{-1}s^{-1}$ have been obtained [43].

1.3.4 Nonlinear Optical Polymers

Nonlinear optics describe the behavior of light in a nonlinear media. In this type of media, the dielectric polarization P responds nonlinearly to the electromagnetic field E of intense light, affecting its behavior (phase, frequency, amplitude, …). The behavior depends on the values of the -nth order susceptibilities. Nonlinear optical materials can be used in information technology applications where light is used to process, transport and store data. The required properties for nonlinear optical materials are low optical losses (either from adsorption or scattering), chemical and optical stability, easy processability and fast response times.

These polymers are very promising for photonic applications because they exhibit a linear electro-optic effect, making it possible to control the refractive index of the media through an applied external E. In order to obtain these materials, nonlinear optical groups need to be contained in the polymer usually through grafting to the side chains or to the backbone. The required behavior is obtained only if the chromophores are oriented by an external electric field at high temperatures and then frozen so that the orientation is kept.

Functional polyimides have been synthetized through Stille polycondensation because traditional methods could affect the stability of the specific groups needed for nonlinear optical applications. Polyimide derivatives with amino chromophore side chains have been produced with density of chromophores usually higher than 50%, with values depending on the considered polymer backbone. It has been found that the density of chromophores has an inverse relation with the orientational stability (and so with the nonlinear optical properties): the more chromophores are loaded the weaker the electro-optic effect is [44].

Another interesting class of nonlinear optical polymers are photorefractive (or PR) polymers. The photorefractive behavior describes a change in the refractive index when the intensity of light varies, under the illumination of low-power lasers. Such materials can be used to record and store optical information, for example holograms. These polymers are usually characterized by photoconductivity and electro-optic effect and are made of a photocharge generator, a charge transporter, a charge trapping center and a nonlinear optical chromopohore. PPT derivatives have been used to obtain PR polymers via Stille polycondensation with a side chain containing an electron-rich amino unit and an electron-withdrawing tricyanodihydrofuran group acting as a chromophore (due to the created strong dipole), and a conjugated backbone adsorbing visible light, acting as a charge generator and transporter [45].

1.3.5 Other Applications

Stile polycondensation can also be used for other more niche applications such as sensor materials due to significant and reproducible properties like luminescence and conductivity. Analyzing units are attached into the polymer so that minor perturbations can be sensed. An example is the synthesis of polythiophene-based sensor polymers where the chelating cyclophane receptor chains grafted to the polymer chain could form specific complexes if traces of metal ions are present. The formed complexes would cause a change in the electrical properties of the material [46].

Liquid crystals are another class of materials that can be synthetized via Stille polycondensation and their use is mainly in electronic display technologies. Its properties are between those of solids and liquids: a liquid crystal can flow like a liquid, but its molecules can organize like a crystal. An example of liquid crystals are some conjugated polymers that derive from PPT or phenylene-thiophene via Stille polycondensation where modifications of the side chains can lead to different physical properties and liquid crystal moieties are present [47].

Recently, hybrid organic–inorganic materials have attracted significant interest as functional materials that can be produced by Stille polycondensation. One important class is metal-containing polymers where heavy metal atoms form an integral part of the backbone or side chains of the polymers. In this case interesting opto-electronic properties are observed due to the mixing of singlet and triplet excited states, high phosphorescence yields, and relatively long emission [48].

1.4 Premise

In this work, Stille coupling reactions will be studied through computational chemistry analysis (density functional theory or DFT) to find out what are the key factors that can influence the coupling reaction between the organohalide substrate and the organostannane (this will be always the same, a (tributylstannyl)ethylene molecule).

In the first trial different tertiary ligands based on phosphorous or arsenic are bonded to palladium: each atom of phosphorous or arsenic will be bonded to palladium and to three identical groups that will be phenyl (or Ph), (para-trifluoromethyl)benzene (or $PhCF_3$) or (para-anysil)benzene (or PhOMe), so that apart from the common $AsPh_3$ and PPh_3 tertiary ligands, other tertiary ligands have been considered both electron-poor (CF_3 containing) and electron-rich (pAn containing). At the same time, also the substrates will change because different halogen atoms bonded to anisole will be considered: in this case iodine, bromine and chlorine will be bonded in para position.

The iodine system has been recently studied by Prof. Imoto, who considered a OMePhI substrate with many different catalysts. Prof. Imoto then mainly focused on four catalysts for this system, the ones which exhibited the highest reaction yields: $AsPh(OMe)_3$, $AsPh_3$, $AsPh(CF_3)_3$ and PPh_3. In this work, the data used for iodine systems come from Prof. Imoto's unpublished work and all the considerations that will be made for such systems derive from a study of the results of the study that Prof. Yumura has kindly provided me.

The novelty of this thesis project, when compared to previous works, is related to the amount of combinations between different substrates (with changing halogens) and different catalysts (with changing substituent groups) that have been considered in order to better understand what are the key factors that influence Stille coupling reactions.

In the second trial, only (para-anysil)benzene substituent groups will be considered in the tertiary ligands (both with phosphorous and arsenic), while the substrates will be (p-iodo)nitrobenzene and iodobenzene. This choice of these species comes from the experimental findings by Prof. Imoto [22], who found that higher production yields have been obtained if NO_2 is considered instead of OMe for the substrate. These reaction yields have also been found to be higher if iodine is considered instead of bromine and chlorine. It is also interesting to consider an unsubstituted iodobenzene molecule in order to see if the absence of a group in para position (and the subsequent lack of steric hindrance) can influence the reaction (the results for these systems come from the work of Prof. Yumura). The different considered substrates will show that not only the considered halogen atoms play a key role in the reaction but also the substituent group can have a strong influence.

2 Methods

2.1 Theoretical Basis

2.1.1 Density Functional Theory (DFT)

Density functional theory is nowadays one of the most used computational methods for molecular electronic structure calculations. The fundamental idea is that the energy of an electronic system is related to the electron probability density ρ. Systems with N_e electrons have a $\rho(r)$ that indicates the total electron density in a certain r point in space. The electronic energy E is treated as a functional of the electron density and is indicated by $E(\rho)$ (so that for a given $\rho(r)$ there is a single corresponding energy).

A lot of advantages are present in DFT methods: this approach uses a single three-dimensional function for an N_e electron constituted molecule, the electron density (way easier than wavefunction approaches where functions have $3N_e$ dimensions and many constraints) and such electron density has no cusps because it does not involve inter-electron distances explicitly (unlike wavefunction approaches).

This approach relies on a certain number of assumptions with the most important one being that the electron density determines the properties of the molecule, and that the energy is correctly given by a variation principle. This assumption was formally proved and summarized in the Hohenberg-Kohn existence theorem. This theorem states that the ground-state energy and all other ground-state electronic properties are uniquely determined by the electron density. The Hohenberg-Kohn existence theorem confirms that the ground-state energy of a molecule can be written as a functional of the ground-state electron density (with the electron-electron potential energy functional given by the sum of a classical Coulombic contribution and a quantum-mechanical contribution):

$$E(\rho) = T(\rho) + V_{ee}(\rho) + \int \rho(r) \upsilon(r) dr$$

Because of this theorem it is sufficient to know the ground-state electron density in order to determine any property of a molecule. But in this case the electron density needs to be constructed by finding the wavefunctions from Schrödinger equation. In order to proceed, the Hohenberg-Kohn variational theorem is used. This theorem states that for a trial density function $\rho'(r)$, the energy functional $E_0(\rho')$ cannot be less than the true ground-state energy of the molecule. The variation of electron density is subject to a constraint:

$$\delta \left\{ E(\rho) - \mu \int \rho(r) dr \right\} = 0$$

For this reason, the ground-state electron density must satisfy:

$$\mu = \upsilon(r) + \frac{\delta E_{HK}(\rho)}{\delta \rho(r)}$$

The next step in DFT calculation is the derivation of a set of one-electron equations from which the electron density ρ can be obtained. In order to generate a solvable set of equations, a hypothetical reference system was considered. This system is characterized by N_e non-interacting electrons in an external potential $\upsilon_{ref}(r)$ selected so that the electron density of the reference system, $\rho_{ref}(r)$, is identical to the true electron density, $\rho(r)$. The hamiltonian for the reference system is:

$$h_{ref} = \sum_{i=1}^{N_e} h_i^{KS}$$

With $h_i^{KS} = -\frac{\hbar^2}{2m_e}\nabla_i^2 + \upsilon_{ref}(r_i)$ and with the one-electron Kohn-Sham orbitals Ψ_m^{KS} that are eigenfunctions of the one-electron Kohn-Sham hamiltonians h_i^{KS}:

$$h_i^{KS}\Psi_m^{KS}(i) = \varepsilon_m^{KS}\Psi_m^{KS}(i)$$

The Slater determinant that represents the ground-state wavefunction of the reference system is:

$$\Psi_{ref} = \left\|\varphi_a^{KS}(1)\varphi_b^{KS}(2)\ldots\varphi_z^{KS}(N_e)\right\|$$

With the φ^{KS} indicating the Kohn-Sham spinorbitals, each of which is a product of a Kohn-Sham spatial orbital Ψ^{KS} and a spin state (α or β).

The total energy functional for the actual molecule is written in terms of the reference system functional and a correction term:

$$\begin{aligned} E(\rho) &= T(\rho) + V_{ee}(\rho) + \int \rho(r)\upsilon(r)dr \\ &= T_{ref}(\rho_{ref}) + J_{ref}(\rho_{ref}) + \int \rho(r)\upsilon(r)dr \\ &+ \left\{T(\rho) + V_{ee}(\rho) - [T_{ref}(\rho_{ref}) + J_{ref}(\rho_{ref})]\right\} \end{aligned}$$

The reference system has been created to have the same electron density as the real system so that:

$$E(\rho) = T_{ref}(\rho) + J(\rho) + \int \rho(r)\upsilon(r)dr + E_{XC}(\rho)$$

With $E_{XC}(\rho) = T(\rho) + V_{ee}(\rho) - [T_{ref}(\rho) + J(\rho)]$ indicating the exchange-correlation energy. Now the expression for μ can be written again:

$$\mu = \upsilon(r) + \frac{\delta E_{HK}(\rho)}{\delta\rho(r)} = \upsilon_{eff}(r) + \frac{\delta T_{ref}(\rho)}{\delta\rho(r)}$$

With $\upsilon_{eff}(r) = \upsilon(r) + \frac{\delta J(\rho)}{\delta\rho(r)} + \frac{\delta E_{XC}(\rho)}{\delta\rho(r)}$. The functional derivatives of *J(ρ)* and E_{XC} are given by:

$$\frac{\delta J(\rho)}{\delta\rho(r)} = j_0 \int \frac{\rho(r')}{|r - r'|}dr'$$

$$\frac{\delta E_{XC}(\rho)}{\delta\rho(r)} = \upsilon_{XC}(r)$$

The effective potential is then expressed by:

$$\upsilon_{eff}(r) = \upsilon(r) + j_0 \int \frac{\rho(r')}{|r - r'|}dr' + \upsilon_{XC}(r)$$

The equation for μ is the same that would be obtained considering free electrons moving in an external potential υ_{eff}. For this reason, the correct form for the electron density is obtained by substituting $\upsilon_{ref}(r)$ with $\upsilon_{eff}(r)$. To find the electron density minimizing the energy functional the Kohn-Sham equation needs to be solved:

$$\left\{h_1 + j_0 \int \frac{\rho(r_2)}{|r_1 - r_2|}dr_2 + \upsilon_{XC}(r_1)\right\}\Psi_m^{KS}(r_1) = \varepsilon_m^{KS}\Psi_m^{KS}(r_1)$$

With $h_1 = -\frac{\hbar^2}{2m_e}\nabla_1^2 + \upsilon(r_1)$.

The most difficult passage is to find the functional $E_{XC}(\rho)$ and so the function $\upsilon_{XC}(r)$. In the years many approximate forms for these terms have been proposed and many others are currently still being studied. One of the most important approximations considers the functional as split into two terms, one exchange functional (which represents the exchange energy) and one correlation functional (which represents the correlation energy):

$$E_{XC}(\rho) = E_X(\rho) + E_C(\rho)$$

Kohn-Sham equations are solved in a self-consistent way where the electron density ρ is initially guessed by using superposition of atomic densities. Then an approximate form of $E_{XC}(\rho)$ is used in order to compute $\upsilon_{XC}(r)$. The set of Kohn-Sham equations is then used to compute an improved electron density ρ from $\rho(r) = 2\sum_m \Psi_m^*(r)\,\Psi_m(r)$. This process is repeated until the electron density and the exchange-correlation energy have converged. The electronic energy is finally computed from $E(\rho)$.

Kohn-Sham orbitals can be computed numerically, or they can be expressed in terms of a set of basis functions: in this latter case solving the Kohn-Sham equations means that the coefficients in the basis set expansion need to be found. The required computational time for DFT calculations if sets of basis functions are used scales as the third power of the number of basis functions (calculations for complex molecules can take a long time in this case) [49].

2.1.2 Gradient Methods

Once the electronic energy is obtained, a lot of molecular properties can be determined, among which the most important is the equilibrium molecular geometry. In order to obtain the equilibrium structures, the derivatives of the potential energy with respect to nuclear coordinates need to be calculated. Usually, gradient methods are used in order to determine energy derivatives analytically because these methods are faster and more accurate.

In polyatomic molecules the potential energy is a function of many nuclear coordinates, q_I. At the equilibrium geometry, each of the forces f_I acting on the nucleus (that are caused by electrons and other nuclei) must disappear, so $f_I = -\frac{\delta E}{\delta q_I} = 0$. In theory, the equilibrium geometry can be found by computing all the forces at a certain geometry and checking if they disappear. If they do not disappear the geometry is changed, and the process is repeated until the forces vanish. Usually this does not happen, but a tolerance level can be determined so that the calculations can be stopped.

To calculate analytical derivatives of the energy with respect to nuclear coordinates it is necessary to compute the derivatives of one-electron and two-electron integrals over the basis functions. These basis functions are centered on atom nuclei so when the derivatives of the integrals are obtained, the derivatives of the basis set functions with respect to nuclear coordinates are required.

A zero gradient individuates a stationary point on the potential surface, but it could be minima, a maxima or a saddle point. In order to distinguish the different types of stationary points, it is necessary to consider the second derivatives of the energy with respect to nuclear coordinates. The second derivatives of the energy with respect to nuclear coordinates are the force constants for normal mode frequencies within the harmonic approximation. The quantities $\frac{\delta^2 E}{\delta q_i q_j}$ characterize the Hessian matrix. A minimum of a one-dimensional potential curve corresponds to a positive second derivative, while a minimum of a multidimensional potential energy surface is defined by the eigenvalues of the Hessian matrix all being positive (the opposite is true for a maximum). A transition state, that corresponds to a first-order saddle point, has one negative eigenvalue and all the others positive.

A lot of algorithms are available for finding stationary points on a potential surface. In general, the stability, reliability, and computational cost of the algorithm as well as its speed of convergence need to be considered. The algorithms can be mainly classified into three groups. The first type uses only the energy, and it is the slowest to converge but it is useful if analytical derivatives are unavailable. The second type uses both the energy and its analytical first derivatives and it is significantly more efficient. Algorithms that use the energy together with its analytical first and second derivatives are the most accurate and efficient methods. Whichever algorithm is used, all nuclear coordinates should be optimized. The optimization is particularly important for transition states, where optimizing a subset of all the nuclear coordinates can individuate a saddle point that changes significantly when all coordinates are optimized [49].

2.1.3 Vibrational Analysis

Non-linear molecules consisting of *N* atoms have *3N-6* displacements that correspond to the vibrations of the molecule. This number of displacements is obtained considering that to specify the location of *N* atoms, *3N* coordinates are needed. The coordinates are then grouped in a useful way: three of the coordinates can specify the position of the center of mass of the molecule with *3N-3* coordinates that will define the position of the atoms with respect to the center of mass. The orientation of non-linear molecules also requires the specification of three angles, so *3N-6* coordinates are left (these coordinates do not change the location of the center of mass or the orientation of the molecule when varied). The displacements along these coordinates correspond to the vibrations of the molecule.

All the atoms take part in the vibrations of the molecule and these vibrations are described after analyzing the variation of potential energy with the position of all the atoms in the molecule. The potential energy depends on all the displacements of the atoms from their equilibrium positions:

$$V = V(0) + \sum_i (\frac{\delta V}{\delta x_i})_0 x_i + \frac{1}{2}\sum_{i,j} (\frac{\delta^2 V}{\delta x_i \delta x_j})_0 x_i x_j + \ldots$$

V(0) could be equal to zero and the first derivatives are all null at equilibrium (all $x_i = 0$) so for small displacements from the equilibrium:

$$V = \frac{1}{2}\sum_{i,j} k_{ij} x_i x_j + \ldots$$

With a generalized force constant $k_{ij} = (\frac{\delta^2 V}{\delta x_i \delta x_j})_0$. A displacement of one atom can influence the restoring force experienced by another as can be deducted from the presence of partial derivatives with respect to two displacements. The above-mentioned sum is over all *3N* displacements of the *N* atoms, so some displacements (rotations and translations of the whole molecule) will have a zero generalized force constant. These displacements need to be disentangled from the true vibrations. The first step is to consider mass-weighted coordinates $q_i = m_i^{1/2} x_i$ where m_i is the mass of the atom with displacement x_i. In this case the potential energy and the kinetic energy of all the atoms are:

$$V = \frac{1}{2}\sum_{i,j} K_{ij} q_i q_j$$

$$E_k = \frac{1}{2}\sum_i m_i \dot{x}_i^2 = \frac{1}{2}\sum_i \dot{q}_i^2$$

With $K_{ij} = (\frac{\delta^2 V}{\delta q_i \delta q_j})_0$ and the dot meaning that it is a derivation with respect to time. The expression for the total energy would be:

$$E = \frac{1}{2}\sum_i \dot{q}_i^2 + \frac{1}{2}\sum_{i,j} K_{ij} q_i q_j$$

The terms where *i* is different from *j* are cross-terms for the potential energy, the most difficult ones to consider. *Q_i*, in which a linear combination of the mass-weighted coordinates *q_i* is considered, can be used to write the total energy in a form deprived of the cross-terms:

$$E = \frac{1}{2}\sum_i \dot{Q}_i^2 + \frac{1}{2}\sum_i \lambda_i Q_i^2$$

When *λ* is equal to zero, *Q* will correspond to translations and rotations. These linear combinations are called normal coordinates because a separation of modes is achieved. The vibrations that correspond to displacements along these normal coordinates are called normal modes of the molecule.

The expression used for the energy is a sum of terms so also the hamiltonian operator, in the position representation, will be a sum of terms:

$$H = \sum_i H_i$$

With $H_i = -\frac{1}{2}\hbar^2 \frac{\delta^2}{\delta Q_i^2} + \frac{1}{2}\lambda_i Q_i^2$. The vibrational wavefunction of the molecule is a product of wavefunctions for each normal mode because the hamiltonian is a sum of terms:

$$\Psi = \Psi_{v_1}(Q_1)\Psi_{v_2}(Q_2)\ldots = \prod_i \Psi_{v_i}(Q_i)$$

In a non-linear molecule *3N-6* factors are present and each of them satisfies a Schrödinger equation:

$$-\frac{1}{2}\hbar^2 \frac{\delta^2 \Psi(Q_i)}{\delta Q_i^2} + \frac{1}{2}\lambda_i Q_i^2 \Psi(Q_i) = E\Psi(Q_i)$$

This is the equation for a harmonic oscillator of unit mass and force constant λ_i. The energy levels of the i-th normal mode are $E_{v_i} = (v_i + \frac{1}{2})\hbar\omega_i$ with $\omega_i = \lambda_i^{1/2}$ and v_i quantum numbers of the modes. The wavefunctions are $\Psi_{v_i}(Q_i) = N_{v_i} H_{v_i}(\alpha_i Q_i) e^{-\frac{\alpha_i^2 Q_i^2}{2}}$ with $\alpha_i = (\frac{\omega_i}{\hbar})^{1/2}$ and N_{v_i} normalization constant. The total vibrational energy of the molecule in the harmonic approximation is:

$$E = (v_i + \frac{1}{2})\hbar\omega_i$$

The total vibrational wavefunction is given by the product of all the $\Psi_{v_i}(Q_i)$ terms. A general vibrational state is defined by i quantum numbers, one for each mode: the ground state has all the quantum numbers equal to zero [49].

In local minima or local maxima geometries all vibrational modes have a positive vibrational frequency, while in transition states (as already discussed in 1.4.2) there is an imaginary mode with a negative vibrational frequency. This can be understood by considering that if we study the vibrations as a harmonic oscillator, in the case of a transition state, the restoring force is not able to return to a local minima or local maxima point but it just returns the configuration to the intermediate state. From the harmonic oscillator theory, the frequency can be expressed in terms of the square of the restoring force so that if the restoring force is negative (as it is in transition states), the frequency becomes an imaginary number, thus the molecule has an imaginary mode.

2.1.4 Hammett Rule

The Hammett rule, developed by L. Hammett in 1937, is used in organic chemistry to describe a linear free energy relationship relating reaction rates and equilibrium constants for a lot of reactions involving benzoic acid derivatives. The only two considered parameters are a substituent constant and a reaction constant. The idea developed intuitively by Hammett is that two aromatic reactants (differing only by the substituent group) involved in two reactions have a free energy of activation that changes proportionally to the Gibbs free energy's change. The basic equation is $\log\frac{K}{K_0} = \sigma\rho$, where K is the equilibrium constant for a given reaction, K_0 is the reference equilibrium constant with a H substituent, σ is the substituent constant (which depends on the substituent), and ρ is the reaction constant (which depends on the type of reaction). The same equation is also true for reaction constants: for a fixed reaction type, the study of σ can reveal a tendency in the reactionrate for a certain reaction, so it is very important to check the substituent constant of the considered groups [50].

2.2 Procedure

In order to obtain the results from the computational DFT calculations .gjf files were created through GaussView 6.0 software [51]: .gjf files contain the initial geometry of the molecules as it is manually created by the user. This .gjf files are later implemented with the instructions needed for the subsequent calculations.

In this study the allocated resources consisted in 8 processor cores on shared memory parallel execution and in 6000000 allocated memory (in words). The used command line consists in 8 keywords that play a key role in the calculations:

- #p means that additional output information is generated. This includes messages at the beginning and end of each link giving assorted machine-dependent information (including execution timing data), as well as convergence information [52].
- opt means that a geometry optimization is carried out. The geometry will be adjusted until a stationary point on the potential surface is found. In the case of transition states the optimization command becomes opt=(calcfc,ts,noeigentest) meaning that the geometry of a transition state is going to be adjusted until a saddle point on the potential surface is found [53].
- freq means that a vibrational analysis is carried out. The vibrational frequencies are computed by determining the second derivatives of the energy with respect to the Cartesian nuclear coordinates and then transforming to mass-weighted coordinates [54].
- b3lyp/gen means that the b3lyp DFT model is used and that the gen (general) basis set is considered. In this case the information about the gen basis set is contained in a specific section at the bottom of the .gjf file [55]. As already discussed in the 2.1.1 section, exchange-correlation functionals are crucial to calculate the system's energy and this model, based on a particular hybrid functional given by the sum of three exchange functionals (local spin density approximation, Hartree-Fock and Becke) and two correlation functionals (local spin density approximation and Lee-Yang-Parr) with some fixed parameters, is the most common

one [56]. In fact, B3LYP calculations can well reproduce experimental date associated to structural and electronic properties of molecules;

- iop means that some internal options can be personalized by the user. In this case iop(2/15=1,5/13=1,1/8=5) and iop(2/15=1,5/13=1) commands have been used [57].
- optcyc=100 means that the maximum number of optimization steps has been set to 100.
- scfcyc=100 means that the maximum number of self-consistent field calculation steps has been set to 100.
- pseudo=read means that the atoms with many electrons are treated by effective core potential. In this case the information about the effective core potential basis set is written at the end of the .gjf file.

After the command line, the overall charge of the system and the overall spin multiplicity are reported. In this case the values are 0 and 1 (singlet state). Then atom's Cartesian coordinates are reported according to how the molecules have been previously organized in GaussView.

At the bottom of the .gjf file, information about the basis set is written. In this case for atoms with many electrons SDD basis set is considered while for atoms with fewer electrons 6-31G** basis set is considered. Also, the pseudopotential considered for atoms with many electrons is written. In this case SDD basis set is considered.

After obtaining the complete .gjf files, the DFT calculations that will follow the instructions contained in the command line need to be carried out through Gaussian 16 software [58]. The calculations will generate a .chk file containing the obtained final geometry and a .out file containing all the information about the optimization process and the vibrational analysis.

The frequencies in the .out files have been checked to see if the calculations were carried out correctly: in the case of local minima only positive vibrational frequencies are required while for transition states a negative frequency is required (an imaginary mode is present).

After checking the frequencies, the energy (in Hartree) associated to every species' final optimization step is converted into kcal/mol and relative total energies for the various steps in the reaction are calculated.

Then the Gibbs free energies (in Hartree) contained in the .out file for every species are studied, converted into kcal/mol and the relative Gibbs free energies are calculated for the various steps in the considered reaction.

The final step consists in plotting the relative Gibbs free energies to obtain the PES (potential energy surface) representation that shows the energy differences involved in the various steps of the reaction. By doing so, the role of the different chemical species in the reaction can be studied in detail.

In order to better understand the mechanism of the reaction, natural population analysis (or NPA) has been carried out on the substrate and on the catalyst to see if different charges caused by different atoms can have a role in the different obtained energy levels. The charges have been obtained in GaussView from the optimized geometries.

A study of the frontier orbitals of the catalyst and the substrate has also been considered in order to see how different orbital energies can lead to a different reaction behavior. Frontier orbital energies have been obtained from the .out files of the optimized geometries.

3 Results

The objective of this thesis work was to understand what are the key factors that can influence the result of Stille coupling reaction by looking at different systems that lead to the same final product. The steps of the reaction have been studied in order to obtain the local minima and the transition states with the associated total energy values and the relative total energies. The reaction for trial 1 is as follows (for trial 2 MeO is changed with NO_2 and H):

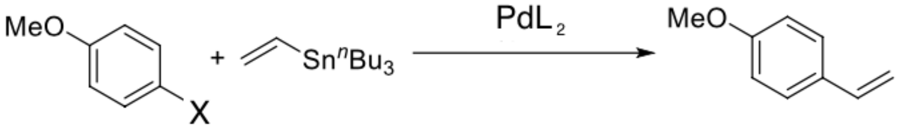

After vibrational analysis the Gibbs free energies and the relative Gibbs free energies have been obtained making it possible to understand the influence of different ligands and substrates on this type of reaction. PESs representations have been drawn from the relative Gibbs free energy values in order to have a more intuitive way of looking at the various steps. From natural population analysis the charges on the main involved species have been calculated so that the results could be better understood. By looking at the electronic population of the orbitals, frontier orbital energies have been obtained and orbital energy gaps have been calculated.

3.1 Trial 1

As already mentioned, the newness of this study lies in the great number of systems that have been studied and compared. For trial 1 a total of 18 systems have been considered and, in every system, the organostannane (tributylstannyl)vinyl has always been kept unchanged:

- Six of them have a substrate consisting of a bromine atom bonded to anisole and a catalyst that changes in every system: half of the systems has a catalyst based on arsenic and the other half of the systems has a catalyst based on phosphorous. The ligands in the catalyst are tertiary ligands that change in every system but that are all equal among the same system: phenyl, (para-trifluoromethyl)benzene and (para-anysil)benzene have been considered with both arsenic and phosphorous;
- Six of them have a substrate consisting of a chlorine atom bonded to anisole and a catalyst that changes in every system: half of the systems has a catalyst based on arsenic and the other half of the systems has a catalyst based on phosphorous. The ligands in the catalyst are tertiary ligands that change in every system but that are all equal among the same system: phenyl, (para-trifluoromethyl)benzene and (para-anysil)benzene have been considered with both arsenic and phosphorous;
- Six of them have a substrate consisting of an iodine atom bonded to anisole and a catalyst that changes in every system: half of the systems has a catalyst based on arsenic and the other half of the systems has a catalyst based on phosphorous. The ligands in the catalyst are tertiary ligands that change in every system but that are all equal among the same system: phenyl, (para-trifluoromethyl)benzene and (para-anysil)benzene have been considered with both arsenic and phosphorous.

3.1.1 Catalysts

The most important species for the reaction to take place is the palladium-based catalyst. The PdL_2 catalyst cannot easily bind the substrate as it is because the arsenic or phosphorous ligands exhibit a considerable bulkiness, so a dissociation of L from PdL_2 is required. From the optimized geometries the bond lengths for the catalyst have been obtained. There is a negligible effect of the type of ligand, but the nature of the ligand (containing arsenic or phosphorus) plays an important role: in arsenic ligands a longer bond length between Pd and As is obtained (around 2,3 Å), while in phosphorous ligands a shorter bond length between Pd and P is obtained (around 2,2 Å).

It is very useful to look at the charge distribution on the dissociated catalyst because it can influence the first step of the reaction. Through NPA, the charge on the palladium atom of PdL has been obtained as shown in Table 1 with only a minor dependence on the bonded ligand and a general order for the negative charge that can be resumed as $As(PhCF_3)_3$ < $AsPh_3$ < $As(PhOMe)_3$ and $P(PhCF_3)_3$ < PPh_3 < $P(PhOMe)_3$.

Table 1 Charges on palladium atoms in PdL for the different ligands

Species	*$AsPh(CF_3)_3$*	*$AsPh_3$*	*$AsPh(OMe)_3$*	*$PPh(CF_3)_3$*	*PPh_3*	*$PPh(OMe)_3$*
Charge	-0,13	-0,16	-0,19	-0,12	-0,16	-0,19

It is also important to study the energy levels associated to the HOMO orbitals of the catalysts. Ligand substituents change the energy associated to the HOMO, especially for the HOMOs whose amplitudes are located on palladium, and on the ligands (HOMO-1, HOMO-2, HOMO-3, and HOMO-4 have amplitudes only on palladium, while HOMO-5 has amplitude mainly on the ligands). PhOMe, Ph and $PhCF_3$ substituents in arsenic catalysts have their HOMOs at respectively -4,55 eV, -4,76 eV and -5,34 eV. In phosphorous ligands, the energy levels associated to the HOMOs for PhOMe, Ph, and $PhCF_3$ substituents are respectively -4,74 eV, -4,80 eV, and -5,27 eV. The optimized geometries of the catalysts are shown in Figure 13.

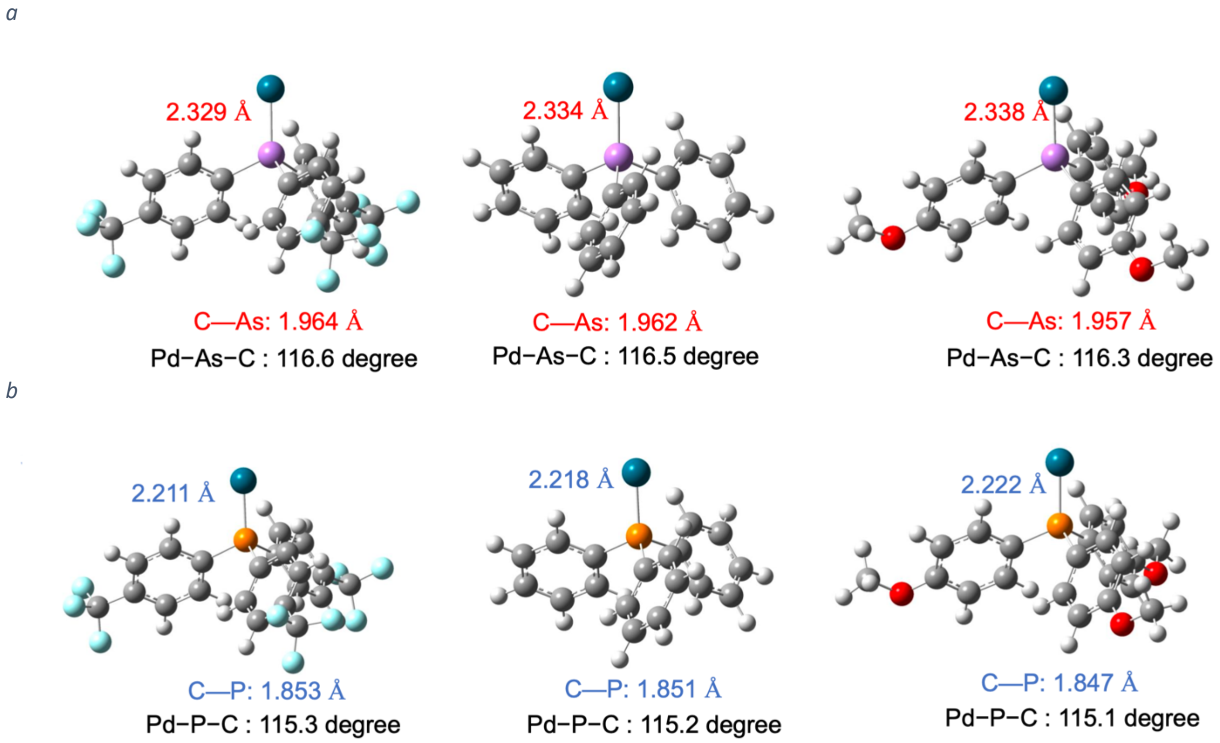

Figure 13 Optimized geometries for the PdL catalysts considered in trial 1 with indications of Pd-As/P and C-As/P bond lengths and Pd-As/P-C angles. (a) Catalysts with arsenic-based ligands; (b) Catalysts with phosphorous-based ligands (Credits to Prof. Yumura)

3.1.2 Substrates

The substrate also plays a very important part in Stille coupling reactions. The different halogen atom can greatly influence the pathway of the reaction and the same is true for the substituted group in para position (which has been kept the same during trial 1). From the optimized geometries the bond lengths have been obtained. Shorter bond lengths are obtained for chlorine (around 1,8 Å), intermediate values are obtained for bromine (around 2,0 Å) and higher values are obtained for iodine (around 2,2 Å) as can be deducted by considering the differences in Pauling electronegativities for the considered halogens (3.16 for Cl, 2.96 for Br and, 2.66 for I).

Through NPA the charges on the different halogens have been calculated as shown in Table 2 with a little negative charge if chlorine is considered, a little positive charge if bromine is considered and a relatively high charge if iodine is considered.

Table 2 Charges on halogen atoms in the various considered substrates

Species	*OMePhCl*	*OMePhBr*	*OMePhI*
Charge	-0,04	0,03	0,13

The σ^* orbitals associated to the different substrates are very important for the study of the reaction. A lower energy σ^* orbital energy is associated to the I-C bond, an intermediate value is associated to the Br-C bond and a higher value is associated to the Cl-C bond. The σ^* orbital representation is shown in Figure 14, while the orbital energies associated to σ^* for the three substrates are reported in Table 3.

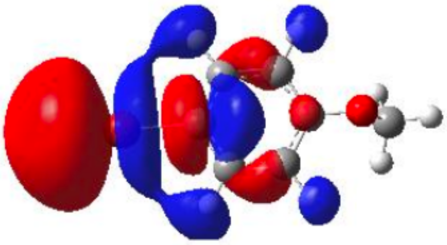

Figure 14 Representation of the substrate's σ orbital (Credits to Prof.Yumura)*

Table 3 Orbital energies associated to the different substrates (energies in eV)

Species	*OMePhCl*	*OMePhBr*	*OMePhI*
σ^* Orbital Energy	0,75	-0,42	-1,09

3.1.3 Catalytic Cycle

According to the considered literature and the recent work by Prof. Imoto, the considered catalytic cycle for the Stille coupling reactions starts between the PdL_2 catalyst and X-Ph-OMe aryl halide substrate, while Bu_3SnEt organostannane is added later. At the beginning, the PdL_2 complex needs to be dissociated in PdL and L. Then, the oxidative addition of the substrate to the resultant PdL complex proceeds, where the C−X bond of X-Ph-OMe is cleaved. The oxidative addition leads to the formation of a MeOPh−PdX−L complex where OMePh, L, and Pd(II) attached by X are aligned linearly. After the oxidative addition, an isomerization takes place in order to form a MeOPh−PdL−X complex where the positions of X and L are exchanged. The product of the isomerization reacts with the organostannane through Pd(II) cation−π interactions, with the beginning of the transmetalation process: here the Pd(II) cation- π complex takes a square-planar structure due to the Pd(II) cation d^8 electronic configuration. In the transmetalation step, the $SnBu_3$ moiety of Bu_3SnEt migrates to the halogen atom, and contemporarily the vinyl moiety migrates to Pd to form a bond between Pd and C. Finally, the transmetalation process leads to Bu_3SnX and a Et−Pd−L where L, vinyl, and Pd attached by MeOPh are aligned linearly. The final step is the reductive elimination step in which the Et−PdOMePh−L complex leads to the coupling of vinyl and OMePh moieties to form the desired OMePhEt and to regenerate Pd−L (that will be a starting species for further catalytic Stille coupling reactions). The considered catalytic cycle is shown in Figure 15 [22].

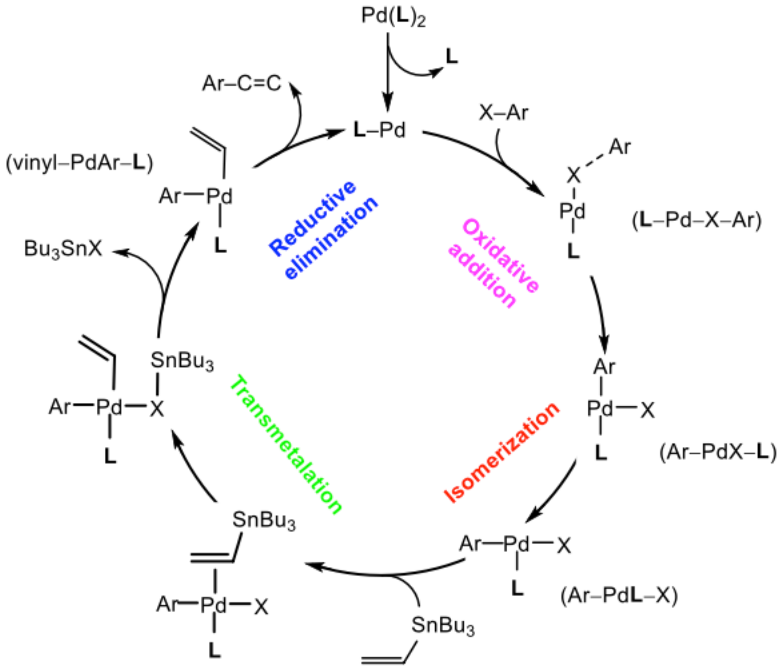

Figure 15 Considered catalytic cycle for the Stille coupling reaction as proposed by Prof. Imoto [22]

To better follow the chosen catalytic cycle, in every system a total of 14 steps in the Stille coupling reaction have been considered (in parenthesis the assigned name to the step as will be indicated in PESs representations):

- The first step is the starting catalyst, a palladium atom bonded to two ligands (L-Pd-L);
- The second step is the ligand dissociation to form a molecule made of a palladium atom bonded to only one ligand, and a free ligand (L-Pd+L);
- The third step is the starting point of the oxidative addition reaction between the catalyst and the substrate (L-Pd--Substrate);
- The fourth step is the three-center transition state involved in the oxidative addition between the catalyst and the substrate (L-Pd--Substrate TS);
- The fifth step is the product of the oxidative addition reaction (Pd_L_X_PhOMe);
- The sixth step is the transition state related to the isomerization of the previously obtained product (Pd--L--X--PhOMe TS);
- The seventh step is the result of the isomerization (Pd_PhOMe_L_X);
- The eighth and nineth step could take place at the same time, and they are two different pathways the reaction can take: the previously obtained isomerized product can react with a free ligand molecule to form a molecule with a palladium atom bonded to two ligands in trans position, an halogen atom and OMePh (Pd_L_MeOPh_L_X) or it can react with the Bu_3SnEt organostannane in order to start the transmetalation (Pd_EtSnBu3_MeOPh_L_X);
- The tenth step is the transmetalation transition state (Pd_Et_MeOPh_L_X--SnBu3 TS);
- The eleventh and twelfth steps are the result of the transmetalation step with the formation of the bond between tin and halogen in the obtained molecule (Pd_Et_MeOPh_L_X-SnBu3)

and the elimination of the newly formed organotin-halogen species (Pd_Et_MeOPh_L+Bu3SnX);

- The thirteenth step is the transition state of the reductive elimination on the T-shaped species (Pd_Et-MeOPh_L TS);
- The fourteenth step is the result of the Stille coupling reaction with the coupling between vinyl and OMePh (L-Pd+MeOPh-Et).

3.1.4 Role of Orbital Interactions

It is very important to consider the frontier orbital interactions involved in the reaction. In the formation of the first complex there is a transfer of electrons from the 4d orbital of the Pd(0) atom (with a d^{10} electronic configuration) to the unoccupied σ^* orbital present between the halogen and the carbon in the X-Ph-OMe substrate. This transfer populates the just mentioned antibonding orbital, thus activating the X-C bond in the substrate. The gap between the HOMO in the catalyst and the LUMO in the substrate is influenced by the considered substrates and ligands in the catalyst.

The difference in orbital energies associated to the LUMO of the substrate come from the different halogen atoms and substituent groups (which in this case are kept the same). The obtained orbital energy values for σ^* greatly influence the activation of the X-C bond of the substrate. An image of the σ^* orbital is shown in Figure 15

In arsenic ligands, the lowest gaps between HOMO (in the catalyst) and LUMO (in the substrate) are observed for PhOMe substituents. The same is true for phosphorous ligands, where the lowest gap is observed with PhOMe substituents, but in this case the values for the gap are still marginally higher than with arsenic ligands.

3.1.5 Obtained Optimized Geometries

The main obtained optimized geometries for one of the systems (Br-Ph-OMe + $Pd(AsPh_3)_2$ is considered as an example) are displayed in Figure 16.

a

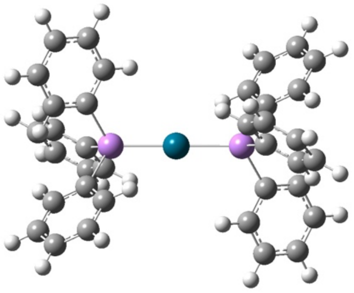

b

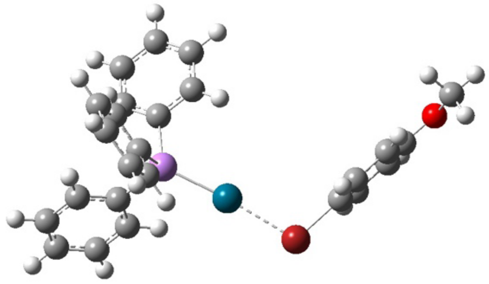

c

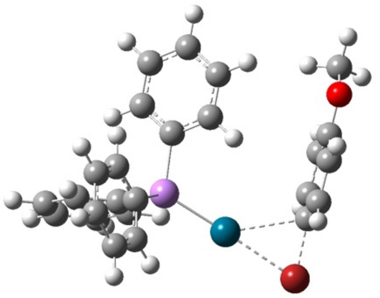

d

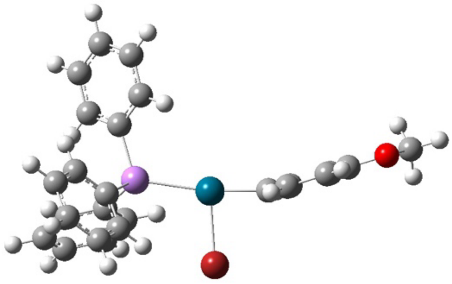

e

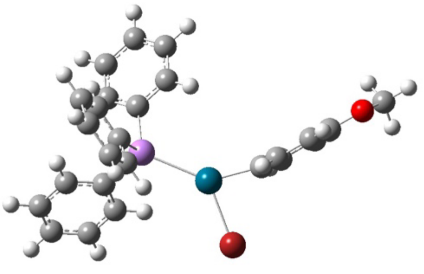

f

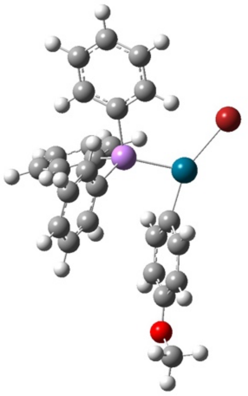

g

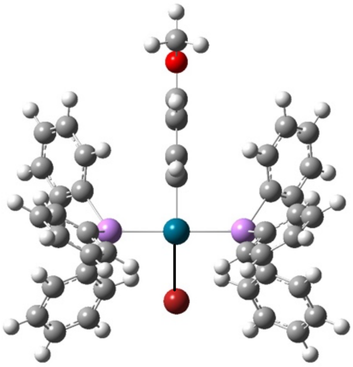

h

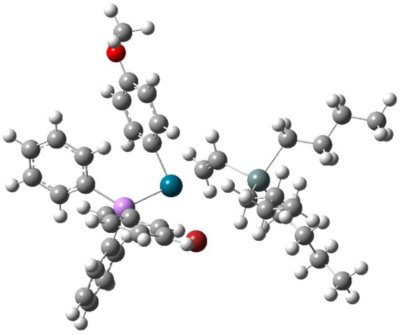

i

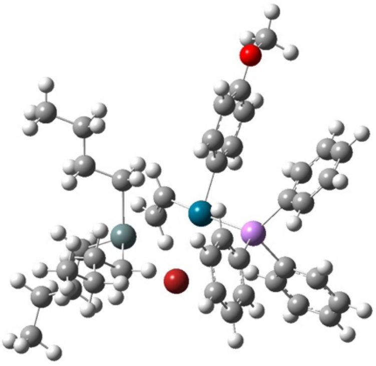

j

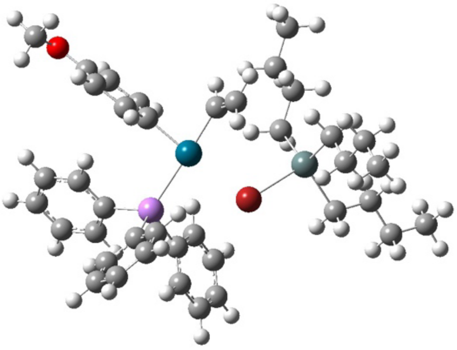

k

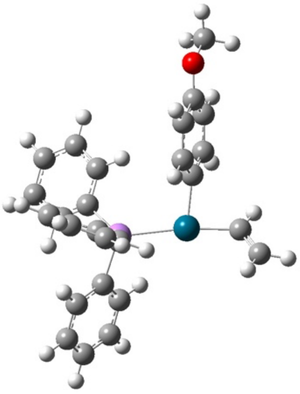

l

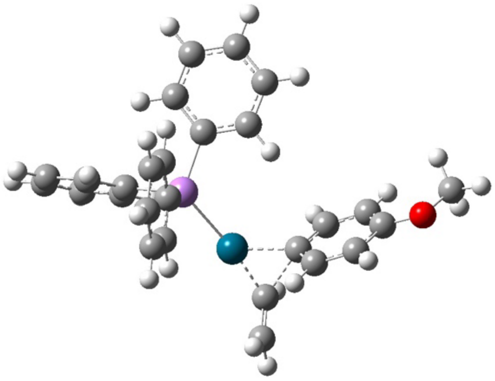

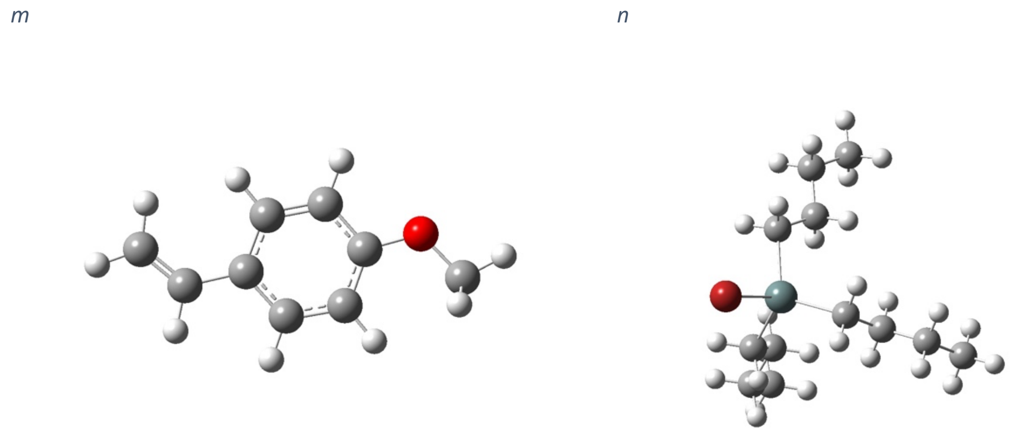

Figure 16 Optimized geometries for the Br-Ph-OMe + Pd($AsPh_3$)$_2$ system. (a) PdL_2 catalyst [L-Pd-L]; (b) first complex [L-Pd--Substrate]; (c) transition state of the oxidative addition [L-Pd—Substrate TS]; (d) result of the oxidative addition [Pd_L_X_PhOMe]; (e) transition state of the isomerization [Pd—L—X—PhOMe TS]; (f) result of the isomerization [Pd_PhOMe_L_X]; (g) alternative pathway with quaternary palladium atom [Pd_L_MeOPh_L_X]; (h) initial state of the transmetalation [Pd_EtSnBu3_MeOPh_L_X]; (i) transition state of the transmetalation [Pd_Et_MeOPh_L_X—SnBu3 TS]; (j) result of the transmetalation with organotin and palladium complex [Pd_Et_MeOPh_L_X-SnBu3]; (k) palladium complex after the transmetalation [Pd_Et_MeOPh_L+Bu3SnX]; (l) transition state of the reductive elimination [Pd_Et-MeOPh_L TS]; (m) final product of the Stille coupling reaction [L-Pd+MeOPh-Et]; (n) final organotin product of the Stille coupling reaction [Bu3SnX]

3.1.6 Br-Ph-OMe + PdL_2 (L = $AsPh_3$, and PPh_3)

The first system that has been considered consists in $AsPh_3$ containing ligands and Br containing substrate. In this case the dissociation of L from PdL_2 in order to obtain the starting PdL catalyst is a very energetically demanding process because an energy difference of 21,62 kcal/mol was calculated. After PdL is obtained, this system reacts by forming the first complex, LPd-Br-Ph-OMe as a result of the binding of PdL with the OMePhBr substrate. This complex is 18,35 kcal/mol unstable relative to the initial state. The obtained complex evolves through a transition state in the oxidative addition step of the Stille coupling reaction being 24,32 kcal/mol unstable relative to the initial state and 5,97 kcal/mol unstable relative to the first complex. The product of the oxidative addition then isomerizes with an energy difference of 10,59 kcal/mol from the initial state, -7,76 kcal/mol from the first complex and 2,95 kcal/mol relative to the reagents involved in this step. The isomerization product reacts with the $SnBu_3Et$ organostannane in the transmetalation step through a transition state with an energy gap of 15,98 kcal/mol measured from the initial state, -2,37 kcal/mol from the first complex and 18,32 kcal/mol relative to the reagents involved in this step. The final reductive elimination step has a transition state with a measured difference of 4,94 kcal/mol from the initial state, -13,41 kcal/mol from the first complex and 4,58 kcal/mol relative to the reagents involved in this step. The PESs representation is shown in Scheme 1.

Scheme 1 Potential energy surfaces representation for the Stille coupling reaction with $AsPh_3$ ligand and OMePhBr substrate

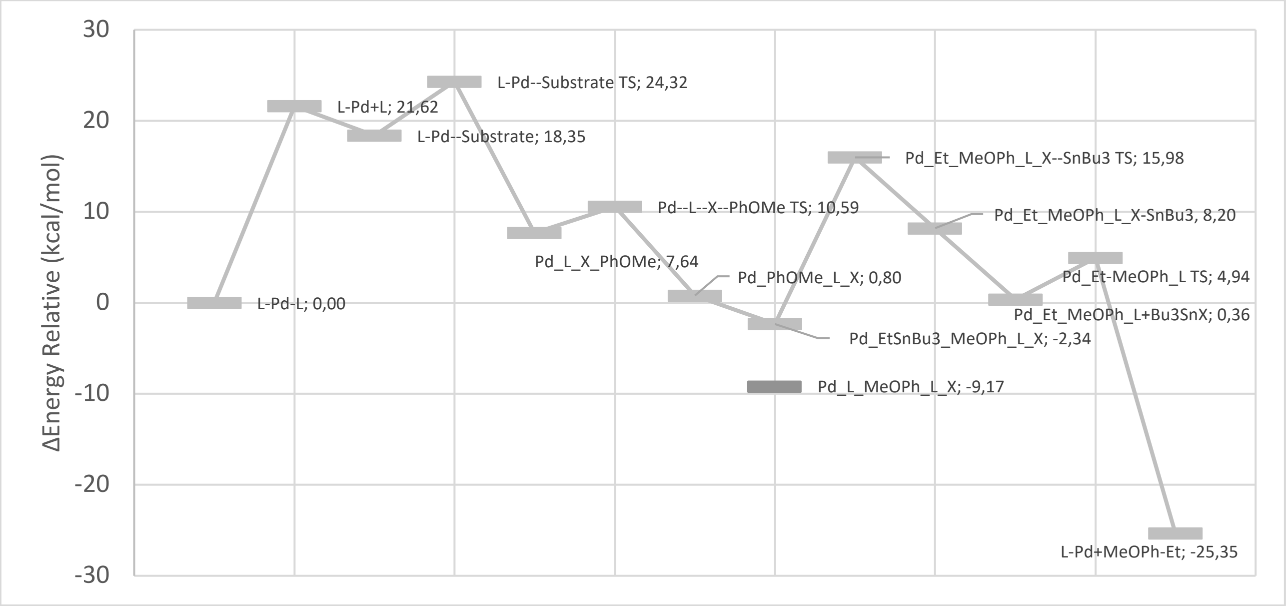

The same system has been studied with phosphorous instead of arsenic in the ligands. In this case the dissociation of L from PdL_2 has an energy gap of 21,82 kcal/mol measured from the initial state. The subsequent complex exhibits an energy difference of 18,87 kcal/mol from the initial state. The transition state in the oxidative addition step has an energy barrier of 24,86 kcal/mol from the initial state and 5,99 kcal/mol from the first complex. The isomerization has an energy difference of 13,13 kcal/mol from the initial state, -5,74 kcal/mol from the first complex and 3,46 kcal/mol relative to the reagents involved in this step. The transmetalation transition state has an energy barrier of 19,98 kcal/mol from the initial state, 1,11 kcal/mol from the first complex and 17,27 kcal/mol relative to the reagents involved in this step. The reductive elimination transition state has an energy barrier of 7,16 kcal/mol from the initial state, -11,71 kcal/mol from the first complex and 3,97 kcal/mol relative to the reagents involved in this step. The PESs representation is shown in Scheme 2.

Scheme 2 Potential energy surfaces representation for the Stille coupling reaction with PPh_3 ligand and OMePhBr substrate

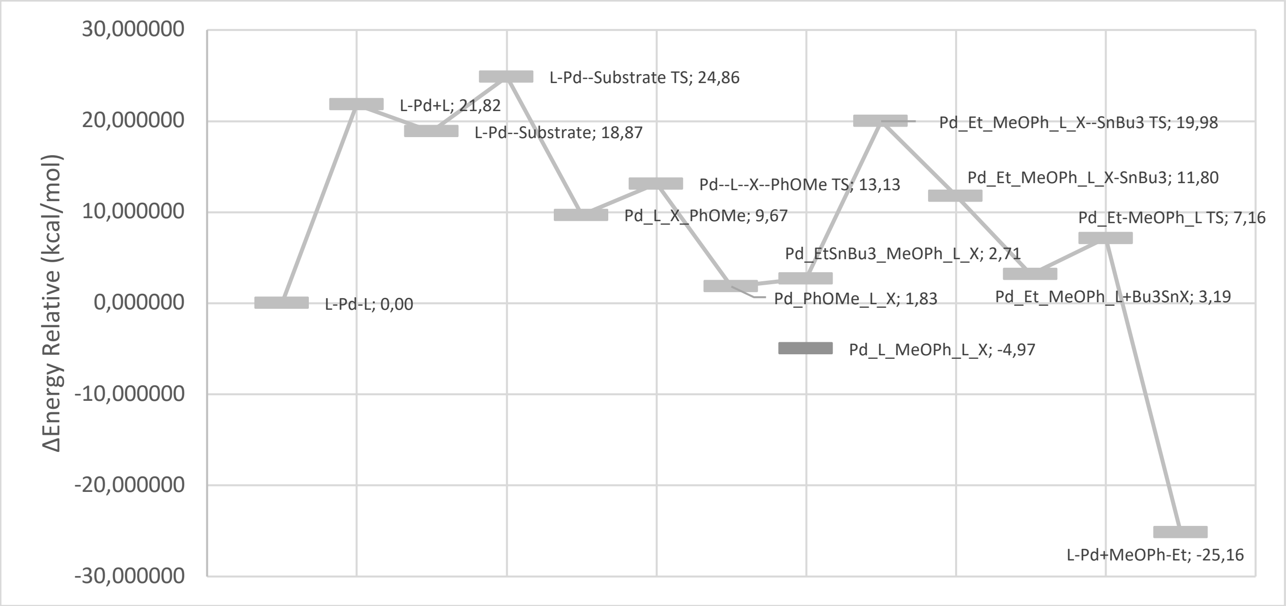

From the obtained values for the energy differences, it is clear that the most difficult steps are the oxidative addition and the transmetalation. In fact, the isomerization and the reductive elimination steps are characterized by relatively low values in the energy, while the oxidative addition and the transmetalation exhibit very high values in energy.

By comparing the reaction of ligands containing phosphorous and ligands containing arsenic there are some interesting considerations that need to be done. First, the PES associated to the dissociation of the catalyst and associated to the first complex seems to be almost independent from the nature of the ligand because similar values have been obtained for phosphorous and arsenic ligands. The same is true for the oxidative addition step where very similar values are obtained among the two systems. Different behaviors emerge when considering the other steps involved in the reaction with significantly lower energy values associated to arsenic ligands in isomerization, transmetalation and reductive elimination when compared to phosphorous ligands: in this case the use of arsenic ligands accelerates the reaction lowering the energy associated to the transition states with a more significant effect on the transmetalation step.

3.1.7 Br-Ph-OMe + PdL_2 (L = $As(PhCF_3)_3$, $P(PhCF_3)_3$, $As(PhOMe)_3$, and $P(PhOMe)_3$)

Other considered systems have tertiary ligands where the substituted groups are changed from Ph_3 to $PhCF_3$ and PhOMe both in arsenic and phosphorous ligands.

In arsenic ligands with the new substituent groups, similar values are obtained for the PESs when compared to the abovementioned Ph_3 substituent group. For the dissociated ligand, the first complex and the oxidative addition transition state lower values are obtained for $PhCF_3$ while higher values are obtained for PhOMe compared to Ph_3. For the isomerization and the reductive elimination, the opposite behavior has been noted with higher values for $PhCF_3$ and lower values for PhOMe. For the transmetalation step, PhOMe has the highest value, $PhCF_3$ has an intermediate value and Ph_3 has the lowest value. In general, a negligible effect of the different ligands is seen on the energies associated to the catalyst dissociation, the transmetalation and the reductive elimination, while a stronger effect is seen on the first complex, the oxidative addition and the isomerization (the strongest effect is visible on the isomerization step with a difference of 2,66 kcal/mol between $As(PhCF_3)_3$ and $As(PhOMe)_3$). A summary of the obtained values for arsenic ligands with a bromine-based substrate is shown in Table 4 (the main values indicate the energy values measured from the initial state, the values in parenthesis indicate the energy values measured from the first complex).

Table 4 Summary of PESs for Stille coupling reactions between PdL_2 and OMePhBr with arsenic ligands (energies in kcal/mol)

L	*PdL+L*	*1st complex*	*TS_{OA}*	*TS_{ISO}*	*TS_{TM}*	*TS_{RE}*
$As(PhCF_3)_3$	21,31	17,60	23,36 (5,76)	12,30 (−5,30)	16,18 (−1,42)	5,49 (−12.10)
$AsPh_3$	21,62	18,35	24,32 (5,97)	10,59 (−7,76)	15,98 (−2,37)	4,94 (−12,11)
$As(PhOMe)_3$	21,79	18,88	24,76 (5,88)	9,64 (−9,24)	16,92 (−1,96)	4,48 (-14,40)

The PESs representation for $As(PhCF_3)_3$ and $As(PhOMe)_3$ ligands can be seen in Scheme 3 and Scheme 4.

Scheme 3 Potential energy surfaces representation for the Stille coupling reaction with As(PhCF₃)₃ ligand and OMePhBr substrate

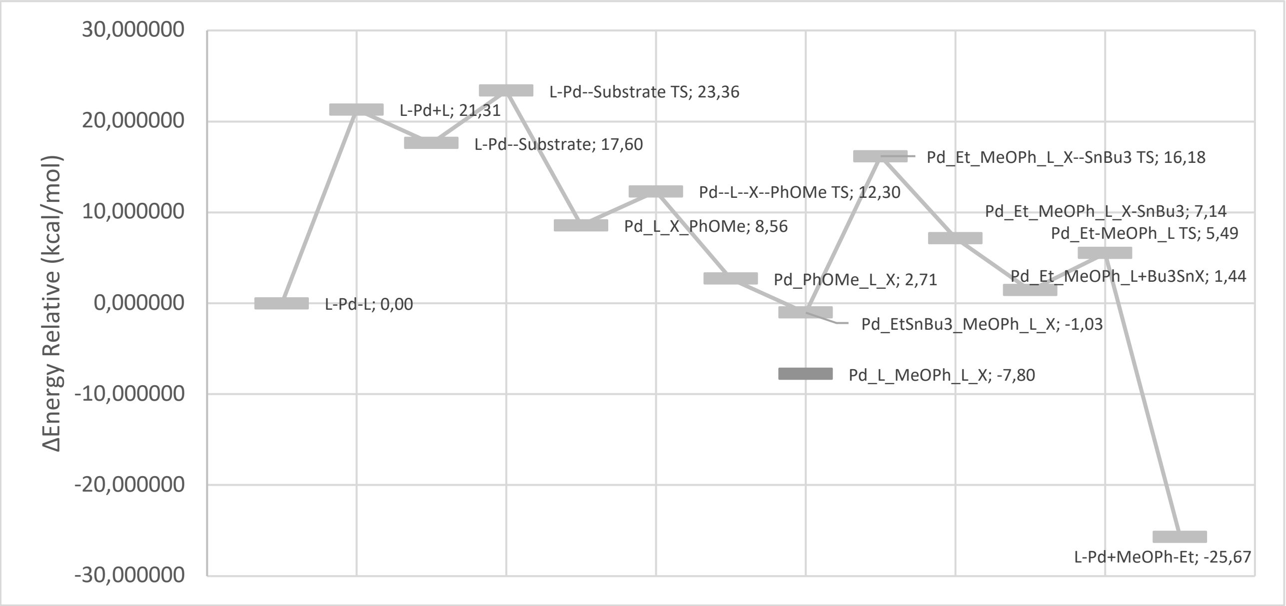

Scheme 4 Potential energy surfaces representation for the Stille coupling reaction with As(PhOMe)₃ ligand and OMePhBr substrate

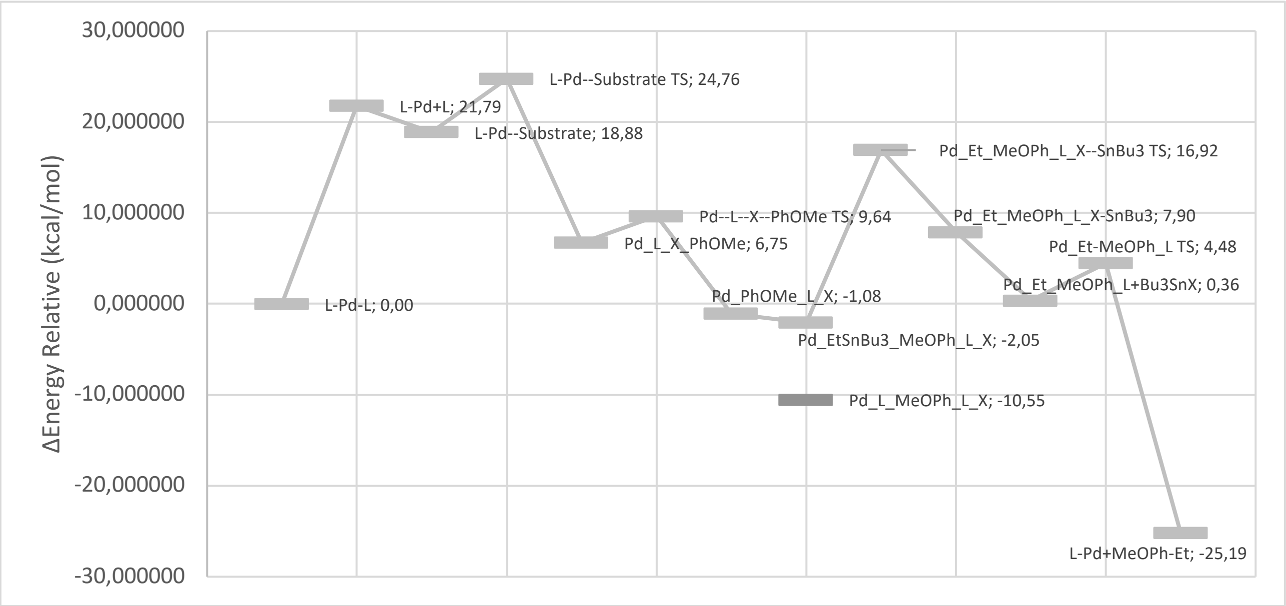

In phosphorous ligands with the same new substituent groups, similar values are obtained for the PESs when compared to Ph_3 substituent group. For the dissociated ligand, the first complex and the oxidative addition transition state lower values are obtained for $PhCF_3$ while higher values are obtained for PhOMe compared to Ph_3. The opposite behavior is observed for the isomerization and the reductive elimination, with higher values for $PhCF_3$ and lower values for PhOMe. For the transmetalation step, PhOMe has the highest value, $PhCF_3$ has an intermediate value and Ph_3 has the lowest value. In general, a negligible effect of the different ligands is seen on the energies associated to the catalyst dissociation, the transmetalation and the reductive elimination, while a stronger effect is seen on the first complex, the oxidative addition and the isomerization (the strongest effect is visible on the isomerization step with a difference of 2,47 kcal/mol between $As(PhCF_3)_3$ and $P(PhOMe)_3$). The results for phosphorous ligands with a bromine-based substrate are summarized in Table 5.

Table 5 Summary of PESs for Stille coupling reactions between PdL_2 and OMePhBr with phosphorous ligands (energies in kcal/mol)

L	*PdL+L*	*1st complex*	TS_{OA}	TS_{ISO}	TS_{TM}	TS_{RE}
$P(PhCF_3)_3$	21,43	17,79	23,76 (5,97)	14,47 (−3,32)	19,74 (1,95)	7,25 (−10,54)
PPh_3	21,82	18,87	24,86 (5,99)	13,13 (-5,74)	19,98 (1,11)	7,16 (−11,71)
$P(PhOMe)_3$	22,17	20,02	25,41 (5,39)	12,00 (−8,02)	20,79 (0,77)	6,55 (-13,47)

The PESs representation for $P(PhCF_3)_3$ and $P(PhOMe)_3$ ligands can be seen in Scheme 5 and Scheme 6.

Scheme 5 Potential energy surfaces representation for the Stille coupling reaction with $P(PhCF_3)_3$ ligand and OMePhBr substrate

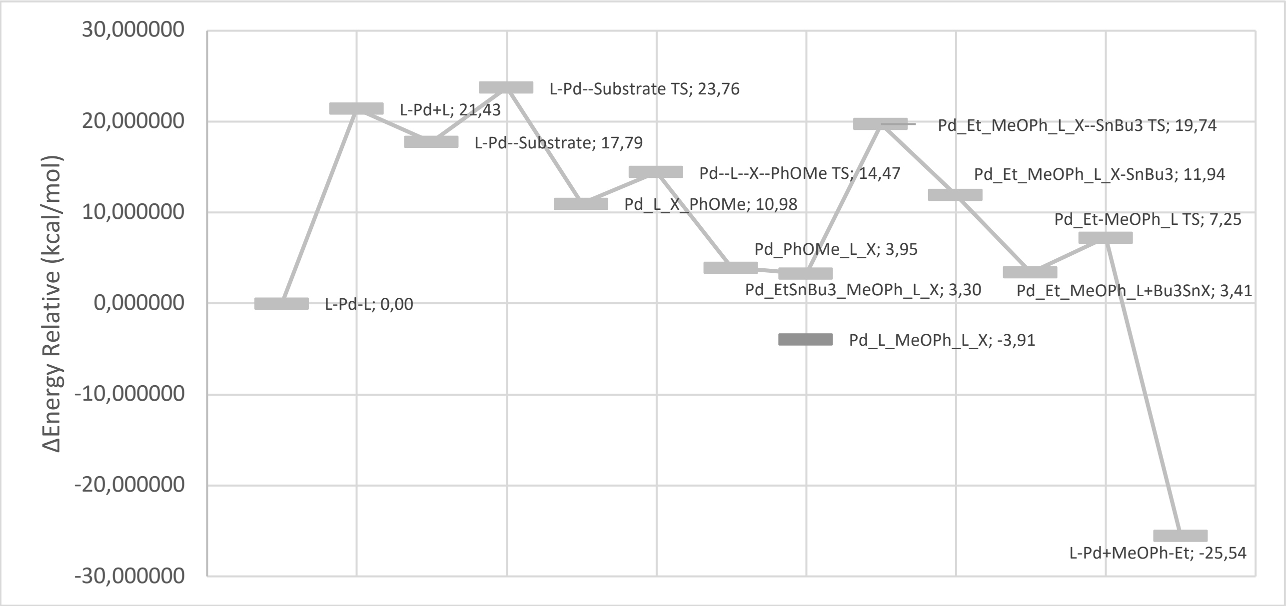

Scheme 6 Potential energy surfaces representation for the Stille coupling reaction with $P(PhOMe)_3$ ligand and OMePhBr

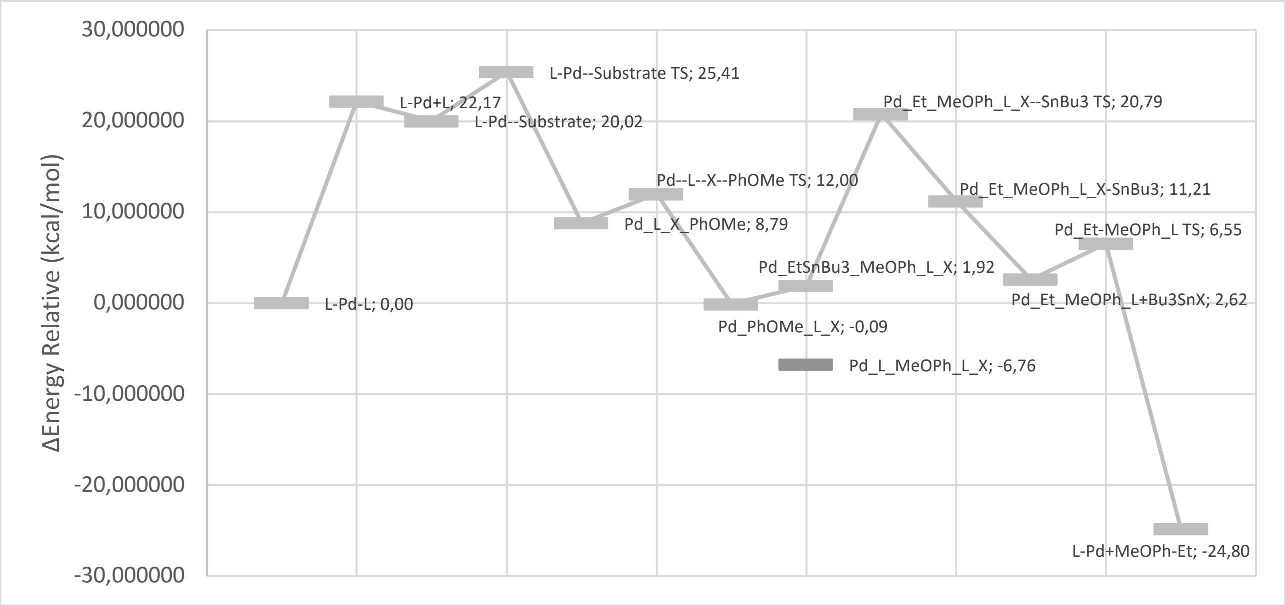

By looking at the values contained in Table 3 and Table 4 the same behavior for arsenic and phosphorous ligands is seen when comparing $(PhCF_3)_3$ and $(PhOMe)_3$ substituted ligands with Ph_3 substituted ligands: the PESs related to the dissociation of the catalyst and to the first complex are almost independent from the nature of the ligand and the same is true for the oxidative addition.

Different behaviors are encountered when considering isomerization, transmetalation and reductive elimination where significantly lower energy values are obtained with arsenic ligands when compared to phosphorous ligands.

3.1.8 Cl-Ph-OMe + PdL_2 (L = $AsPh_3$, and PPh_3)

When the halogen atoms in the substrate are changed, the results of the calculations can differ significantly. The same systems that have just been considered have also been studied with OMePhCl and OMePhI substrates in order to better understand the effects of different halogen atoms.

The first system with a chlorine-based substrate that has been considered has $AsPh_3$ ligand. In this case the dissociation of L from PdL_2 in order to obtain the starting PdL catalyst has the same energy difference of 21,62 kcal/mol that was already calculated. The system then reacts by forming the first complex, LPd-Cl-Ph-OMe, with an energy gap of 19,95 kcal/mol from the initial state. The obtained complex evolves through a transition state in the oxidative addition step of the Stille coupling reaction with an energy barrier of 24,59 kcal/mol from the initial state and 4,64 kcal/mol from the first complex. The product of the oxidative addition then isomerizes with an energy difference of 13,65 kcal/mol from the initial state, -6,30 kcal/mol from the first complex and 2,75 kcal/mol relative to the reagents involved in this step. The isomerization product reacts with the organostannane in the transmetalation step through a transition state characterized by an energy barrier of 12,88 kcal/mol from the initial state, -7,07 kcal/mol from the first complex and 10,22 kcal/mol relative to the reagents involved in this step. The final reductive elimination step has a transition state with an energy barrier of 4,94 kcal/mol from the initial state, -15,01 kcal/mol from the first complex and 4,58 kcal/mol relative to the reagents involved in this step. The PESs representation is shown in Scheme 7.

Scheme 7 Potential energy surfaces representation for the Stille coupling reaction with $AsPh_3$ ligand and OMePhCl substrate

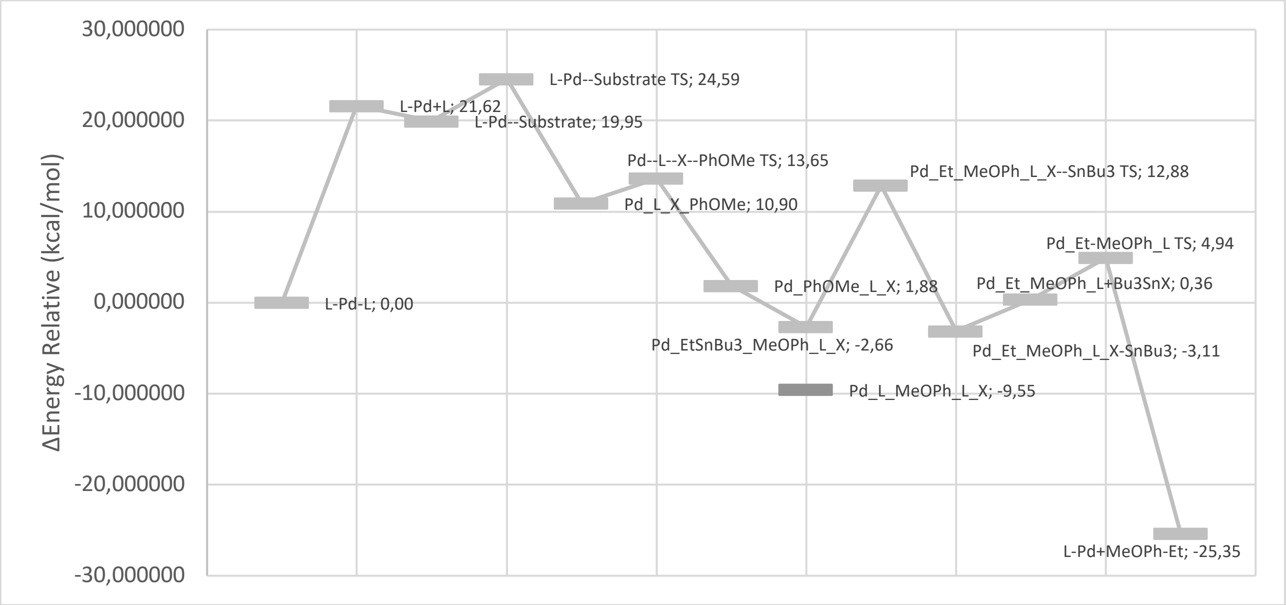

The same substrate has been studied with PPh_3 instead of $AsPh_3$ in the catalyst. In this case the dissociation of L from PdL_2 has an energy difference of 21,82 kcal/mol measured from the initial state. The subsequent complex is 20,17 kcal/mol unstable relative to the initial state. The transition state in the oxidative addition step has an energy barrier of 25,00 kcal/mol from the initial state and 4,83 kcal/mol from the first complex. The isomerization has an energy gap of 15,92 kcal/mol from the initial state, -4,25 kcal/mol from the first complex and 3,26 kcal/mol relative to the reagents involved in this step. The transmetalation transition state has an energy barrier of 16,98 kcal/mol from the initial state, -3,19 kcal/mol from the first complex and 16,39 kcal/mol relative to the reagents involved in this step. The reductive elimination transition state has an energy barrier of 7,17 kcal/mol from the initial state, -13,00 kcal/mol from the first complex and 3,98 kcal/mol relative to the reagents involved in this step. The PESs representation is shown in Scheme 8.

Scheme 8 Potential energy surfaces representation for the Stille coupling reaction with PPh3 ligand and OMePhCl substrate

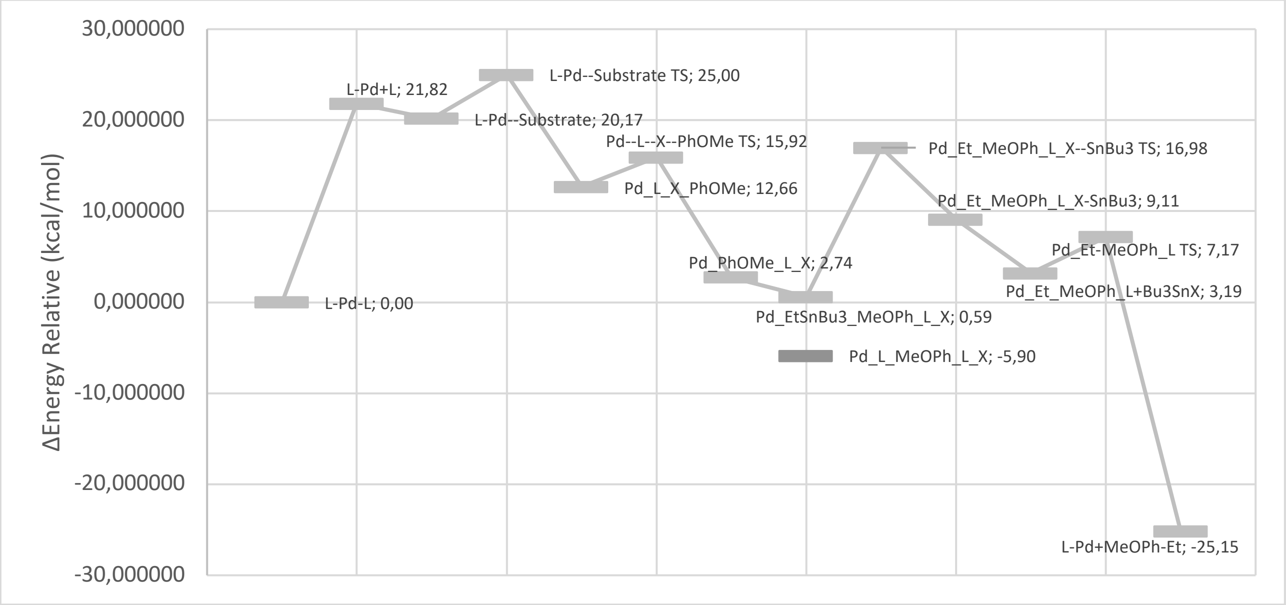

From the obtained values for the energy differences, it is once again clear that the catalyst dissociation is a very demanding process. Apart from this step, the most difficult processes are the oxidative addition, the isomerization and the transmetalation. In these systems, the reductive elimination step is characterized by relatively low values in the energy, while the oxidative addition, the isomerization and the transmetalation exhibit very high values in those energy values. In particular, the oxidative addition process is the most difficult one because it is characterized by the highest values.

By comparing the reaction of ligands containing phosphorous and ligands containing arsenic there are some similarities and some differences. PESs associated to the dissociation of the catalyst and to the first complex seem to be almost independent from the nature of the ligand because similar values have been obtained for phosphorous and arsenic ligands. The same is true for the oxidative addition step where very similar values are obtained for the two systems. Important differences are evident when considering isomerization, transmetalation and reductive elimination, steps where the arsenic ligands significantly decrease the energy levels when compared to phosphorous ligands: this effect is very significant in the transmetalation step.

3.1.9 Cl-Ph-OMe + PdL_2 (L = $As(PhCF_3)_3$, $P(PhCF_3)_3$, $As(PhOMe)_3$, and $P(PhOMe)_3$)

When other substituent groups are considered for the ligands with Cl-based substrates, a very similar behavior to Br-based substrates is observed with the same trend in the values that has already been described.

In arsenic ligands ($As(PhCF_3)_3$ and $As(PhOMe)_3$) a negligible effect of the different ligands is seen on the energies associated to the catalyst dissociation, to the first complex, to the oxidative addition and to the reductive elimination, while a stronger effect is seen on the isomerization and on the transmetalation (the strongest effect is visible on the isomerization step with a difference of 1,74 kcal/mol between As($PhCF_3$)$_3$ and As(PhOMe)$_3$). A summary of the obtained values for arsenic ligands with a chlorine-based substrate is shown in Table 6.

Table 6 Summary of PESs for Stille coupling reactions between PdL_2 and OMePhCl with arsenic ligands (energies in kcal/mol)

L	*PdL+L*	*1st complex*	TS_{OA}	TS_{ISO}	TS_{TM}	TS_{RE}
As($PhCF_3$)$_3$	21,31	20,66	24,13 (3,47)	14,80 (−5,86)	13,60 (−7,06)	5,49 (−15,17)
$AsPh_3$	21,62	19,95	24,59 (4,64)	13,65 (−6,30)	12,88 (−7,07)	4,94 (−15,01)
As(PhOMe)$_3$	21,79	20,15	25,05 (4,90)	13,06 (−7,09)	14,13 (−6,02)	4,48 (-15,67)

The PESs representation for As($PhCF_3$)$_3$ and As(PhOMe)$_3$ ligands can be seen in Scheme 9 and Scheme 10.

Scheme 9 Potential energy surfaces representation for the Stille coupling reaction with As($PhCF_3$)$_3$ ligand and OMePhCl substrate

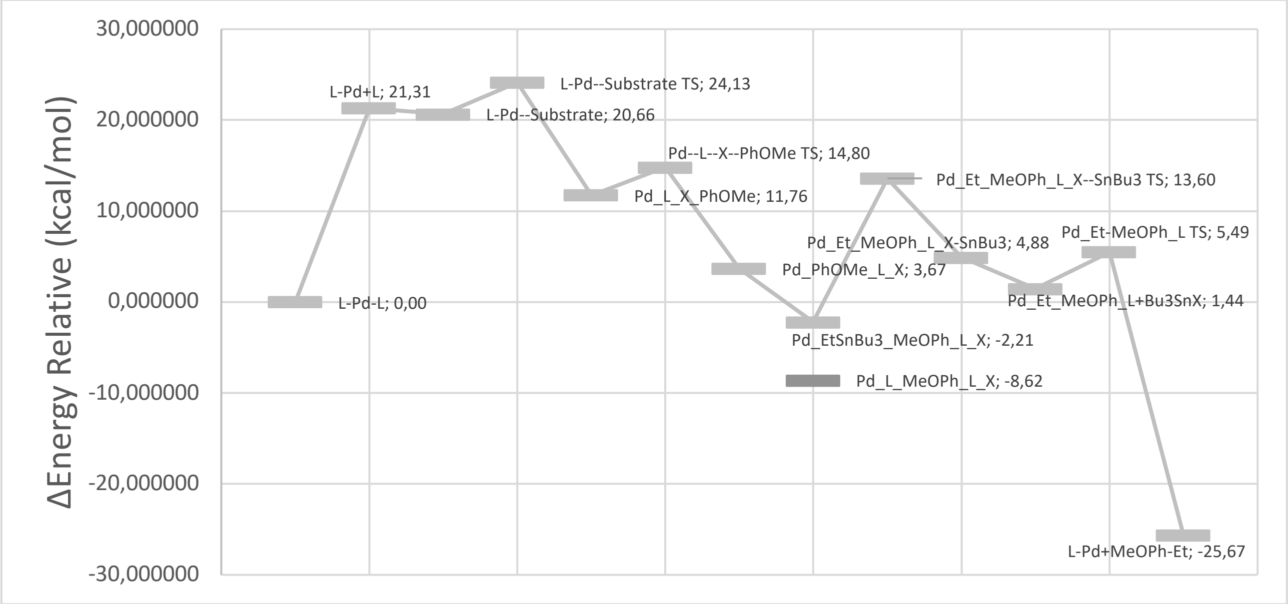

Scheme 10 Potential energy surfaces representation for the Stille coupling reaction with As(PhOMe)$_3$ ligand and OMePhCl substrate

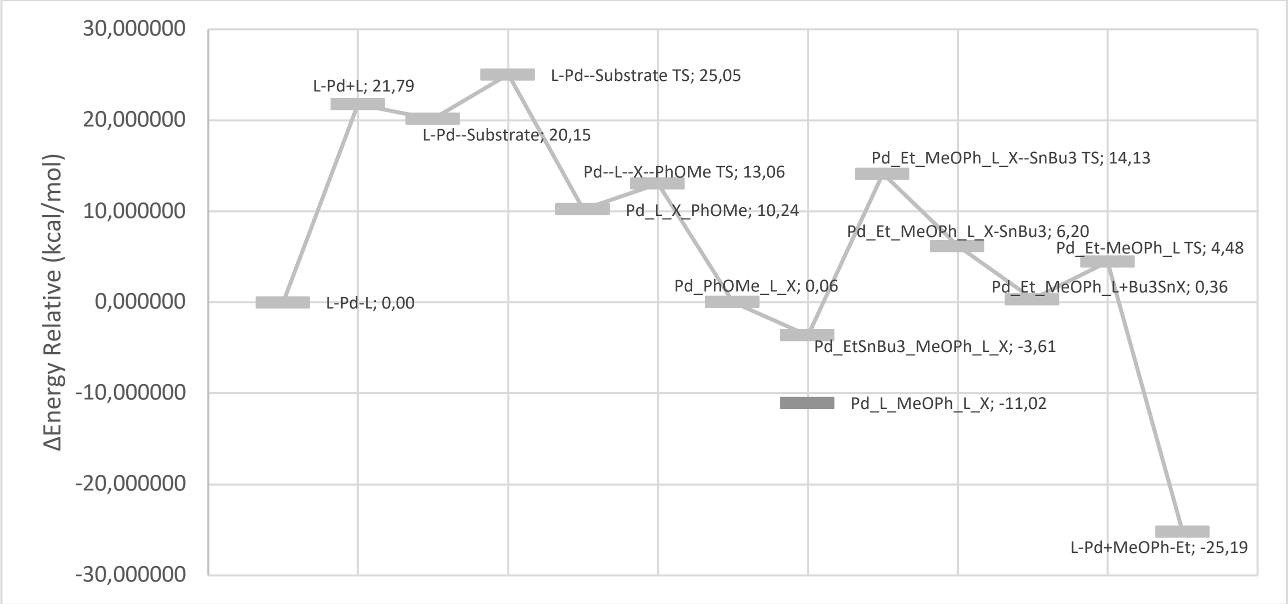

In phosphorous ligands (P($PhCF_3$)$_3$ and P(PhOMe)$_3$) a negligible effect of the different ligands is seen on the energies associated to the catalyst dissociation, to the transmetalation and to the reductive elimination, while a stronger effect can be noted on the first complex formation, on the oxidative addition and on the isomerization (the strongest effect is visible on the isomerization step with a difference of 2,60 kcal/mol between $P(PhCF_3)_3$ and $P(PhOMe)_3$). A summary of the obtained values for phosphorous ligands with a chlorine-based substrate is shown in Table 7.

Table 7 Summary of PESs for Stille coupling reactions between PdL_2 and OMePhCl with phosphorous ligands (energies in kcal/mol)

L	*PdL+L*	*1st complex*	TS_{OA}	TS_{ISO}	TS_{TM}	TS_{RE}
$P(PhCF_3)_3$	21,43	18,28	23,70 (5,42)	17,85 (−0,43)	17,34 (-0,94)	7,25 (−11,03)
PPh_3	21,82	20,17	25,00 (4,83)	15,92 (-4,25)	16,98 (-3,19)	7,17 (−13,00)
$P(PhOMe)_3$	22,17	20,65	25,56 (4,91)	15,25 (−5,40)	17,57 (-3,08)	6,55 (-14,10)

The PESs representation for $P(PhCF_3)_3$ and $P(PhOMe)_3$ ligands can be seen in Scheme 11 and Scheme 12.

Scheme 11 Potential energy surfaces representation for the Stille coupling reaction with $P(PhCF_3)_3$ ligand and OMePhCl substrate

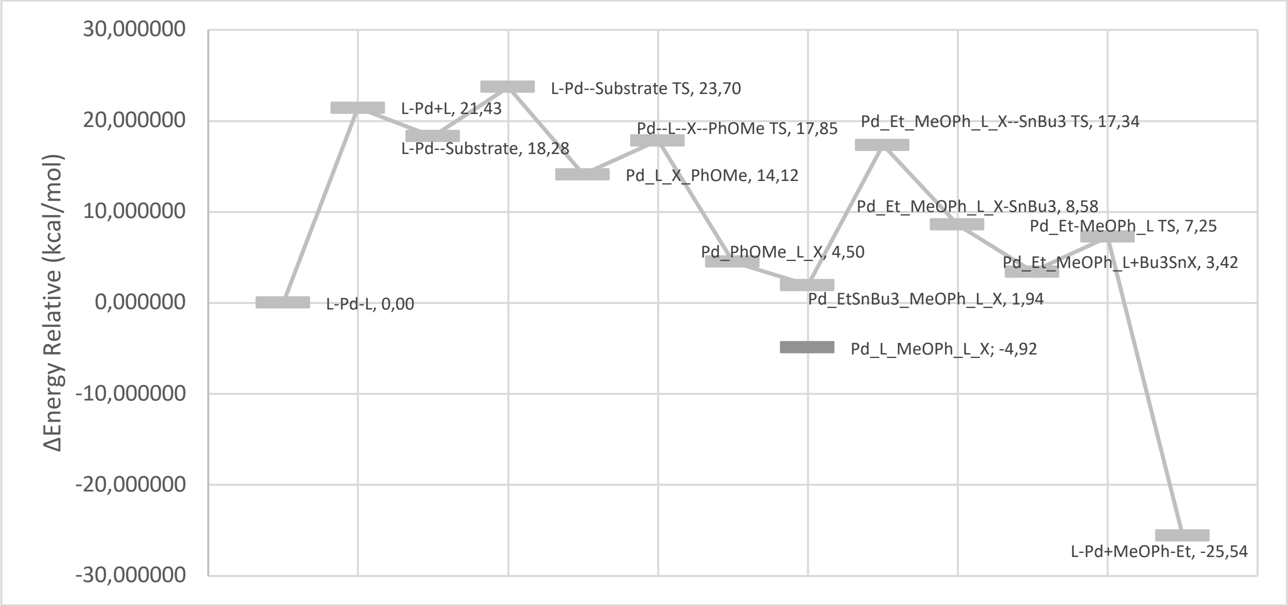

Scheme 12 Potential energy surfaces representation for the Stille coupling reaction with $P(PhOMe)_3$ ligand and OMePhCl substrate

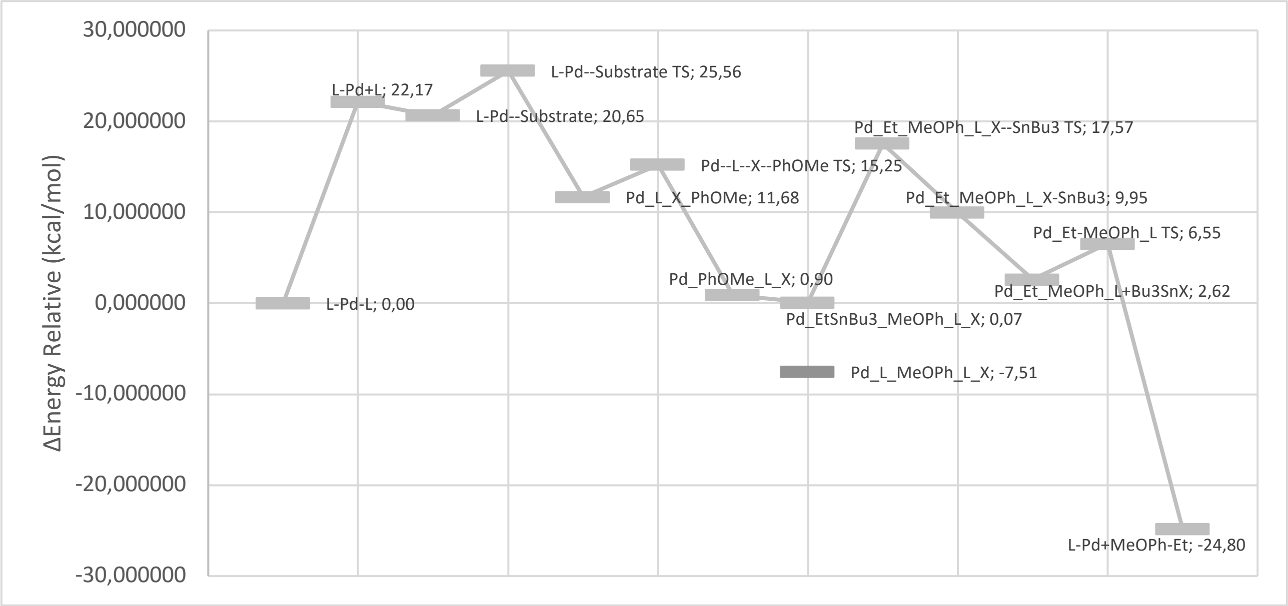

The values obtained for the reaction between the various catalysts and OMePhCl show that similar energies for the dissociation of the catalyst and the oxidative addition are obtained with arsenic and phosphorous ligands. There is a significantly lower energy associated to the $P(PhCF_3)_3$ ligand when compared to $As(PhCF_3)_3$ for the first complex (2,38 kcal/mol lower energy). In the isomerization, in the transmetalation and in the reductive elimination steps there are important differences in the energy values obtained for the two types of ligands, with arsenic ligands that have much lower energies when compared to phosphorous ligands.

3.1.10 I-Ph-OMe + PdL_2 (L = $AsPh_3$, and PPh_3)

The last systems that have been studied for trial 1 consist in the same catalysts that have already been discussed, reacting with OMePhI (as already mentioned, the data utilized below in 3.1.5 and 3.1.6 for iodine-systems comes from Prof. Imoto's work [22]). The first system with an iodine-based substrate that has been considered has $AsPh_3$ as the ligand: in this case the dissociation product of PdL_2 is 21,62 kcal/mol more unstable than the initial state. The obtained dissociated catalyst reacts with the substrate to obtain the first complex with a 15,07 kcal/mol difference from the initial state. The obtained complex evolves through a transition state in the oxidative addition step with an energy barrier of 22,26 kcal/mol from the initial state and 7,19 kcal/mol from the first complex. The obtained product then isomerizes with an energy difference of 5,96 kcal/mol from the initial state, -9,11 kcal/mol from the first complex and 2,70 kcal/mol relative to the reagents involved in this step. In the transmetalation step, a transition state characterized by an energy barrier of 18,67 kcal/mol from the initial state, 3,60 kcal/mol from the first complex and 18,98 kcal/mol relative to the reagents involved in this step was calculated. The last step, the reductive elimination has a transition state with an energy barrier of 6,23 kcal/mol from the initial state, -8,84 kcal/mol from the first complex and 3,81 kcal/mol relative to the reagents involved in this step. The PESs representation is shown in Scheme 13.

Scheme 13 Potential energy surfaces representation for the Stille coupling reaction with $AsPh_3$ ligand and OMePhI substrate

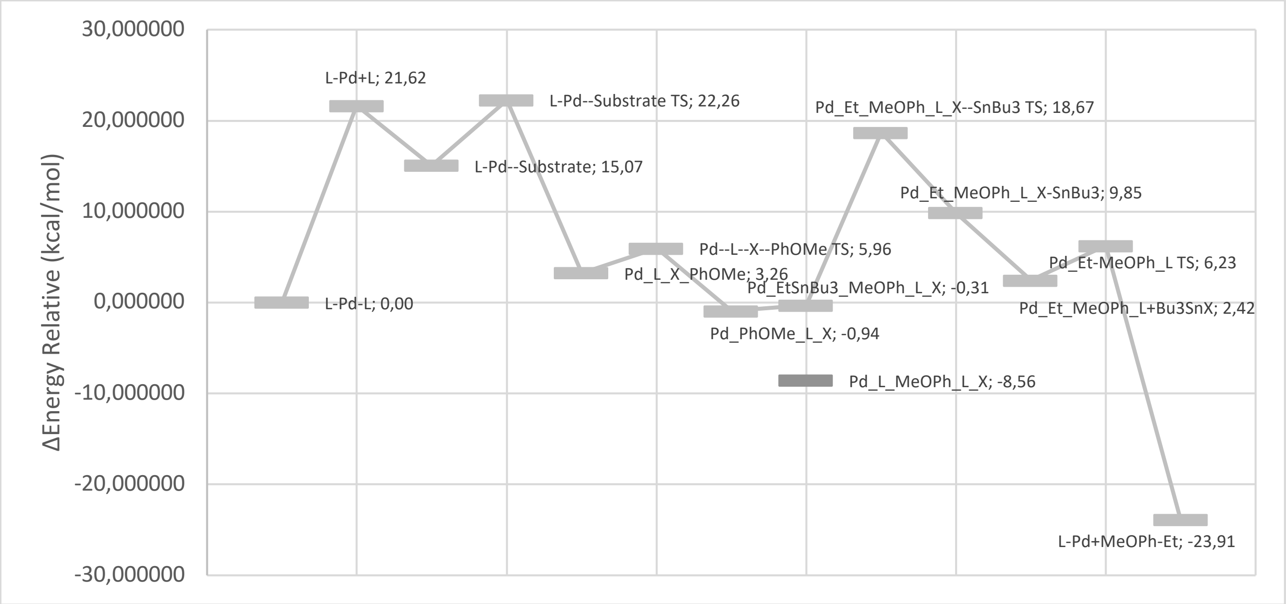

The same substrate has been studied with a catalyst containing PPh_3 instead of $AsPh_3$. In this case the dissociation of L from PdL_2 is 21,82 kcal/mol unstable relative to the initial state and the obtained first complex exhibits an energy gap of 16,04 kcal/mol from the initial state. The transition state in the oxidative addition step has an energy barrier of 22,88 kcal/mol from the initial state and 6,76 kcal/mol from the first complex. The isomerization has an energy difference of 8,48 kcal/mol from the initial state, -7,56 kcal/mol from the first complex and 10,70 kcal/mol relative to the reactants involved in this step. The transmetalation transition state has an energy barrier of 22,40 kcal/mol from the initial state, 6,36 kcal/mol from the first complex and 18,78 kcal/mol relative to the reagents involved in this step. The last step has a transition state with an energy barrier of 8,56 kcal/mol from the initial state, -7,48 kcal/mol from the first complex and 3,90 kcal/mol relative to the reagents involved in this step. The PESs representation is shown in Scheme 14.

Scheme 14 Potential energy surfaces representation for the Stille coupling reaction with PPh_3 ligand and OMePhI substrate

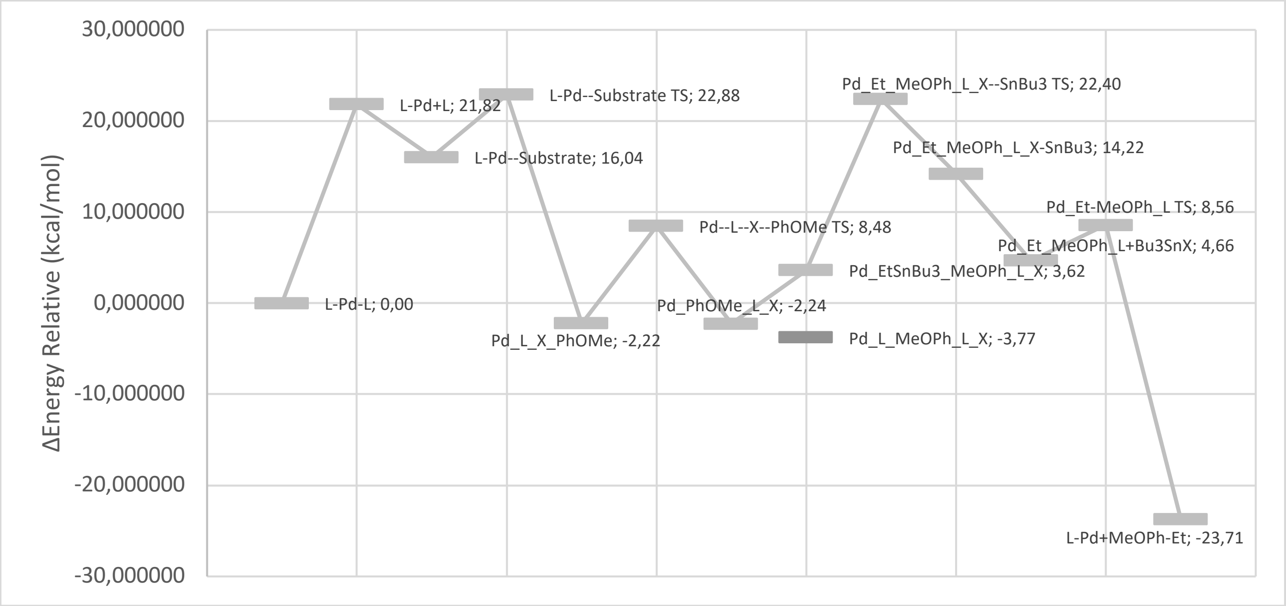

The obtained values show that the dissociation of the ligand is still characterized by a high energy level as it has been noted for Br-based and Cl-based substrates. The oxidative addition and the transmetalation steps are characterized by elevated energy levels, while the isomerization and the reductive elimination steps show way lower values in energy. The energy associated to the first complex is intermediate with values between 15,07 kcal/mol for $AsPh_3$ and 16,04 kcal/mol for PPh_3.

The PESs associated to the dissociation of the catalyst and to the first complex seem to be almost independent from the nature of the ligand with only marginally higher values associated to phosphorous ligands. In the oxidative addition and reductive elimination steps a similar tendency has been found with the value of PPh_3 ligands being 0,62 kcal/mol higher for oxidative addition and 2,33 kcal/mol higher for reductive elimination when compared to $AsPh_3$ ligands. Important differences are evident when considering isomerization and transmetalation where arsenic ligands significantly decrease the energy levels when compared to phosphorous ligands (by 2,52 kcal/mol and by 3,73 respectively).

3.1.11 I-Ph-OMe + PdL_2 (L = $As(PhCF_3)_3$, $P(PhCF_3)_3$, $As(PhOMe)_3$, and $P(PhOMe)_3$)

The other substituent groups in the ligands have also been considered for the reaction with I-based substrates.

In arsenic ligands ($As(PhCF_3)_3$ and $As(PhOMe)_3$), almost no effect of the different ligands is seen on the energies associated to the catalyst dissociation, to the oxidative addition and to the transmetalation. In the first complex similar energy values have been obtained for all the ligands, with $As(PhCF_3)_3$ showing a marginally lower energy. In the isomerization step, $As(PhCF_3)_3$ ligands exhibited higher values when compared to the other ligands. For the reductive elimination step the highest values were calculated for $As(PhCF_3)_3$, intermediate values were obtained for $AsPh_3$ and the lowest values were noted for $As(PhOMe)_3$, but the differences are almost negligible. A summary of the obtained values for arsenic ligands with a I-based substrate is shown in Table 8.

Table 8 Summary of PESs for Stille coupling reactions between PdL_2 and OMePhI with arsenic ligands (energies in kcal/mol)

L	PdL+L	1st complex	TS_{OA}	TS_{ISO}	TS_{TM}	TS_{RE}
$As(PhCF_3)_3$	21,17	14,07	21,22 (7,15)	7,45 (−6,62)	19,05 (4,98)	6,92 (−7,15)
$AsPh_3$	21,62	15,07	22,26 (7,19)	5,96 (−9,11)	18,67 (3,60)	6,23 (−8,84)
$As(PhOMe)_3$	21,79	15,15	21,50 (6,35)	5,43 (−9,72)	19,34 (0,44)	6,19 (-8,96)

The PESs representation for $As(PhCF_3)_3$ and $As(PhOMe)_3$ ligands can be seen in Scheme 15 and Scheme 16.

Scheme 15 Potential energy surfaces representation for the Stille coupling reaction with $As(PhCF_3)_3$ ligand and OMePhI substrate

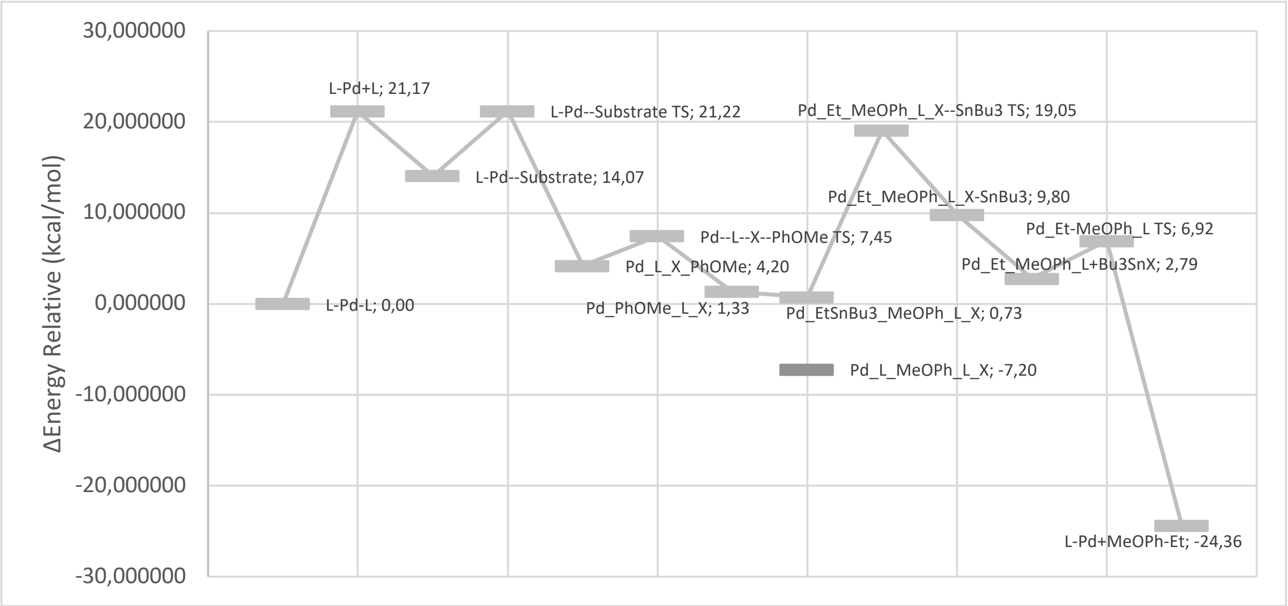

Scheme 16 Potential energy surfaces representation for the Stille coupling reaction with $As(PhOMe)_3$ ligand and OMePhI substrate

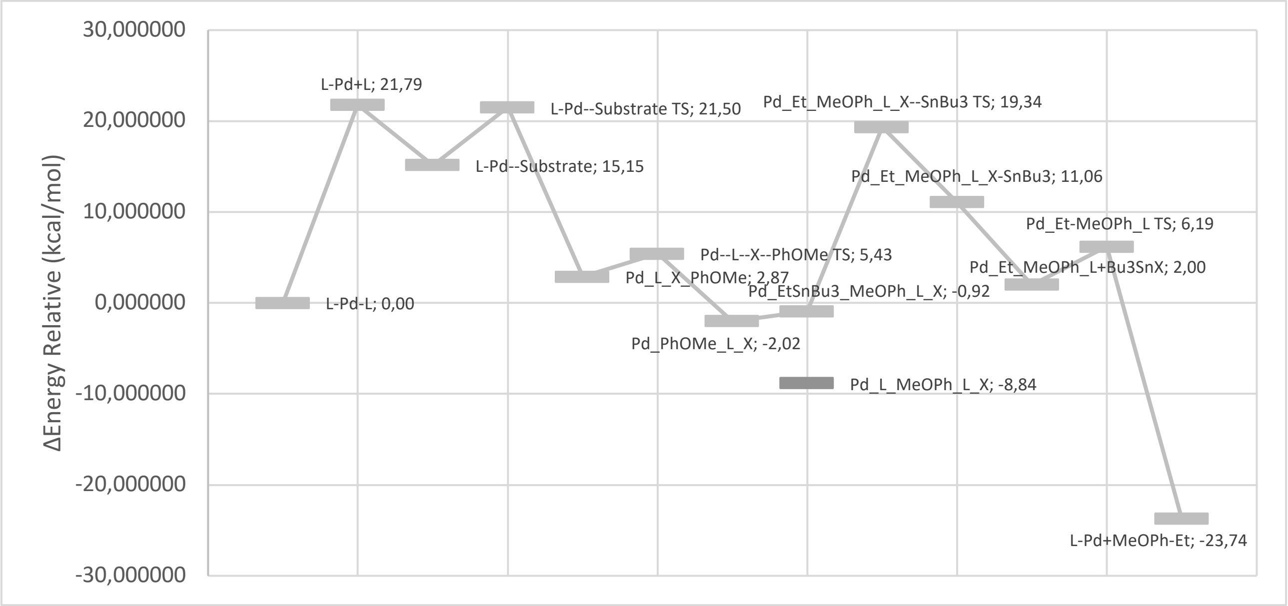

In phosphorous ligands ($P(PhCF_3)_3$ and $P(PhOMe)_3$) a negligible effect of the different ligands is seen on the energies associated to the catalyst dissociation, to the oxidative addition and to the reductive elimination, while a stronger influence of the ligand has been found on the to the energy associated to the first complex (with $P(PhCF_3)_3$ showing a significant lower value when compared to the other ligands), on the transmetalation (with higher values when compared to PPh_3) and on the isomerization: isomerization in particular exhibited the largest difference between the different ligands with lower values for $P(PhOMe)_3$ and higher values for $P(PhCF_3)_3$ when compared to PPh_3. A summary of the obtained values for phosphorous ligands with a iodine-based substrate is shown in Table 9.

Table 9 Summary of PESs for Stille coupling reactions between PdL_2 and OMePhI with phosphorous ligands (energies in kcal/mol)

L	*PdL+L*	*1st complex*	TS_{OA}	TS_{ISO}	TS_{TM}	TS_{RE}
$P(PhCF_3)_3$	21,43	14,92	21,92 (7,00)	10,50 (−4,42)	23,77 (8,85)	8,81 (−6,11)
PPh_3	21,82	16,04	22,88 (6,84)	8,48 (-7,56)	22,40 (6,36)	8,56 (−7,48)
$P(PhOMe)_3$	22,17	16,49	22,51 (6,02)	7,93 (−8,56)	23,48 (6,99)	8,81 (-7,68)

The PESs representation for $P(PhCF_3)_3$ and $P(PhOMe)_3$ ligands can be seen in Scheme 17 and Scheme 18.

Scheme 17 Potential energy surfaces representation for the Stille coupling reaction with $P(PhCF_3)_3$ ligand and OMePhI substrate

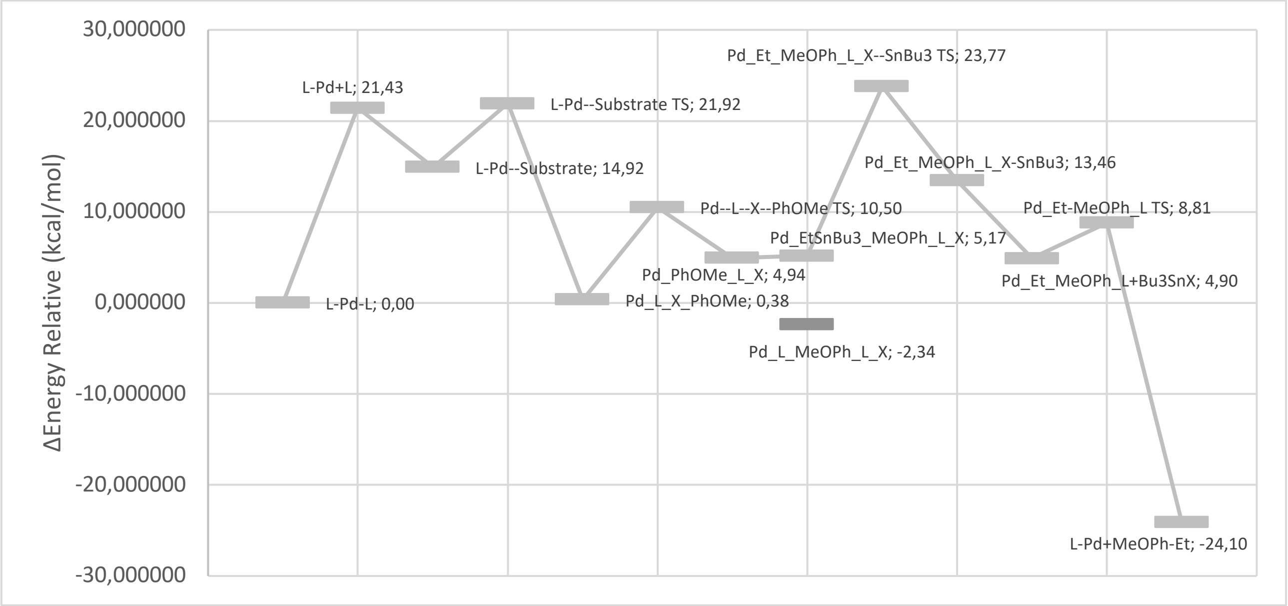

Scheme 18 Potential energy surfaces representation for the Stille coupling reaction with $P(PhOMe)_3$ ligand and OMePhCl substrate

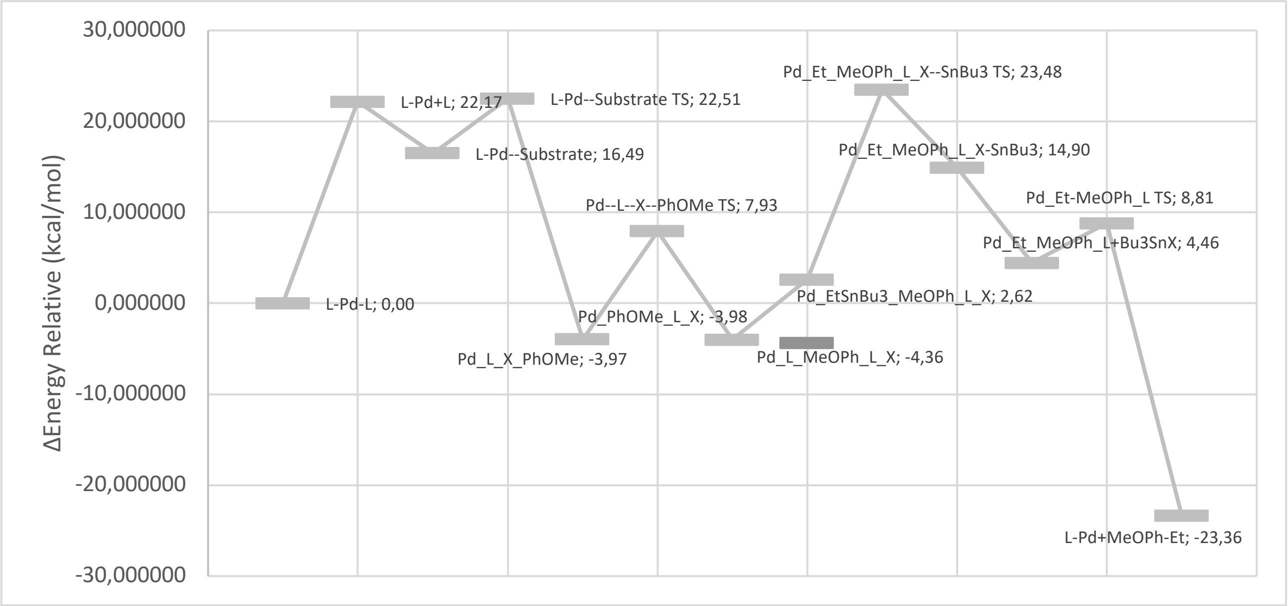

The values obtained for the reaction with OMePhI as the substrate show that similar energies for the dissociation of the catalyst and for the oxidative addition are obtained for arsenic and phosphorous ligands (with only marginally lower values obtained for arsenic ligands). The first complex has similar energy levels among the different type of ligands, but usually phosphorous ligands show higher values of energy. In the isomerization and in the transmetalation steps there are important differences in the energy values obtained for the two types of ligands, with arsenic ligands that have much lower energies when compared to phosphorous ligands. In the reductive elimination step, lower values have been obtained for arsenic ligands when compared to phosphorous ligands, with a difference around 2,5 kcal/mol.

3.1.12 Comparative Analyses for the Catalytic Systems

Now the results of the different systems can be compared to point out the effect of the various halogen atoms.

First, let us focus on the energetics on arsenic systems tabulated in Table 10. Similar energy values for the catalyst dissociation have been calculated with all the halogens and substituents. The catalytic dissociation is one of the energy-demanding steps, thus, the energy level of PdL+L should be a good criterion to compare the energy levels of transition states in the reaction, and to judge whether further reaction steps can easily proceed or not. That is, if a transition state in further reaction steps is higher in energy than PdL+L, the corresponding step will become an energy-demanding step too, and the reaction will hardly proceed. For the first complex, I-based substrates show much lower energies when compared to Br-based and Cl-based substrates.

The energy associated to the oxidative addition, comparable for Br-based and Cl-based substrates, is higher than the corresponding catalytic dissociation. In contrast, significantly lower values have been calculated for I-based substrates, making the transition state energetically comparable to the state of PdL+L.

In the isomerization step very low energy values have been calculated for I-based substrates, intermediate values have been obtained for Br-based substrates and higher values have been noted for Cl-based substrates (the gap between the values for I-based substrates and Br-based substrates is much larger than the gap between the values for Br-based substrates and Cl-based substrates).

The transmetalation step is characterized by higher energy values for I-based substrates, intermediate values for Br-based substrates, and lower values for Cl-based substrates (the lower values are always obtained for arsenic ligands).

For the reductive elimination step, the energy associated to the transition state is dependent on the halogen atom considered. Almost the same values have been calculated for chlorine and bromine substrates, while higher values have been obtained for iodine systems.

In summary, in arsenic systems, the oxidative addition process is the rate-determining step for Stille-coupling reactions, and the energy associated to this step was minimized by utilizing I-based substrates.

Table 10 Summary of PESs for Stille coupling reactions between PdL_2 and the different substrates with the various arsenic ligands (energies in kcal/mol) ordered by their position on the periodic table

L	PdL+L	1st complex	TS_{OA}	TS_{ISO}	TS_{TM}	TS_{RE}
$Cl\_As(PhCF_3)_3$	21,31	20,66	24,13 (3,47)	14,80 (−5,86)	13,60 (−7,06)	5,49 (−15,17)
Cl_AsPh_3	21,62	19,95	24,59 (4,64)	13,65 (−6,30)	12,88 (−7,07)	4,94 (−15,01)
$Cl\_As(PhOMe)_3$	21,79	20,15	25,05 (4,90)	13,06 (−7,09)	14,13 (−6,02)	4,48 (-15,67)
$Br\_As(PhCF_3)_3$	21,31	17,60	23,36 (5,76)	12,30 (−5,30)	16,18 (−1,42)	5,49 (−12.10)

Br_AsPh$_3$	21,62	18,35	24,32 (5,97)	10,59 (−7,76)	15,98 (−2,37)	4,94 (−12,11)
Br_As(PhOMe)$_3$	21,79	18,88	24,76 (5,88)	9,64 (−9,24)	16,92 (−1,96)	4,48 (-14,40)
I_As(PhCF$_3$)$_3$	21,17	14,07	21,22 (7,15)	7,45 (−6,62)	19,05 (4,98)	6,92 (−7,15)
I_AsPh$_3$	21,62	15,07	22,26 (7,19)	5,96 (−9,11)	18,67 (3,60)	6,23 (−8,84)
I_As(PhOMe)$_3$	21,79	15,15	21,50 (6,35)	5,43 (−9,72)	19,34 (4,19)	6,19 (-8,96)

Next, let us turn our attention on the energetics of phosphorous systems tabulated in Table 11, by comparing with the values obtained for arsenic systems. Similar energy values for the catalyst dissociation have been calculated with all the halogens and the substituents when compared to arsenic systems, so the same considerations remain valid.

High energy values for the oxidative addition processes in phosphorous systems were obtained, similarly to arsenic systems, thus, the oxidative addition is an energy-demanding step also in phosphorous systems, in addition to catalytic dissociation. Note that in this case, the energies associated to oxidative addition's transition state decrease with Cl > Br > I.

DFT calculations also found a destabilizing effect of phosphorous ligands on the transition states of isomerization and transmetalation. In this case, the energies associated to isomerization's transition state grow in the order I < Br < Cl, while the opposite is true for the transmetalation. The high values obtained for the transmetalation mean that this is a rate-determining step, in addition to the catalytic dissociation and oxidative addition.

For the reductive elimination step, the same trend observed for arsenic ligands is observed for phosphorous ligands, but the obtained values are higher in this case.

In conclusion, the comparative analyses found that the oxidative addition in Stille coupling reactions is an energy demanding step both in arsenic and phosphorous systems, in addition to the catalytic dissociation indispensable to begin the reaction. By changing the halogen atom attached to the substrate, we can modulate the energy levels of oxidative addition's transition state and in fact, the use of I-based substrates stabilizes the associated energy level making it comparable to the catalytic dissociation (and this is true for both arsenic and phosphorous systems). On the other hand, different types of palladium catalysts with different ligands can strongly influence the energy levels of the transition states associated to isomerization and transmetalation. In fact, the use of arsenic ligands can effectively stabilize both transition states, while such stabilizing effects cannot be found with phosphorous ligands. As a result, for phosphorous systems, the transmetalation process becomes an energy-demanding step in addition to the oxidative addition and the catalytic dissociation. Finally, the combination of arsenic-containing catalysts and I-based substrates seems to be the best species to be used in Stille coupling reactions. All the different effects involved in the various steps will be discussed in the discussion part.

Table 11 Summary of PESs for Stille coupling reactions between PdL$_2$ and the different substrates with the various phosphorous ligands (energies in kcal/mol) ordered by their position on the periodic table

L	PdL+L	1st complex	TS$_{OA}$	TS$_{ISO}$	TS$_{TM}$	TS$_{RE}$
Cl_P(PhCF$_3$)$_3$	21,43	18,28	23,70 (5,42)	17,85 (−0,43)	17,34 (-0,94)	7,25 (−11,03)
Cl_PPh$_3$	21,82	20,17	25,00 (4,83)	15,92 (-4,25)	16,98 (-3,19)	7,17 (−13,00)
Cl P(PhOMe)$_3$	22,17	20,65	25,56 (4,91)	15,25 (−5,40)	17,57 (-3,08)	6,55 (-14,10)
Br P(PhCF$_3$)$_3$	21,43	17,79	23,76 (5,97)	14,47 (−3,32)	19,74 (1,95)	7,25 (−10,54)
Br_PPh$_3$	21,82	18,87	24,86 (5,99)	13,13 (-5,74)	19,98 (1,11)	7,16 (−11,71)
Br_P(PhOMe)$_3$	22,17	20,02	25,41 (5,39)	12,00 (−8,02)	20,79 (0,77)	6,55 (-13,47)
I_P(PhCF$_3$)$_3$	21,43	14,92	21,92 (7,00)	10,50 (−4,42)	23,77 (8,85)	8,81 (−6,11)

I_PPh_3	21,82	16,04	22,88 (6,84)	8,48 (-7,56)	22,40 (6,36)	8,56 (−7,48)
$I\_P(PhOMe)_3$	22,17	16,49	22,51 (6,02)	7,93 (−8,56)	23,48 (6,99)	8,81 (-7,68)

To further optimize catalytic reactivity of Stille coupling reactions, different substituent groups can be considered in the substrate. The obtained results will be presented in trial 2.

3.2 Trial 2

In order to see if also the substituent group bonded to the substrate has a role in the behavior of the reaction, four additional systems have been considered with two different substrates and the same p-anysil ligand in every system (with the ligand containing arsenic and phosphorous). The first considered substrate is (p-iodo)nitrobenzene, while the second substrate is iodobenzene. The data reported for iodobenzene’s systems have been calculated by Prof. Yumura who allowed me to use them in this thesis project to have a more complete point of view.

The characteristics of the catalyst like the geometry, the charge and the orbital configuration have remained the same as in 3.1. Different features have been obtained for the new substrates. With NO_2 as the substituent, a different charge on the halogen atom of the substrate has been found through NPA and the same is true for H: in the first case a charge of 0,17 has been obtained, while in the second case a charge of 0,11 has been obtained. The I-C bond length is also influenced by the presence of the new substituent group, with 2,1 Å bond length for NO_2 and 2,2 Å bond length for H. By looking at the frontier orbitals of the substrates, a LUMO+1 (associated to the σ^* orbital) at an orbital energy of -1,61 eV has been obtained for NO_2, while a LUMO at an orbital energy of -1,08 eV has been obtained for H.

The catalytic cycle proposed by Prof. Imoto is still considered as reference and the obtained PESs representations follow the steps that have already been mentioned in the previous section.

The first system that has been considered has an arsenic-based ligand and NO_2PhI as the substrate: in this case the dissociation product of PdL_2 is 21,79 kcal/mol more unstable than the initial state. The obtained dissociated catalyst reacts with the substrate to obtain the first complex with a 16,11 kcal/mol difference from the initial state. The obtained complex evolves through a transition state in the oxidative addition step with an energy difference of 19,93 kcal/mol from the initial state and 3,82 kcal/mol from the first complex. The obtained product then isomerizes with an energy difference of 2,75 kcal/mol from the initial state, -13,36 kcal/mol from the first complex and 2,56 kcal/mol relative to the reagents involved in this step. In the transmetalation step, the transition state is characterized by an energy barrier of 13,31 kcal/mol from the initial state, -2,80 kcal/mol from the first complex and 17,26 kcal/mol relative to the reagents involved in this step was calculated. The last step, the reductive elimination has a transition state 0,93 kcal/mol more unstable from the initial state, -15,18 kcal/mol from the first complex and 3,76 kcal/mol from the reagents involved in this step. The PESs representation is shown in Scheme 19.

Scheme 19 Potential energy surfaces representation for the Stille coupling reaction with As(PhOMe)$_3$ ligand and NO$_2$PhI substrate

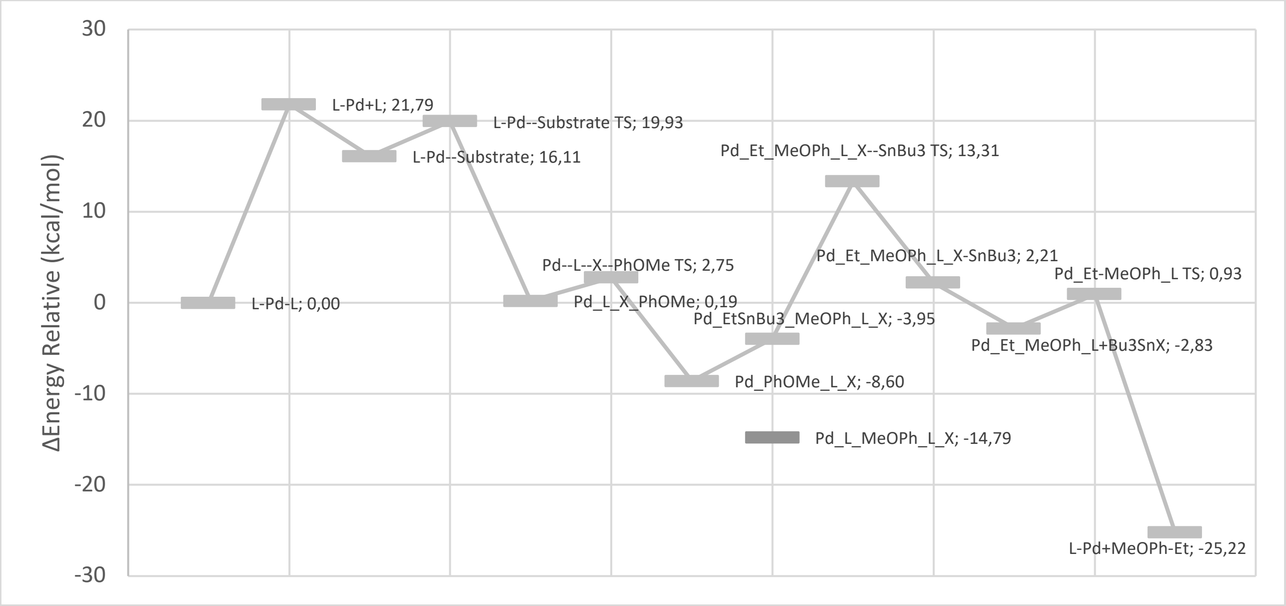

Then P(PhOMe)$_3$ has been considered as the ligand with NO$_2$PhI as the substrate. In this case the dissociation of L from PdL$_2$ is 22,17 kcal/mol unstable relative to the initial state and the obtained first complex exhibits an energy gap of 17,28 kcal/mol from the initial state. The transition state in the oxidative addition step has an energy barrier of 23,00 kcal/mol from the initial state and 5,72 kcal/mol from the first complex. The isomerization has an energy difference of 4,97 kcal/mol from the initial state, -12,31 kcal/mol from the first complex and 3,30 kcal/mol relative to the reactants involved in this step. The transmetalation transition state has an energy barrier of 17,15 kcal/mol from the initial state, -0,13 kcal/mol from the first complex and 18,01 kcal/mol relative to the reagents involved in this step. The last step has a transition state with an energy barrier of 2,94 kcal/mol from the initial state, -14,34 kcal/mol from the first complex and 3,94 kcal/mol relative to the reagents involved in this step. The PESs representation is shown in Scheme 20.

Scheme 20 Potential energy surfaces representation for the Stille coupling reaction with P(PhOMe)$_3$ ligand and NO$_2$PhI substrate

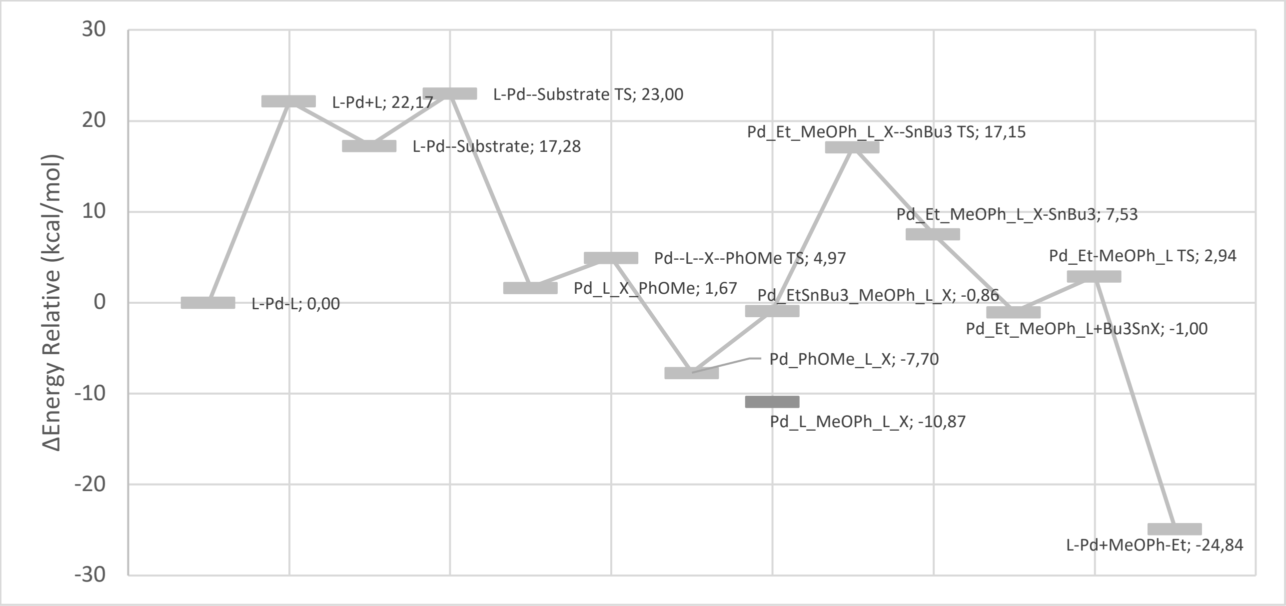

A summary of the obtained energy values for the two considered systems is shown in Table 12.

Table 12 Summary of PESs for Stille coupling reactions between PdL_2 and NO_2PhI with arsenic and phosphorous ligands (energies in kcal/mol)

L	PdL+L	1st complex	TS_{OA}	TS_{ISO}	TS_{TM}	TS_{RE}
$As(PhOMe)_3$	21,79	16,11	19,93 (3,82)	2,75 (−13,36)	13,31 (−2,80)	0,93 (-15,18)
$P(PhOMe)_3$	22,17	17,28	23,00 (5,72)	4,97 (−12,31)	17,15 (−0,13)	2,94 (-14,34)

The PESs associated to the dissociation of the catalyst and to the first complex seem to be practically independent from the nature of the ligand with only slightly smaller values associated to arsenic ligands. Important differences are evident when considering oxidative addition, isomerization, transmetalation and reductive elimination, where arsenic ligands significantly decrease the energy levels when compared to phosphorous ligands (by 3,07 kcal/mol, by 2,22 kcal/mol, by 3,84 kcal/mol, and by 2,01 kcal/mol respectively).

The third considered system has an arsenic-based ligand and iodobenzene as the substrate: in this case the dissociation product of PdL_2 is 21,79 kcal/mol more unstable than the initial state. The obtained dissociated catalyst reacts with the substrate to obtain the first complex with a 15,40 kcal/mol difference from the initial state. The obtained complex evolves through a transition state in the oxidative addition step with an energy difference of 21,31 kcal/mol from the initial state and 5,91 kcal/mol from the first complex. The obtained product then isomerizes with an energy difference of 5,43 kcal/mol from the initial state, -9,97 kcal/mol from the first complex and 10,27 kcal/mol relative to the reagents involved in this step. In the transmetalation step, the transition state is characterized by an energy barrier of 18,67 kcal/mol from the initial state, 3,27 kcal/mol from the first complex and 20,20 kcal/mol relative to the reagents involved in this step was calculated. The last step, the reductive elimination has a transition state 6,25 kcal/mol more unstable from the initial state, -9,15 kcal/mol from the first complex and 4,80 kcal/mol from the reagents involved in this step. The PESs representation is shown in Scheme 21.

Scheme 21 Potential energy surfaces representation for the Stille coupling reaction with $As(PhOMe)_3$ ligand and PhI substrate

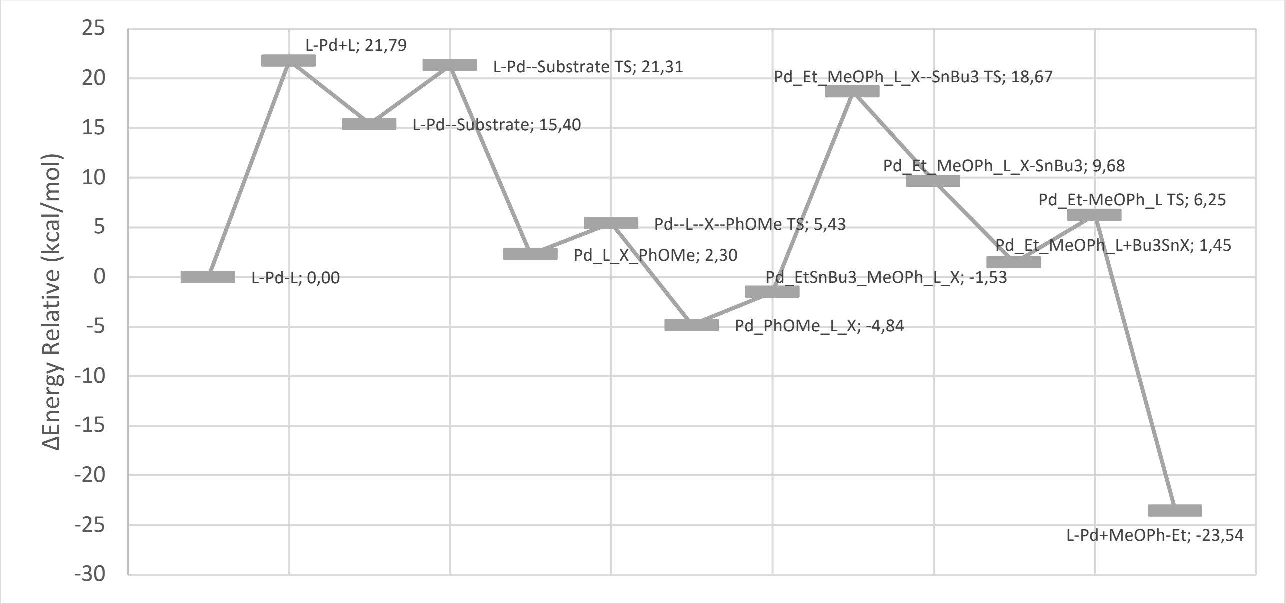

Then $P(PhOMe)_3$ has been considered as the ligand with Ph-I as the substrate. In this case the dissociation of L from PdL_2 is 22,17 kcal/mol unstable relative to the initial state and the obtained first complex exhibits an energy gap of 16,66 kcal/mol from the initial state. The transition state in the oxidative addition step has an energy barrier of 22,48 kcal/mol from the initial state and 5,82 kcal/mol from the first complex. The isomerization has an energy difference of 7,90 kcal/mol from the initial state, -8,76 kcal/mol from the first complex and 3,82 kcal/mol relative to the reactants involved in this step. The transmetalation transition state has an energy barrier of 22,95 kcal/mol from the initial state, 6,29 kcal/mol from the first complex and 21,82 kcal/mol relative to the reagents involved in this step. The last step has a transition state with an energy barrier of 8,21 kcal/mol from the initial state, -8,45 kcal/mol from the first complex and 4,55 kcal/mol relative to the reagents involved in this step. The PESs representation is shown in Scheme 22.

Scheme 22 Potential energy surfaces representation for the Stille coupling reaction with P(PhOMe)$_3$ ligand and PhI substrate

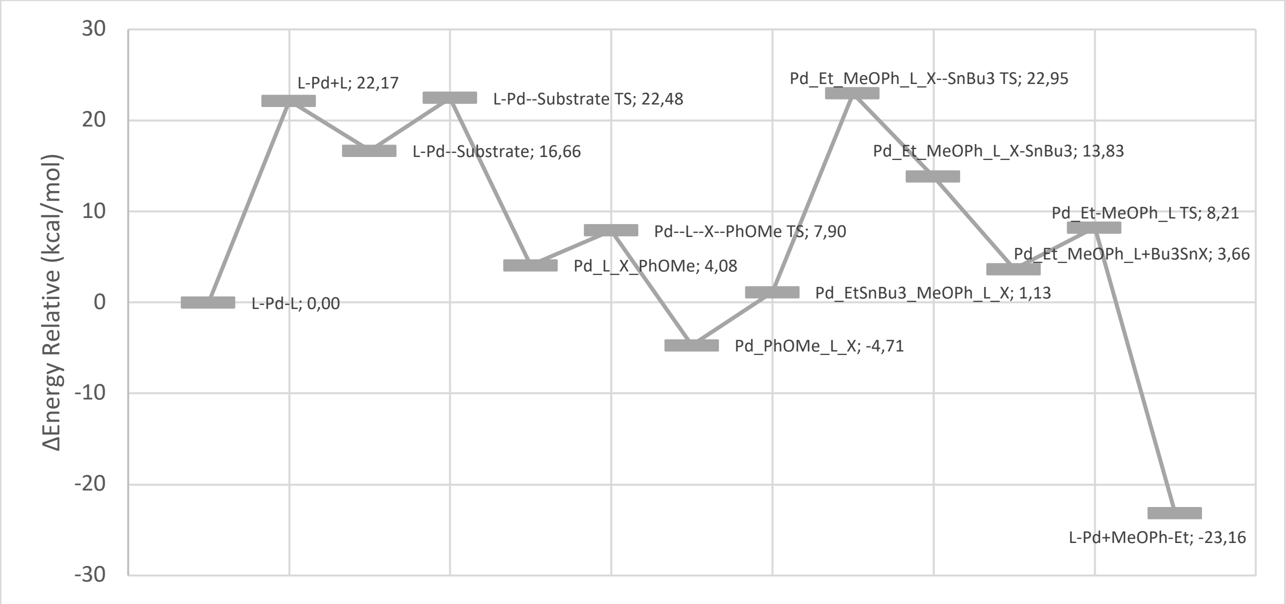

A summary of the obtained energy values for the two considered systems is shown in Table 13. It is worth mentioning that no alternative route has been calculated for these two systems.

Table 13 Summary of PESs for Stille coupling reactions between PdL$_2$ and PhI with arsenic and phosphorous ligands (energies in kcal/mol)

L	PdL+L	1st complex	TS_{OA}	TS_{ISO}	TS_{TM}	TS_{RE}
As(PhOMe)$_3$	21,79	15,40	21,31 (5,91)	5,43 (−9,97)	18,67 (3,27)	6,25 (-9,15)
P(PhOMe)$_3$	22,17	16,66	22,48 (5,82)	7,90 (-8,76)	22,95 (6,29)	8,21 (-8,45)

The PESs related to the dissociation of the catalyst and to the first complex for arsenic ligands and phosphorous ligands are similar with only slightly smaller values for arsenic systems. In the oxidative addition a similar behavior has been found with the value associated to phosphorous ligands being only 1,17 kcal/mol higher when compared to arsenic ligands. Important differences are evident when considering isomerization, transmetalation and reductive elimination, where arsenic ligands significantly decrease the energy levels when compared to phosphorous ligands (by 2,47 kcal/mol, by 4,28kcal/mol, and by 1,96 kcal/mol respectively).

Comparative analyses found that for both substrates, the catalyst dissociation and the oxidative addition are again energy demanding steps (both in arsenic and phosphorous systems). By changing the substituent group bonded to the substrate, very similar energy values for the oxidative addition have been obtained in all the cases, with slightly lower values associated to NO_2PhI when compared to iodobenzene for arsenic ligands (the opposite is observed for phosphorous ligands). The use of arsenic ligands can also stabilize the transition states associated to the oxidative addition, while such stabilizing effects cannot be found with phosphorous ligands. Isomerization is dependent on the type of substrate and ligand because lower values are obtained for NO_2PhI when compared with iodobenzene, and for arsenic ligands when compared to phosphorous ligands. A strong effect of the considered substrate is also visible on the transmetalation process because much lower energy values are associated to the transition states of this step for NO_2PhI substrates. As already reported, arsenic ligands have a stabilizing effect in the transmetalation step, meaning that for this type of ligand, lower energy values are obtained when compared to phosphorous ligands. The same exact behavior reported for the isomerization step is observed for the reductive elimination step.

When comparing the results from trial 1 and trial 2 similar values have been obtained for the energy associated to the first complex. The same is true for the oxidative addition step, indicating that a more important role needs to be attributed to the considered halogen rather than to the considered substituted group. It is very interesting to note that the use of NO_2PhI makes it possible to significantly lower the energy associated to the transition states of isomerization, transmetalation, and reductive elimination, while the use of PhI leads to almost same values observed in trial 1 for these steps (only marginally smaller values are obtained). These results indicate that, as an improvement from trial 1, the use of NO_2PhI as the substrate with arsenic ligands (and in particular p-anysil containing ligands) can make the Stille coupling reaction even easier.

4 Discussion

After checking the results, it is easy to note that there are important differences in the behavior of the reaction if different ligands and substrates are considered.

4.1 Trial 1

4.1.1 Catalyst Dissociation

The catalyst dissociation is a process that is independent from the considered substrate because this step of the reaction only involves the catalyst and no other species. This step is necessary because the considered ligands are bulky, making the reaction almost impossible if PdL_2 is the catalyst species. Very similar PESs values were found across all the systems for this step and a small dependence on the type of ligand was noted: usually lower values are associated to the same type of ligand if arsenic is considered instead of phosphorous because in this species Pd-As bond lengths are longer than Pd-P bond lengths. It has also been observed that in arsenic ligands and phosphorous ligands a trend $(PhCF_3)_3 < Ph_3 < (PhOMe)_3$ is present in the energy values and this could be due to the difference in the As-C (or P-C) bond lengths that for every group of ligands decreases in the just mentioned order.

4.1.2 Oxidative Addition

In order to study the oxidative addition, the stability of the first complex (LPd-X-Ph-OMe) needs to be considered. The stability of the first complex can be understood by looking at the charge distribution on the palladium atom in the dissociated catalyst and on the halogen atom in the substrate. The charge on the palladium atom of the catalyst (the values are shown in Table 1) does not depend on the nature of the ligand because almost the same values of charge have been calculated for arsenic ligands and the corresponding phosphorous ligands. The charge depends on the substituent groups that are bonded to arsenic or phosphorous atoms because groups like anisole are electron-rich leading to a more negative charge on the palladium atom when compared to phenyl (which has an intermediate behavior) and $PhCF_3$ (which is electron-poor leading to less negative charge on the palladium atom).

The charge on the halogen atom of the substrate depends on the Pauling electronegativity of the different halogen atoms, which has a role in shortening the C-X bond length: chlorine is the most electronegative halogen atom among the three leading to the shorter C-X bond length and a slightly negative charge on itself, bromine has an intermediate electronegativity leading to an intermediate bond length and a slightly positive charge on itself and iodine is the least electronegative halogen leading to the longer C-X bond length and a significant positive charge on itself.

When considering the formation of the first complex, the charges on the two involved species are very important because they can stabilize or destabilize the product of this step. In fact, when considering chlorine systems there is a repulsive electrostatic interaction between the two reactants due to the negative charges that are present on both: the effect is more evident in the order $(PhCF_3)_3 < Ph_3 < (PhOMe)_3$ because of the more negative charge on the palladium atom that grows in that order with the different substituent groups. For this reason, the transition state for the oxidative addition is at a higher energy level than the dissociated catalyst, indicating a destabilized first complex. When considering bromine systems there is a negative charge on the palladium atom and a slightly positive charge on the bromine atom. As a result, only a very small attractive electrostatic interaction can take place without succeeding in stabilizing the first complex due to the very small positive charge on the bromine atom. The same behavior of chlorine systems is found in bromine systems with the destabilizing effect that is more evident in the order $(PhCF_3)_3 < Ph_3 < (PhOMe)_3$

because of the more negative charge on the palladium atom that grows in that order with the different substituent groups. When considering iodine systems, the same negative charges are present on the palladium atoms of the ligands, but the iodine atom has a positive charge (way higher than in bromine systems) that can stabilize the first complex: in these systems the transition state for the oxidative addition is always at a lower energy value indicating an easier step.

The different values of charge that lead to higher stability for the first complex and the subsequent transition state, mean that there are different relative bond strengths for Pd-X and OMePh-X. The Pd-X and OMePh-X bond strengths both decrease in the order Cl > Br > I, but the OMePh-X bond strength decreases more quickly than that of Pd-X explaining the trend of the calculated energies.

Orbital interactions play a key role in the oxidative addition step because a transfer of electrons from the HOMO of the catalyst to the LUMO of the substrate takes place. The populating of the antibonding orbitals causes the activation of X-C bonds which is seen in the transition state for this step. It is very important to consider the energy differences between the LUMO of the substrate (σ* orbital) and the HOMO of the catalyst (d-block orbitals) because this difference indicates how easily the oxidative addition can take place.

The orbital energy of σ* depends on the considered halogen in the substrate with an increase in the energy with I < Br < Cl: due to the lower energy levels, the energy difference is smaller for I containing-substrates, thus indicating an easier electron transfer which activates the I-C bond. Ligands are also very important because different ligands change the energy associated to the HOMO: electron transfer is favored as the orbital energy of the HOMO gets closer to the energy of the σ* orbital of the substrate. In arsenic ligands the associated orbital energy goes with PhOMe > Ph > $PhCF_3$ indicating that the oxidative reaction should be easier for Pd-As$(PhOMe)_3$ when compared to the other catalysts. The reaction between Pd-As$(PhOMe)_3$ and I-Ph-OMe is characterized by the lowest orbital energy gap (3,46 eV) which means that from an orbital interactions' point of view this is the preferred combination of species for the oxidative addition. For phosphorous ligands the oxidative addition step is easier if PhOMe is considered as the substituent because of the lower orbital energy gap observed in this case: by combining Pd-P$(PhOMe)_3$ and I-Ph-OMe a gap of 3,65 eV is obtained. For the other substituent groups in phosphorous ligands, the gap grows in the order Ph > $PhCF_3$. The slightly higher minimum orbital energy gap obtained for arsenic ligands when compared to phosphorous ligands indicates that the best catalysts to use if only orbital interactions are considered, are arsenic ligands (this is not true for $PhCF_3$ because the HOMO associated to $PPhCF_3$ is slightly closer to zero than the HOMO associated to $AsPhCF_3$).

4.1.3 Isomerization

In the isomerization step, steric effects are very important: arsenic ligands lead to lower values for the isomerization transition because of a longer Pd-As distance that makes it easier for the molecule to isomerize when compared to phosphorous ligands.

Bond strengths are also very important because if the molecule has less strong bonds between the atoms, it is easier for those bonds to break. In this case, a change in the halogen atom leads to different energy values for the isomerization step with the lowest value associated to iodine substrates, intermediate values for bromine and the highest values for chlorine substrates. This behavior is caused by the different electronegativities that influence the Pd-X bond strengths, with the bond strength that grows in the order I < Br < Cl. A change in the ligand can also influence the Pd-C bond involved in this step and in fact a trend $(PhCF_3)_3$ > Ph_3 > $(PhOMe)_3$ is observed in the energies associated to the isomerization.

4.1.4 Transmetalation

In the transmetalation step arsenic ligands lead to lower values in energy when compared to the phosphorous ligands with the same substituent groups. This is mainly due to Pd-As longer bond length that can relieve steric repulsions (that are much more important in transmetalation than in oxidative addition because of the organostannane presence) between the halogen atom and the ligand and between PhOMe and the ligand. Less steric repulsions mean that the organostannane attack can take place in an easier way, thus leading to lower energy values associated to the transition state of arsenic ligands.

The halogen atom that is present is also important because when chlorine-based substrates are considered usually lower values in the activation energies are calculated: more electronegative halogen atoms like chlorine lead to lower activation barriers because of the size that makes them less sterically hindering and because of the bond strengths for Sn-Cl and Pd-Cl. The size gets larger when going down the seventh group of the periodic table meaning that larger atoms are more sterically repulsive (Cl < Br < I). The values for the bond strength increase in the same order but the observed trend is explained by the fact that Sn-X bond strength increases faster than Pd-X bond strength.

Even if a very small contribution to transmetalation energy levels can be attributed to different substituent groups in the ligands (due to the different steric effects), no significant differences in the calculated valued have been found regarding the use of diverse substituent groups.

4.1.5 Reductive Elimination

Reductive elimination is usually characterized by low energetic values, meaning that this step can take place easily. There is a dependence on the halogen atom for this step, due to the difference in bond dissociation energies between X-C bond in the substrate and X-Sn bond in the newly formed X-$SnBu_3$ species. The considered ligand also influences the energy associated to this step, due to its energy being considered in the relative energy: in this case, a trend $(PhCF_3)_3$ > Ph_3 > $(PhOMe)_3$ in the energies is noted.

4.2 Trial 2

The results obtained in trial 2 confirm what has been observed in trial 1: arsenic ligands lead to lower energy values when compared to phosphorous ligands. For this reason, in this discussion of trial 2, the focus will be on arsenic ligands.

In this trial, the dissociation of the catalyst is exactly the same described in trial 1 so the same considerations made in 4.1.1 remain valid.

The use of NO_2PhI as the substrate for the Stille coupling reaction has led to much lower energy values associated to the oxidative addition, while similar values to trial 1 have been obtained for a PhI substrate. In order to study this step, it is important to consider the stability of the first complex. The charge on the palladium atom of the catalyst is the same as before, while the charge on the substrate is increased by the presence of NO_2 and decreased by the presence of H. The fact that the charge on the halogen atom is increased by NO_2 substituents when compared to the other substrates means that there is a stronger stabilizing effect on the first complex when compared to trial 1. It is also very important to consider orbital interactions because the presence of different substituent groups on the substrate change the orbital energies, thus influencing the easiness related to this step. In trial 2, for a NO_2PhI substrate there is an energy difference between the σ* orbital of the substrate and the HOMO of the catalyst of 2,94 eV with arsenic ligands. For an iodobenzene substrate, an energy difference between the LUMO and the HOMO of 3,47 eV with arsenic ligands has been calculated. It is also clear that the type of substrate considered in trial 2 leads to different values of the orbital energy gap with NO_2PhI substrate that has a lower orbital energy gap when compared to PhI. It is also very interesting to compare the results of trial 2 with the results of trial 1: in trial 2 much lower gaps have been obtained for an NO_2PhI substrate when compared to an OMePhI substrate (which has similar values to the ones obtained for PhI), so the new used NO_2PhI substrate is preferable for the oxidative addition step. It is very interesting to plot the activation energies for oxidative addition against the substituent constants of the three variating groups bonded in the substrate. The constants are 0,74 for NO_2, 0 for H, and -0,16 for OMe. The results are shown below in Scheme 23:

Scheme 23 Plot of activation energies for the oxidative addition (measured from the first complex) against the substituent constants of the considered groups

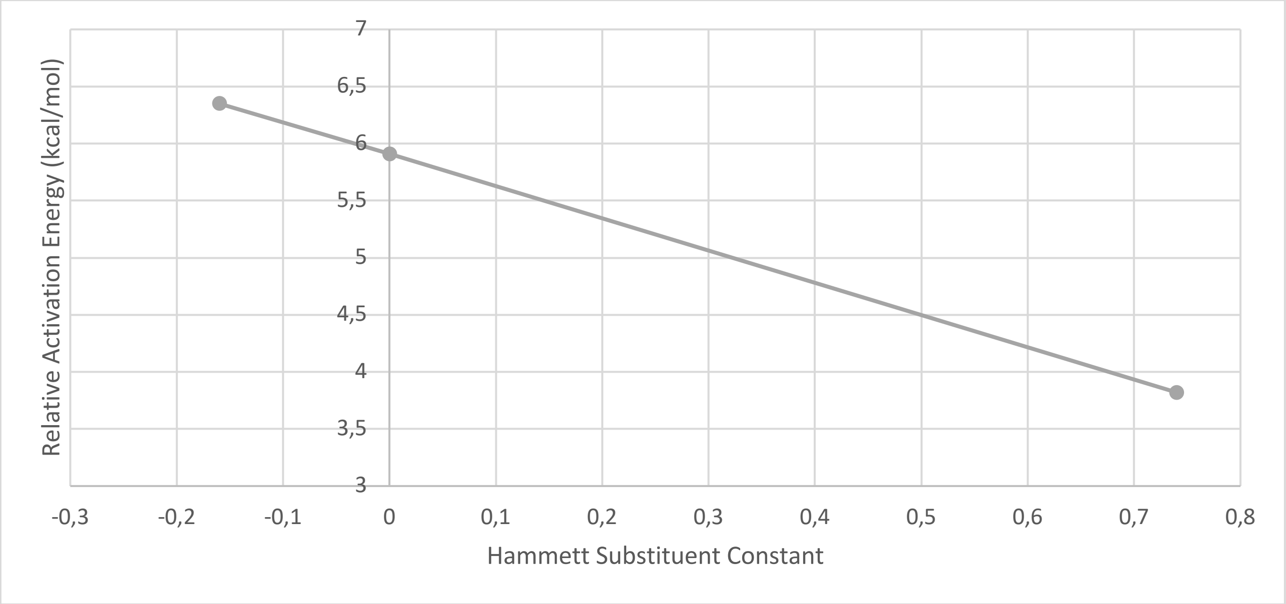

A linear relation has been found between the activation energy and the substituent constant, and, according to the Hammett rule, higher values of the substituent constant mean that a higher reaction rate should be observed (which is shown here by lower activation energies).

In the isomerization step, the Pd-C bond strength between the substrate and the palladium atom is like the one in trial 1, so similar energy values have been obtained for a PhI substrate when compared to OMePhI. Lower values have been obtained if NO_2PhI is considered as the substrate due to the lower Pd-C bond strength caused by the presence of an electron-withdrawing group (in trial 1 the substituent group was an electron-donating group).

In the transmetalation step, the reactivity is enhanced by the presence of NO_2 in the substrate because of its electronic effect on the molecule. This means that the palladium atom can bond the ethylene moiety of the organotin more easily due to the presence of the new substrate, and this is confirmed by the lower energy values associated to this step in the first system of trial 2. The other considered substrate led to similar values when compared to trial 1 meaning that the effect of OMe is similar to the effect of H.

The reductive elimination energy associated to the first system of trial 2 is significantly smaller when compared to PhI and OMePhI (which have similar values). This behavior is due to the different bond strength between the carbon atom of the substrate and the palladium atom, with the same considerations that have been previously made regarding the isomerization process.

5 Conclusion

In this work many different systems have been considered in order to study how the different catalysts and substrates can influence the Stille coupling reaction: the influence on the reaction has been studied through the energy levels obtained via DFT calculations.

Trial 1 showed that arsenic ligands lead to significantly lower energy values for the transition states of isomerization, transmetalation and reductive elimination when compared to phosphorous ligands. These results mean that transmetalation is a rate-determining step only for phosphorous ligands, while oxidative addition energy levels are comparable among the two systems meaning that this is a rate-determining step with both catalyst types. The use of electron-donating groups in the catalyst leads to more stable transition states in isomerization and reductive elimination when compared to Ph or electron-withdrawing groups, while similar values are obtained for oxidative addition and transmetalation. Different halogen atoms attached to the substrate lead to the energies associated to oxidative addition and isomerization growing in the order I < Br < Cl, while the opposite behavior is observed for transmetalation and reductive elimination. For this trial, the best combination of species is an arsenic catalyst (with electron-donating groups that lead to the smaller energy differences when compared to the first complex) and an iodine-based substrate.

Trial 2 confirmed that arsenic ligands are preferable, and that the use of electron-withdrawing groups attached to the substrate (instead of the previously considered electron-donating groups) can lead to significantly smaller energies associated to the transition states of oxidative addition, isomerization, transmetalation, and reductive elimination.

In conclusion, after the deep study of many different systems, the best species to consider for a Stille coupling reaction are arsenic ligands with electron-donating groups like p-anysil, and iodine-based substrates with electron-withdrawing groups like NO_2. Additional studies would be needed in the future to better understand the mechanisms behind these findings and to discover new species that can further enhance the reaction yields. The main focus in the future needs to be on the catalyst dissociation, on the oxidative addition and on the transmetalation because these steps are the most difficult ones, due to the high energies observed, much higher than the ones associated to isomerization and reductive elimination.

6 Aknowledgements

Firstly, I would like to thank Prof. Yumura for all the help he gave me in writing this thesis and the patience he has had during these difficult months of remote work. Without your help nothing of this could have been made.

I would also like to thank Prof. Imoto and his group for giving me part of their results for iodine systems so that I could use them to carry out a more complete work.

I would like to thank Mr. Fukuura for helping me a lot during the first phases of my work when I was completely lost in the use of Gaussian. Your help has been greatly appreciated.

Thanks to all the professors I virtually met during my courses at KIT, everyone has been very kind and helpful with me.

Thanks also to all the professors from the Politecnico di Torino I met during my master's degree, and in particular Prof. Sangermano who was my co-supervisor from Italy during this difficult year.

A great thanks goes to Giulia, who really helped me with the difficulties I encountered in the last year, without your presence by my side I would have probably not succeeded.

Finally, I would thank my parents, who really supported me during the pandemic and who motivated me to do my best all the time.

7 References

[1] G. M. J. Cowie, Polymers : chemistry and physics of modern materials, Boca Raton: CRC Press, 2008.

[2] «name-reaction.com,» [Online]. Available: https://www.name-reaction.com/stille-cross-coupling.

[3] D. E. C. Azarian, «Reaction of organic halides with R3MMR3 compounds (M = Si, Ge, Sn) in the presence of Tetrakis(triarylphosphine) palladium,» *Journal of Organometallic Chemistry,* vol. 117, 1976.

[4] M. M. T. Kosugi, «Reaction of allyltin compounds II. Facile preparation of allyl ketones via allyltins,» *Journal of Organometallic Chemistry,* vol. 129, 1977.

[5] S. J., «The palladium-catalyzed cross-coupling reactions of organotin reagents with organic electrophiles,» *Angewandte Chemie,* vol. 25, pp. 508-524, 1986.

[6] Z. Y. L. Bao, «Synthesis of conjugated polymer by the Stille coupling reaction,» *Chemistry of Materials,* vol. 5, pp. 2-3, 1993.

[7] «organic-chemistry.org,» [Online]. Available: https://www.organic-chemistry.org/namedreactions/stille-coupling.shtm.

[8] A. E. P. Casado, «On the configuration resulting from oxidative addition of RX to Pd(PPh3)4 and the mechanism of the cis-to-trans isomerization of [PdRX(PPh3)2] complexes (R = Aryl, X = Halide),» *Organometallics,* vol. 17, pp. 954-959, 1998.

[9] C. B. C. Cordovilla, «The Stille reaction, 38 years later,» *ACS Catalysis,* vol. 5, pp. 3040-3053, 2015.

[10] M. M. D. Portnoy, «Mechanism of aryl chloride oxidative addition to chelated palladium(0) complexes,» *Organometallics,* vol. 12, pp. 1665-1673, 1993.

[11] P. E. A. Espinet, «The mechanisms of the Stille reaction,» *Angewadtie Chemie,* vol. 43, pp. 4704-4734, 2004.

[12] V. R. G. Farina, «Recent avances in the Stille reaction,» *Advanced Metallic Oganic Chemistry,* vol. 5, pp. 1-53, 1996.

[13] A. E. P. Casado, «Mechanism of the Stille reaction. 2. Couplings of aryl triflates with vinyltributyltin. Observation of interme- diates. A more comprehensive scheme,» *Journal of the American Chemical Society,* vol. 122, pp. 11771-11782, 2000.

[14] A. E. P. Casado, «Mechanism of the Stille reaction. 1. The transmetalation step. Coupling of R1I and R2SnBu3 catalyzed by trans-[PdR1IL2] (R1 = C6Cl2F3; R2 = Vinyl, 4-Methoxyphenyl; L = AsPh3),» *Journal of the American Chemical Society,* vol. 120, pp. 8878-8985, 1998.

[15] J. H. J. Louie, «Transmetalation involving organotin aryl, thio- late, and amide compounds. An unusual type of dissociative ligand substitution reaction,» *Journal of the American Chemical Society,* vol. 117, pp. 11598-11599, 1995.

[16] B. H. F. Carsten, «Stille polycondensation for synthesis of functional materials,» *Chemical Reviews,* vol. 111, pp. 1493-1528, 2011.

[17] Z. Y. L. Bao, «Exploration of the Stille coupling reaction for the syntheses of functional polymers,» *Journal of the American Chemical Society,* vol. 117, pp. 12426-12435, 1995.

[18] A. S. L. Littke, «Pd/P(-Bu)3: a mild and general cata- lyst for Stille reactions of aryl chlorides and aryl bromides,» *Journal of the American Chemical Society,* vol. 124, pp. 6343-6348, 2002.

[19] C. C. E. Amatore, «Rates and mechanism of the formation of zerovalent palladium complexes from mixtures of Pd(OAc)2 and tertiary phosphines and their reactivity in oxidative additions,» *Organometallics,* vol. 14, pp. 1818-1826, 1995.

[20] C. B. A. Amatore, «Rate and mechanism of the oxidative addition of phenyl iodide to Pd0 ligated by triphenylarsine: evidence for the formation of a T-shaped complex [PhPdI(AsPh3)] and for the decelerating effect of CH2=CH–SnBu3 by formation of [Pd0(η2-CH2=CH–SnBu3)(AsPh3)2,» *Chemical European Journal,* vol. 7, pp. 2134-2142, 2001.

[21] V. K. B. Farina, «Large rate accelerations in the Stille reaction with Tri-2-furylphosphine and triphenylarsine as palladium ligands: mechanistic and synthetic implications,» *Journal of the American Chemical Society,* vol. 113, pp. 9585-9595, 1991.

[22] H. C. A. Imoto, «Tertiary arsine ligands for Stille coupling reaction,» *Wiley-VCH,* 2021.

[23] K. M. T. Lam, «DFT Studies on the Effect of the Nature of the Aryl Halide Y-C6H4-X on the Mechanism of Its Oxidative Addition to Pd0L versus Pd0L2,» *Organometallics,* vol. 26, pp. 758-760, 2007.

[24] A. L. Z. Ariafard, «Effect of the Leaving Ligand X on Transmetalation of Organostannanes (vinylSnR3) with LnPd(Ar)(X) in Stille Cross-Coupling Reactions. A Density Functional Theory Study,» *Organometallics,* vol. 25, pp. 5788-5794, 2006.

[25] W. S. J. Scott, «Palladium-catalyzed coupling of vinyl triflates with organostannanes. Synthetic and mechanistic studies,» *Journal of the American Chemical Society,* vol. 108, pp. 3033-3040, 1986.

[26] V. L. L. Farina, «On the nature of the “copper effect” in the Stille cross-coupling,» *Journal of Organic Chemistry,* vol. 59, pp. 5905-5911, 1994.

[27] K. F. G. Menzel, «Room-temperature Stille cross-couplings of alkenyltin reagents and functionalized alkyl bromides that possess beta hydrogens,» *Journal of the American Chemical Society,* vol. 125, pp. 3718-3719, 2003.

[28] S. L. V. Mee, «Significant enhancement of the Stille reaction with a new combination of reagents-copper(I) iodide with cesium fluoride,» *Chemistry,* vol. 11, pp. 3294-3308, 2005.

[29] C. B. A. Amatore, «Mechanism of the Stille reaction catalyzed by palladium ligated to arsine ligand: PhPdI(AsPh3)(DMF) is the species reacting with vinylstannane in DMF,» *Journal of the American Chemical Society,* vol. 125, pp. 4212-4222, 2003.

[30] C. Kappe, «Controlled microwave heating in modern organic synthesis,» *Angewadtie Chemie,* vol. 43, pp. 6250-6284, 2004.

[31] L. B. Z. Yu, «Conjugated, liquid crystalline polymers,» *Angewadtie Chemie,* vol. 32, pp. 1345-1347, 1993.

[32] X. M. S. Zhan, «A high-mobility electron-transport polymer with broad absorption and its use in field-effect transistors and all-polymer solar cells,» *Journal of the American Chemical Society,* vol. 129, p. 7246–7247, 2007.

[33] P. Z. X. Cheng, «Binary additives synergistically boost the efficiency of all-polymer solar cells up to 3.45%,» *Energy Environmental Science,* vol. 7, pp. 1351-1356, 2014.

[34] H. F. A. Yan, «A high-mobility electron-transporting polymer for printed transistors,» *Nature,* vol. 457, p. 679–686, 2009.

[35] Z. Z. C. He, «Enhanced power-conversion efficiency in polymer solar cells using an inverted device structure,» *Nature Photonics,* vol. 6, pp. 591-595, 2012.

[36] J. Y. Y. You, «A polymer tandem solar cell with 10.6% power conversion efficiency,» *Nature Communications ,* vol. 4, p. 1446, 2013.

[37] J. B. D. Burroughes, «Light-emitting diodes based on conjugated polymers,» *Nature,* vol. 347, pp. 539-541, 1990.

[38] J. W. C. Tian, «Photophysical properties, self-assembled thin films, and light-emitting diodes of poly(p-pyridylviny1ene)s and poly(p-pyridinium viny1ene)s,» *Chemical Materials,* vol. 7, pp. 2190-2198, 1995.

[39] J. k. K. Ohshita, «Synthesis of silicon-bridged polythiophene derivatives and their applications to EL device materials,» *Journal of Polymeric Science,* vol. 45, pp. 4588-4596, 2007.

[40] I. H. M. McCulloch, «Liquid-crystalline semiconducting polymers with high charge-carrier mobility,» *Nature Materials,* vol. 5, pp. 328-333, 2006.

[41] T. D. J. Lei, «Influence of alkyl chain branching positions on the hole mobilities of polymer thin-film transistors,» *Advanced Materials,* vol. 24, pp. 6457-6461, 2012.

[42] G. T. B. Schwartz, «Flexible polymer transistors with high pressure sensitivity for application in electronic skin and health monitoring,» *Nature Communication,* vol. 4, p. 1859, 2013.

[43] J. H. A. Lee, «Solution-processable ambipolar diketopyrrolopyrrole-selenophene polymer with unprecedentedly high hole and electron mobilities,» *Journal of the American Chemical Society,* vol. 134, pp. 20713-201721, 2012.

[44] H. W. L. Saadeh, «A new synthetic approach to novel polymers exhibiting large electrooptic coefficients and high thermal stability,» *Macromolecules,* vol. 33, pp. 1570-1576, 2000.

[45] W. Y. L. You, «Fully functionalized photorefractive polymer with infrared sensitivity based on novel chromophores,» *Macromolecules,* vol. 36, pp. 7014-7019, 2003.

[46] M. S. T. Marsella, «Design of chemoresistive sen- sory materials: polythiophene-based pseudopolyrotaxanes,» *Journal of the American Chemical Society,* vol. 117, pp. 9832-9841, 1995.

[47] K. G. H. Kawabata, «Liquid crystalline π-conjugated copolymers bearing a pyrimidine type mesogenic group,» *Materials,* vol. 2, pp. 22-37, 2009.

[48] C. W. W. Ho, «Metal-containing polymers: facile tuning of pho- tophysical traits and emerging applications in organic electronics and photonics.,» *Coordination Chemistry Reviews,* vol. 255, pp. 2469-2502, 2011.

[49] P. F. R. Atkins, Molecular Quantum Mechanics, Oxford University Press, 2011.

[50] A. W. A. McNaught, IUPAC. Compendium of Chemical Terminology, Oxford: Blackwell Scientific Publications, 1997.

[51] «Gaussian.com,» [Online]. Available: https://gaussian.com/gaussview6/.

[52] «Gaussian.com,» [Online]. Available: https://gaussian.com/route/.

[53] «Gaussian.com,» [Online]. Available: https://gaussian.com/opt/.

[54] «Gaussian.com,» [Online]. Available: https://gaussian.com/freq/.

[55] «Gaussian.com,» [Online]. Available: https://gaussian.com/dft/.

[56] A. Becke, «Density-functional thermochemistry. III. The role of exact exchange,» *Journal of Chemical Physiscs,* vol. 98, p. 5648–5652, 1993.

[57] «Gaussian.com,» [Online]. Available: https://gaussian.com/iop/.

[58] «Gaussian.com,» [Online]. Available: https://gaussian.com/gaussian16/.